Research Doctorate School in Biological and molecular Sciences

DOCTORATE THESIS

Student: **Iacopo Petrini**
e-mail: **petrinii@mail.nih.gov**

Supervisor: **Giuseppe Giaccone**
e-mail: **giacconeg@mail.nih.gov**

Doctorate Program: **Molecular and Experimental Oncology**

Year: **2012**

TITLE OF THE PROJECT

Genomic Aberrations of Thymic Epithelial Tumors

Department/Laboratory/Institution: **Medical Oncology Branch/Thoracic Oncology Laboratory/National Cancer Institute.**

Abstract

Thymic epithelial tumors (TETs) are rare neoplasms classified in thymoma and thymic carcinoma. According to the 2004 WHO classification, thymomas are further subdivided into five subcategories (A, AB, B1, B2, B3), depending on cancer cell shape, degree of atypia and number of intratumoral thymocytes. Surgical resection is recommended for localized tumors, but systemic therapy is the choice for metastatic and not resectable neoplasms. Usually, TETs respond to chemotherapeutic drugs but their effect lasts only for a limited time, thus, new targeted-molecules are currently under evaluation. However, the efficacy of biologic therapies in TET is scant, to date. The main limitation is the lack of a robust rationale to target specific molecules, mainly because the aberrations driving TET growth are obscure.

The aim of this project is to clarify the molecular aberration driving the TET growth.

Firstly, the frequency of aberrations described in TET case-reports has been evaluated. The presence of BRD4-NUT fusion gene was tested in 148 TETs, but resulted in a rare event, observed in only one thymic carcinoma. Similarly, no KIT mutations were detected in the 13 TETs sequenced. Reviewing literature data, KIT was mutated in only 9% of thymic carcinomas.

Therefore, a systematic screening for new genomic aberrations in TET was started using whole genome sequencing to evaluate the presence of mutations, translocation and copy number (CN) aberrations in a B3 thymoma. The translocation t(11;X)(q14.2;q25), the presence of 7 single nucleotide mutations and 1 INDEL were observed together with CN gain of chromosome 1q, 5, 7, X and CN loss of 3p, 6, 13 and part of chromosome 11q.

In order to identify which one of these genomic aberrations was recurrent and therefore candidate to drive TET growth, whole exome sequencing and array comparative genomic hybridization (CGH) were adopted. 26 tumors were screened by array CGH and 5 selected to be sequenced using tumor and normal DNA. The identified mutations were confirmed and tested for expression using transcriptome sequencing. The sequencing demonstrated a remarkably heterogeneous pattern of mutations. Recurrent were the amplification of BCL2, observed in 4 thymic carcinomas, and the inactivation of CDKN2A caused by a frame-shift INDEL and 2 CN losses.

Because BCL2 and CDKN2A are more likely to be mutated by CN aberrations, 59 formalin fixed paraffin embedded tumors were evaluated using array CGH. Data confirmed the presence of focal CN loss of CDKN2A and amplification of BCL2 as recurrent events in TETs and suggest a possible prognostic role for these CN aberrations. Immunohistochemistry confirmed the lack of P16INK4 expression in tumors with CDKN2A CN loss and showed a poor prognosis for patients with negative staining. P16INK4 is a well-known tumor suppressor gene involved in the control of cell cycle through the binding of CDK4 and 6.

The role of anti apoptotic BCL2 family proteins was elucidated using 3 TET cell lines because these molecules could represent targets for therapy. A siRNA approach demonstrated that the expression of BCL2 and MCL1, two anti-apoptotic proteins, was necessary for TET cell line growth. GX15-070, a BH3 mimetic inhibitor of anti-apoptotic BCL2 family members, reduced proliferation of TET cell-lines in vitro, through the induction of autophagy and necroptosis. Gx15-070 inhibited tumor growth in the xenograft model established using TY82 thymic carcinoma cell line; therefore this drug may be tested for patients' treatment.

1. Introduction

1.1 Normal thymus

Macroscopic structure

Microscopic structure

Physiological function of the thymus

1.2 Definition of thymic epithelial tumors

1.3 Epidemiology

1.4 Etiology

1.5 Staging

1.6 Histological classification of thymic epithelial tumors

Gross pathological and histological features of thymic epithelial tumors

Clinical relevance of WHO classification

Reproducibility of WHO classification

1.7 Treatment of thymic epithelial tumors

Surgery

Subtotal resection

Salvage surgery

Radiotherapy

Postoperative radiotherapy

Radiotherapy for thymic carcinoma

Systemic therapy

Palliative chemotherapy

Neoadjuvant chemotherapy

Targeted therapy

1.8 Paraneoplastic syndromes

1.9 Molecular aberrations of thymic epithelial tumors

1. Introduction

1.1 Normal thymus

Macroscopic structure

The thymus is a median organ located in the anterior mediastinum. Starting from fetal life, it increases its dimension reaching maximum size during adolescence and decreases thereafter. In the adolescent the thymus extends from the fourth costal cartilage upward to the lower border of the thyroid gland. The sternum and the sternohyoidei and sternothyreoidei muscles cover the thymus. Back, the thymus confines with the pericardium and a layer of fascia, which covers the aortic arch and the great vessels. In the neck, it partially wraps the frontal part of the trachea. The thymus consists of two lateral lobes that are occasionally united and frequently differ in size. This organ presents a soft lobulated surface when cut and a pinkish-gray color.

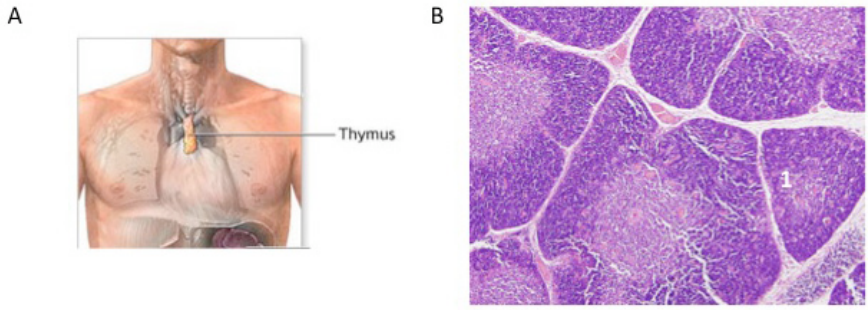

Figure1.1: Normal thymus. (A) Schematic representation of the thymus. (B) Microscopic structure of the thymus.

Microscopic structure

A fibrous capsule wraps each lateral lobe of the thymus and protrudes septa of a delicate areolar tissue within the organ; therefore it presents a lobular aspect. The lobules vary in size and have an irregular shape being, in the interior portion fused together. Each follicle is divided into two main regions on histological grounds, the cortex and the medulla; and each of these regions contains several ultrastructurally and phenotypically distinct types of thymic epithelial cells and immature lymphocytes (thymocytes).

The thymic cortex is composed by network of epithelial cells mixed with abundant thymocytes; these stroma cells form an adventitia to the blood vessels in the periphery of lobules.

In the medulla the epithelial cells are prevalentand are organized in a coarse reticulum whereas the thymocytes are relatively fewer in number. Hassall corpuscles are nest-like bodies observed in thymic medulla. These corpuscles are composed of central granular cells wrapped by several layers of epithelioid cells. The cortico-medullary junction separates the two distinct portions. Just outside the cortex, the sub-capsular zone defines a functionally differentiated region of the thymus.

Stromal cells, mainly thymus epithelium, interdigitating cells, and macrophages constitute the thymic microenvironment, but other components, such as nerves, endothelium, fibroblasts, and connective tissue are represented as well.

Distinct regions of the thymus contain different populations of epithelial cells. Electron microscopy analyses have identified six types of thymic epithelial cells: type 1 cells are present in the capsule and septa and surround the perivascular spaces of the

cortical capillaries; types 2, 3 and 4 form a graded series in the cortex, ranging from electron-lucent metabolically active to electron-dense dying forms; type 5 cells are rare, medullary unspecialized epithelial cells, while type 6 cells form the major medullary population and contribute to Hassall's corpuscles.

Expression of cytokeratin 5 (K5) and K8 distinguishes epithelial cell subpopulations of the thymus. The more prominent cortical and medullary subsets are K8+K5– and K8–K5+, respectively. Cells of the cortico–medullary junction are K5+K8+. The presence of a common stem cell of endodermic origin, able to generate such epithelial subpopulations, has been demonstrated and is characterized by MTS20+MTS24+K8+K5+ phenotype[1]. Therefore, the epithelial component of the thymus entirely originates from the endoderm of the third pharyngeal pouch, whereas the fibroblast and the capsule originate from mesoderm of the neural crest. The cells originating from the neural crest wrap the thymic primordium and this interaction is necessary to the normal development of thymus[2]. Moreover, the precursors of thymic epithelial cells are able to start their maturation process but necessitate the interaction with thymocytes to differentiate into the mature phenotype[3].

Physiological function of the thymus

The thymus has a central role in the immune system because it is required for T-cell differentiation and repertoire selection. The stromal cells of the thymus sustain and drive the maturation of the thymocytes that migrate in this organ from the bone marrow. T-cell development is characterized by the progression through several phenotypically distinct stages, defined as double negative (DN), double positive (DP) and single positive (SP) based on expression of the co-receptors CD4 and CD8. The DN subset is further subdivided into four stages (DN1–3 and DN4/pre-DB) by the

differential expression of CD44 and CD25. Thymocytes occupy different regions of the thymus according to their maturative stages suggesting an highly ordered migration (Figure 1.2).

T-cell precursors access the thymus at the cortico–medullary junction and migrate progressively to the subcapsular zone of the outer cortex; thereafter thymocytes move back through the cortex and into the medulla, from where they egress to the periphery in the form of mature T lymphocytes. Migrating through the cortex, thymocytes undergo the positive selection for those cells presenting a T cell receptor able to recognize the major histocompatibility complex. Passing through the medulla, thymocytes are exposed to the negative selection that removes those T-cell precursors able to recognize self-antigens. This process is also known as central tolerance and it is promoted by the ectopic expression of tissue-restricted self-antigens in the medullary cells of the thymus. The expression of tissue-restricted self-antigens mirrors virtually all tissues of the body, irrespective of developmental or spatio-temporal expression patterns. The autoimmune regulator gene (AIRE) promotes the expression of peripheral antigens in medullary cells. The subversion of thymic architecture and the abnormal properties of neoplastic thymic epithelial cells in thymomas can brake the central tolerance and are considered responsible for the increased number of autoimmune diseases observed in these tumors.

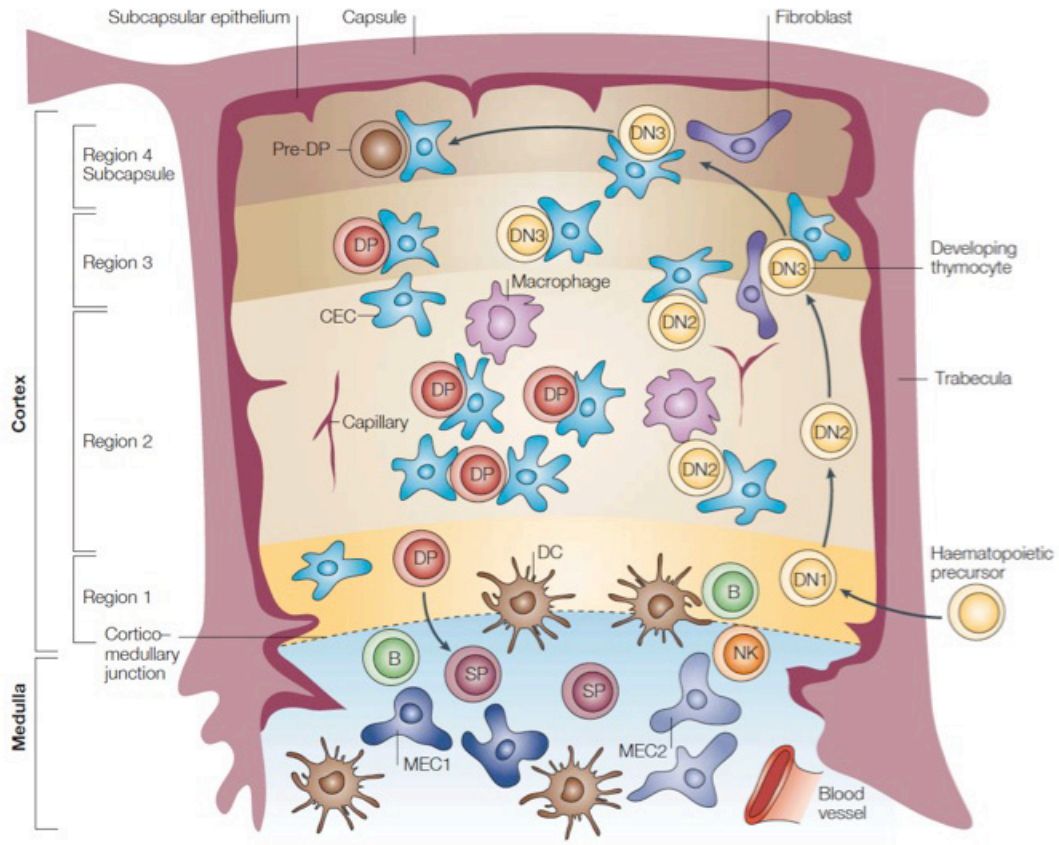

Figure 1.2: Modified from Blackburn CC, et al.[3]; the thymic lobule is divided into cortex and the medulla. Different types of epithelial cells constitute the stroma of thymic medulla (MEC) and cortex (CEC). The thymic cortex has been separated into 4 regions. In region 1, the cortico–medullary junction, is the site of entry into the thymus and contains DN1 cells. In region 2, cells differentiate to the DN2 stage, undergo a proliferative clonal expansion, and lose B- and natural killer (NK)-cell potential. In region 3, DN3 cells rearrange their T-cell receptor (TCR) β-chain. In region 4 DN cells become CD4+CD8+ DP. DP cells migrate back through the cortex to differentiate into the medulla either in CD4+ or CD8+ SP cells. B: B lymphocytes and DC: dendritic cells.

1.2 Definition of thymic epithelial tumors

Thymoma and thymic carcinoma are neoplasms originating from the epithelial cells of the thymus; therefore, they are defined thymic epithelial tumors to distinguish them from lymphomas that arise from thymic lymphocytes and thymocytes (immature lymphocytes of the thymus). Levine and Rosai have introduced such distinction in 1976[4]. Previous publications indiscriminately named thymomas also those tumors originating from thymic lymphocytic component.

1.3 Epidemiology

Thymic epithelial tumors (TETs) are the most frequent primary tumors of the mediastinum, however they are rare. In the mediastinum, metastases are the most commonly diagnosed masses, while primary tumors are among the most rare human neoplasms comprising less than 1% of all adult cancers. TETs comprise about 25% of primary mediastinal cancers (Figure 1.3 A).

Three population-based studies have estimated the incidence of TETs in the Netherlands, Sweden and USA. According to the Dutch cancer register, the incidence of TETs is 0.32/100 000 person-year[5], while, according to the Swedish register, 0.23 in female and 0.27 in male[6]. In the Nederlands, the incidence progressively increased by 6% between 1995 and 2003. Data on US population are more difficult to interpret, because the Surveillance, Epidemiology and End Results (SEER) database collects only data on malignant thymomas. The definition of malignant thymomas was based on an obsolete classification and limited to those cases with capsular invasion. Due to the stage at the diagnosis and the evidence of capsular invasion, not all thymomas have been captured by SEER registries, because they could be interpreted as benign tumors by pathologist or clinicians. Because such cases have not been recorded in the US cancer registries, the reported estimated incidence of 0.13/100 000 person-year underestimates the global incidence of TETs in US, including only a subgroup of cases considered "malignant thymomas"[7]. Such results come back in line with European estimations, considering that 35.5% of TETs were classified malignant and 64.5% benign in the Swedish population[6].

TETs are exceedingly uncommon in children and young adults; the incidence rises in middle age, and peaks in the seventh decade of life. The median age at the

presentation is 60 years, with most patients older than 40 years[6]. Surprisingly, the increase in thymoma incidence with age appears in striking contrast to the progressive age-related involution of the thymus. Similarly, the incidence decline at the oldest ages is unexplained.

TET incidence is higher in Asians/Pacific Islanders and African Americans than Caucasian and Hispanics, among the ethnic groups studied in SEER database[7].

Patients affected by TET present a reduced overall survival[6], despite the possible indolent behavior of a subgroup of them (Figure 1.3B). Patients with either malignant or benign tumors have a shorter survival compared to the control group which was constituted by subjects randomly selected from the Swedish population database, without any history of cancer and matched by gender and age[6].

The evaluation of secondary malignancy after the diagnosis of TET is relevant to understanding the etiology and the biology of these tumors. An increased risk of specific neoplasms could indicate that those cancers share genetic or environmental risk factors. Moreover, an elevated risk for specific cancers succeeding thymoma may suggest that the immune dysregulation caused by thymoma predisposes to those cancers. Retrospective reports suggest a broadly increased risk for cancer in patients treated for thymoma, with possible relation to genetic predisposition or to immune disturbance. In those studies the frequency of secondary malignancy ranged between 28 and 8%[8-10]. In the SEER database, 66 out of 733 (9%) patients with a diagnosis of malignant thymoma successively developed a secondary tumor. However, the corresponding standardized incidence ratio (SIR)[@], that approximates the relative risk for cancer associated with thymoma, was only 1.5; which was a more modest elevation than that depicted in the hospital-based series[7]. Among the specific

malignancy, only an increased risk for non-Hodgkin's lymphoma (7 cases) was supported by SEER data for a SIR of 4.7[7]. The increased risk for secondary non-Hodgkin's lymphoma was confirmed in the Swedish register (SIR 6.3) and reported together with an increased risk of non-melanoma skin cancer (SIR 10.6) and cervix cancer (SIR 6.9) that were not evaluated in the US study[6]. These observations have been related to the immune system alteration associated with thymic impairment, since a significantly risk increase of non-melanoma skin cancer, non-Hodgkin's lymphoma and cancer of the cervix, are strongly associated with severe immune disorders such as acquired immunodeficiency syndrome (AIDS). A complementary approach can be adopted to examine cancer registry data searching for thymoma risk following other primary malignancy. A report, based on SEER data, showed only a modestly elevated risk of developing thymoma after different cancers (SIR 1.33), without any relation to a particular tumor type[11]. The lack of an increased risk for developing thymoma in non-Hodgkin's lymphoma patients supports the hypothesis that the elevated risk of secondary non-Hodgkin's lymphoma after thymoma arises from immune disturbance consequent to thymoma. Moreover, the absence of an increased thymoma risk in lung or breast cancer and in Hodgkin's lymphoma patients, all of which are frequently treated by radiation therapy to the chest, argues against a role played by ionizing radiation as a risk factor for thymoma. Such data regarding risk of secondary cancers do not suggest tobacco or alcohol as candidate risk factors for thymoma. There are not data concerning the role of occupation, environmental exposures, or diet and nutrition.

@ Note: the standardized incidence ratio (SIR) is the ratio of the observed-to-expected number of cases: if SIR =1 the incidence of secondary malignancy is the same of the reference population whereas it is increased when SIR >1.

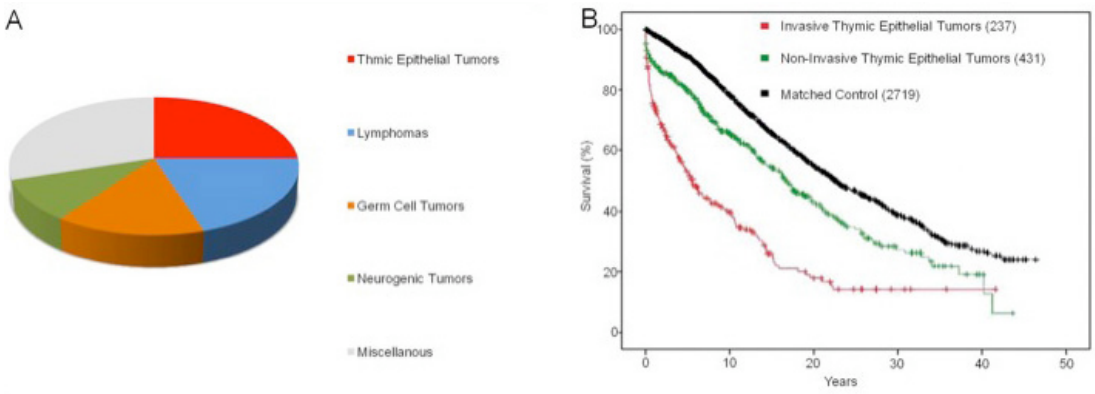

Figure 1.3: Epidemiology data of thymic epithelial tumors. (A) Depicts the frequency of primary tumor of the mediastinum in adults. (B) Modified from Gadalla SM, *et al.*[6]; Survival curves for benign and malignant thymoma patients and their matched controls

1.4 Etiology

The etiology of TETs is largely unknown. Based on case-reports, viral etiology has been evaluated as a possible cause of TETs. Two cases of human foamy virus in patients with thymoma or myasthenia gravis have been reported[12,13], however subsequent larger studies did not confirm these findings[14,15]. Similarly, the infection of human T-cell lymphotropic virus type 1 has been described in myasthenia gravis patients, some of whom had thymoma[16], but, again, these findings were not confirmed[14].

More convincing evidences indicate Epstein Barr virus (EBV) as a possible cause of lymphoepithelioma-like thymic carcinoma, since viral infection has been confirmed in these tumors[17-20] and its histological features resemble those of nasopharyngeal carcinoma: tumors caused by EBV in a subset of patients.

An higher frequency of neuroendocrine thymic carcinomas has been reported in patients affected by Multiple endocrine neoplasm 1 (MEN1) syndrome[21,22], however, the incidence (8%) of thymic tumors remains an infrequent finding in MEN1 patients. About 25% of patients with thymic carcinoids have a positive history of MEN1[23].

1.5 Staging

Thymomas are an heterogeneous group of tumors according to histological features and malignant behavior. There are tumors that present a favorable prognosis growing into the thymic capsule; such tumors can even reach large dimensions, up to bulky masses, but they remain limited to the thymus borders. Other tumors present a more aggressive behavior invading the mediastinal structures. Usually, these more aggressive tumors start invading the thymic capsule, thereafter the mediastinal fat and finally, infiltrate other mediastinal organs. Diffusion in the pericardial and pleural cavities are the most common ways of dissemination. Less frequently, advanced thymomas present a metastatic spread colonizing distant organs such as liver, lung or bone than regional lymph nodes. On the other hand thymic carcinomas usually are aggressive diseases with early invasion of regional structure as well as metastatic spread[24].

To evaluate TETs it is necessary to organize them according to their extent of spread, therefore they are classified according a specific staging system. The stage at the diagnosis is one of the most important prognostic factors for TETs and contributes to define the framework of treatment of these neoplasms. In 1981, Masaoka has proposed a staging system that has been widely accepted during the last decades and is currently adopted in most centers (Table 1.1). Beside Masaoka staging system, recently, several authors have proposed a TNM based classification: Yamakawa and Masaoka *et al.*[25], Tsuchiya *et al.*[26] at the National Cancer Center Hospital of Japan, the WHO committee[24] and Bedini *et al.*[27] at the National Cancer Institute of Italy. The TNM schema proposed by Yamakawa and Masaoka is reported in table 1.2. The Masaoka staging system empathizes the importance of local invasion and is mainly designed for thymomas which present nodal metastasis only in 3.2% of patients[28].

Conversely, a larger number of thymic carcinomas display nodal spread (32.6%), thus, the presence of N1, N2 or N3 diffusion could segregate patients upon survival.

Kondo *et al.* have evaluated the prognostic implication of nodal spread among the stage IVB in a large series of TETs. However, the authors did not show any significant difference. Consequently, they concluded that Yamakawa and Masaoka TNM system represents an excellent predictor for the prognosis even in thymic carcinomas where the N and/or M influence the prognosis more than the T factor[29]. A proper sub classification of the N and/or M factors necessitates large-scale studies including resectable and unresectable tumors[29]. Therefore, in the flowing chapters stages are referred to the system reported in table 11.

Table 1.1: Masaoka staging system

I	Macroscopically encapsulated tumor, with no microscopic capsular invasion
IIa	Microscopic invasion into the capsule
IIb	Macroscopic invasion into surrounding fatty tissue or mediastinal pleura
IIIa	Macroscopic invasion into neighboring organs without invasion of great vessels
IIIb	Macroscopic invasion into neighboring organs with invasions of great vessels
IVa	Pleural or pericardial metastases
IVb	Lymphogenous or hematogenous metastasis

Table 1.2: TNM Classification of Thymic Epithelial Tumors (Yamakawa and Masaoka [25])

T factor
T1: Macroscopically completely encapsulated and microscopically no capsular invasion
T2: Macroscopically showing adhesion or invasion into surrounding fatty tissue or mediastinal pleura, or microscopic invasion into capsule
T3: Invasion into neighboring organs, such as pericardium, great vessels, and lung
T4: Pleural or pericardial dissemination

N factor
N0: No lymph node metastasis
N1: Metastasis to anterior mediastinal lymph nodes
N2: Metastasis to intrathoracic lymph nodes except anterior mediastinal lymph nodes
N3: Metastasis to extrathoracic lymph nodes

M factor
M0: No hematogenous metastasis
M1: Hematogenous metastasis

Stage I	T1	N0	M0
Stage II	T2	N0	M0
Stage III	T3	N0	M0
Stage IVA	T4	N0	M0
Stage IVB	any T	N1-3	M0
Or	any T	anyN	M1

1.6 Histological Classification of thymic epithelial tumors

The classification of TETs based upon their histological features has been one of the most debated topics between pathologists. In 1961, Barnatz et al. from the Mayo clinic presented the first widely accepted classification of TETs by which thymomas were divided in four categories: predominantly lymphocytic, predominantly epithelial, mixed and predominantly spindle cells. During the following years, several subsequent classifications (Table 1.3) have been proposed and criticized, until 1999, when the World Health Organization (WHO) committee chaired by Dr. Rosai presented a proposal of classification that encountered large agreement between pathologists. That proposal has been integrated and accepted as a formal classification in 2004 by a WHO committed chaired by Dr. Muller-Hermelink[24,30].

Table 1.3: Historical classification of thymic epithelial tumors

Classification	Year	Categories: Thymoma					Thymic carcinoma
Barnatz	1961	Predominantly spindle cells	Mixed	Predominantly Lymphocytic		Predominantly Epithelial	
Verley and Hollmann	1985	Spindle Cell		Lymphocyte rich		Differentiated epithelial cell rich	Undifferentiated epithelial cell tumors
Levine and Rosai	1978	Benign thymoma (encapsulated)			Malignant Thymoma Type I (Invasive)		Malignant Thymoma Type II (Thymic carcinoma)
Marino and Muller-Hermelink	1989	Medullary Thymoma	Mixed Thymoma	Cortical Thymoma	Predominantly Cortical Thymoma	Well differentiated Thymic Carcinoma	
Shimosato and Mukai	1997	By extent (Circumscribed, Invasive, Metastatic)		By histology (Lymphocytic mixed and epithelial)	By cell type (Spindle, Polygonal, Polygonal-Oval)		By atypia (Absent, slight, moderate, marked)
Kuo	2000	Spindle cell thymoma	Mixed	Organoid	Small polygonal	Large polygonal cell	Squamoid thymoma
WHO (Rosai)	1999	A	AB	B1	B2	B3	C
Suster and Moran	1999	Well-differentiated thymoma				Moderately differentiated thymic neoplasm	Poorly differentiated tumors
WHO (Muller-Hermelink)	2004	A	AB	B1	B2	B3	Thymic Carcinoma

According to this classification, a clear cut distinction has been defined between thymomas, organotypic tumors that mimics the structure of normal thymus, and thymic carcinomas, more aggressive neoplasms that do not resemble the structure of normal thymus but those of carcinomas originating in organs other than thymus.

Gross pathological and histological features of thymic epithelial tumors

Thymomas are classified in A, B histotypes, depending on the shape of epithelial cells and their nuclei.

A type thymomas present bland spindle/oval epithelial tumor cells with few or no lymphocytes. Grossly, they are usually encapsulated and easily separable from the surrounding organs even in case of tumors with conspicuous dimension. When cut, the surface appears white with vague lobulation. Cystic structures and calcification of the capsules can be observed. Microscopically, the tumor cells present bland nuclei with disperse chromatin and inconspicuous nuclei. Tumor cells are arranged in solid sheets without any particular pattern, neither distinct lobules nor dissecting fibrous bands typical of other type of thymomas. Type A cells can form cystic o glandular structure, glomeruloid bodies, rosettes or meningioma-like whorls. Perivascular spaces are less commonly seen than in other types of thymomas and even if type A is a thymocyte poor thymoma, spindle cells micronodules in a lymphoid stroma can be observed at places. Mitotic figures are infrequent. Necrosis can be appreciated in case of lobular infarct. Rarely, thymic carcinoma can arise in type A thymoma, usually accompanied by necrotic areas, which examination reveals hyperchromatic anaplastic nuclei and or mitotic figures indicating the presence of carcinoma[24].

Type B thymomas show epithelial cells with a predominantly round or polygonal appearance and are further classified in B1, B2 and B3, according to an increasing degree of atypia of the tumor cells and to a decreasing extent of thymocytes[24].

Type B1 thymomas display tumor epithelial cells scattered in a prominent population of immature non-neoplastic thymocytes resembling the structure of normal

thymus cortex. Usually, B1 thymomas are encapsulated grayish masses. Thick fibrous septa protruding from the capsule can be observed, as well as cystic spaces or small hemorrhagic and necrotic areas. Microscopically, the neoplastic epithelial cells are scant, small, with very little atypia and submerged by non-neoplastic thymocytes. The tumor cells are oval with pale round nuclei and small nucleoli, although some cells may be large and occasionally have conspicuous nucleoli. B1 thymomas are usually organized in a lobular structure even if sheets architectures can be sometime appreciated. Either thick or thin fibrous bands separate lobules of various sizes. Perivascular spaces are not as frequent as in other B thymomas. Pale areas of medullary differentiation are always present, composed of more loosely packed thymocytes; Hassall's corpuscles are less frequent than in medulla of normal thymus[24].

Type B2 thymomas are characterized by large polygonal epithelial tumor cells arranged in a loose network containing numerous immature T lymphocytes. Grossly, B2 thymomas can be encapsulated, circumscribed or invasive of the surrounding tissues and organs. When cut, the surface presents tan-colored nodules separated by white fibrous septa and can be soft or firm. Cysts, hemorrhages and fibrosis can be appreciated. Microscopically, the large polygonal tumor cells present large nuclei with an open chromatin pattern with prominent central nucleoli. Commonly, B2 thymomas are organized in large lobules with delicate septa, resembling the normal architecture of thymic cortex. The tumor epithelial cells form palisades around perivascular spaces and along septa, large sheets of tumor cells occasionally can be observed. Medullary islands are missing or infrequent and Hassall's corpuscles are an exceptional finding. Tumor cells are usually outnumbered by non-neoplastic immature lymphocytes[24].

B3 thymomas are composed from medium size round or polygonal epithelial tumor cells with slight atypia; these cells are mixed with a minor component of intraepithelial thymocytes. Commonly, B3 thymomas are not encapsulated and present an infiltrative border with extension to the mediastinal fat or the surrounding organs. The cut surface appears firm and lobulated in grey and white nodules by fibrous septa. Soft yellow or red foci, cyst formation or hard calcification are common both in large and small tumors. Usually, neoplastic cells are polygonal with round or elongated nuclei often folded or grooved. Commonly, B3 cell nuclei are smaller and with less prominent nucleoli than in B2 thymomas. In a minority of cases, more atypical, enlarged and hypercromatic nuclei are observed. Other rare variants present either polygonal cells with nuclei similar to B2 thymomas or partial clear cell changes. Focal or extensive structure of spindle cells can be observed. B3 thymomas with anaplasia are a small group of tumor showing an high degree of atypia but conserving the organoid structure of thymomas. Tumor cells form lobules that are separated by thick fibrous and hyalinized septa. Tumor cells grow in palisades around perivascular spaces and along septa resulting in the formation of tumor cell sheets with a vaguely solid or epidermoid appearance[24].

AB thymomas are composed of a lymphocytes-poor type A and a more lymphocyte-rich type B component. Usually, AB thymomas are encapsulated. The cut surface shows a lobular structure divided, by fibrous septa, in tan colored nodules of variable sizes. All the histological features of type A thymomas are represented in the A component. Conversely, the B component is peculiar and differs from B1, B2 or B3 thymomas; it is characterized by small polygonal tumor cells with small round, oval or spindle nuclei showing disperse chromatin and small nucleoli. The A and B

components either form discrete separate nodules or intermix together. The growth pattern consists of nodular and diffuse areas[24].

The 2004 WHO classification depicts separate additional categories: the micronodular thymoma with lymphoid stroma, the metaplastic thymoma and a group of rare thymomas. Micronodular thymoma is characterized by cystic tumor areas of variable size and by multiple discrete or confluent nodules of epithelial cells, separated by lymphocytic stroma that might contain follicles with germinal center. Tumor epithelial cells of microcystic thymoma are slender or pulp spindle with bland looking oval nuclei and small nucleoli. Metaplastic thymomas do not present a lobulated growth pattern and are characterized by a biphasic architecture comprising epithelial islands intertwining with boundless of spindle cells. The tumor cells are polygonal, ovaloid or plump spindle, with oval vesicular nuclei, small distinct nucleoli and an amount of lightly eosinophilic cytoplasm. Rare thymomas are defined: microscopic thymoma, sclerosing thymoma and lipofibroadenoma of the thymus, a neoplasm that occasionally occurs adjacent to a conventional type B1 thymomas. Microscopic thymoma depicts the multifocal proliferation (<1mm in diameter) that can occur in the thymus of myasthenia gravis patients without a macroscopically evident tumor. The sclerosing thymoma exhibits the features of a conventional thymoma in terms of epithelial cell morphology and thymocytes content, but with an exuberant collagen rich stroma[24].

Table 1.4: Thymoma histotypes

Type A
Type AB
Type B1
Type B2
Type B3
Micronodular thymoma
Metaplastic thymoma
Rare thymomas
Microscopic thymoma
Sclerosing thymoma
Lipofibroadenoma of the thymus

Thymic carcinomas regroup all non-organotypic malignant epithelial neoplasms other than germ cell tumors. Carcinomas are named according to their differentiation and are listed in table 1.5.

Table 1.5: Thymic carcinoma histotypes

Squamous cell carcinoma
Basaloid carcinoma
Mucoepidermoid carcinoma
Lymphoepithelioma-like carcinoma
Sarcomatoid carcinoma
Clear cell carcinoma
Papillary adenocarcinoma
Non-papillary adenocarcinoma
Carcinoma with t(15;19) translocation
Undifferentiated carcinoma of the thymus
Thymic neuroendocrine tumors
Well differentiated neuroendocrine carcinomas
Typical carcinoid
Atypical carcinoid
Poorly differentiated neuroendocrine carcinomas
Non-small cell neuroendocrine carcinoma
Small cell neuroendocrine carcinoma

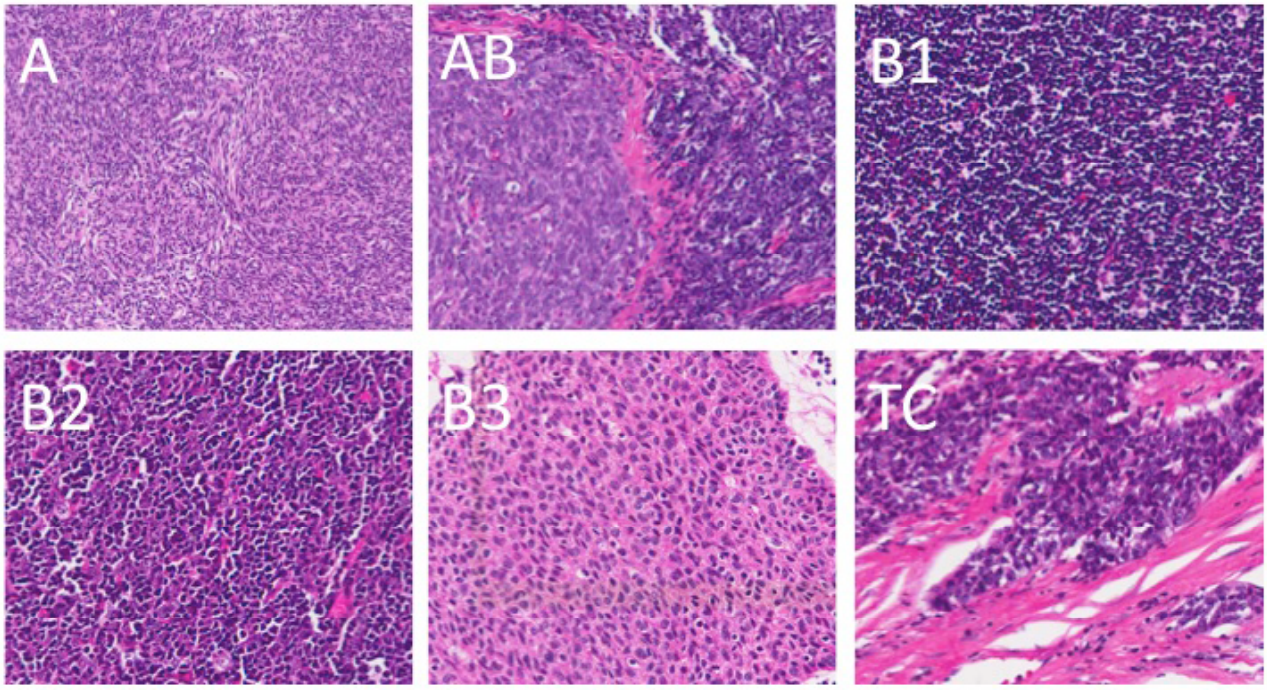

Figure 1.4: microscopy appearance of thymic epithelial tumors according to their histotype. Images were captured at 20x magnifications.

Squamous cell carcinoma of the thymus is a tumor of the epithelial cells of the thymus resembling the features of those squamous cell carcinomas originating in organs other than thymus. Squamous cell carcinomas at the diagnosis usually infiltrate the surrounding organs and tissues. At the cut surface, lobulation and fibrous septa are not evident, whereas foci of necrosis and hemorrhage are common features. Tumor cells are large polygonal with or without evidence of keratinization and presenting vesicular or hyperchromatic nuclei. Cells are arranged in nests and cords divided by fibrohyaline-stroma[24].

Basaloid carcinoma is composed by compact lobules of tumor cells with peripheral palisading and a basophilic staining pattern due to a high nuclear-

cytoplasmatic ratio. Basaloid carcinoma frequently originates in micronodular thymic cysts. Generally, basaloid carcinomas are well-circumscribed, grey masses surrounded by a thin fibrous capsule with focal hemorrhage and cystic formations. Microscopically, the cells are small, columnar, round or spindle with hyperchromatic round nuclei, scant cytoplasm and indistinct borders[24].

Mucoepidermoid carcinoma is a rare variety of thymic carcinomas characterized by the presences of squamous cells and cells producing mucous. The cut surface of these tumors looks nodular with fibrous bands and mucinous appearance[24].

Lymphoepithelioma-like carcinoma is characterized by a sincitial growth of undifferentiated carcinoma cells accompanied by lymphoplasmacytic infiltration. It may or may not be associated with EBV infection. Macroscopically, the tumor is solid with yellow/white areas of necrosis. The tumor cells present large vesicular nuclei with open chromatin and show indistinct plasma membrane. Lymphocytes are admixed with the carcinoma cells, that growth in nests or anastomosing cords[24].

Sarcomatoid carcinoma resembles soft tissue sarcoma morphology and, usually, is constituted by a sarcomatoid and a carcinoma component. The carcinomatous component comprises clusters and sheets of poorly differentiated epithelial cells with nuclear prominent atypia and occasional squamous differentiation. Spindle tumor cells with pleomorphic nuclei characterize the sarcomatoid component, these cells show distinct nucleoli and frequent mitotic figures organized in fascicules and storiform arrays[24].

Clear cell carcinoma is a rare variety composed from polyhedral tumor cells with optically clear cytoplasm with slight cellular pleomorphism and nuclear atypia. Tumor cut surface shows solid or cystic regions without any evidence of hemorrhage

or necrosis. Tumor cells grow in nests, lobules or sheets surrounded by a dense fibrous stroma that confers a lobular architecture[24].

Papillary adenocarcinoma is rare and characterized by a prominent papillary pattern of growth. Tumor cells have eosinophilic clear cytoplasm and round ovaloid nuclei with condensed chromatin and few small prominent nucleoli. Few cells are positive for mucine stating. Tumor cells grow in tubulopapillary structure of uniform cuboid to columnar cells, mainly lying in a monolayer but occasionally showing a glomeruloid arrangement. Non-papillary adenocarcinoma differentiation of thymic carcinoma is more extremely rare with only three cases described in literature[24].

Carcinoma with t(15;19) translocation is a rare carcinoma of unknown histogenesis arising in the mediastinum and other midline organs of young people. Undifferentiated cells, vigorously mitotic, grow in sheets that form syncytia with inter epithelial lymphocytes[24].

Undifferentiated thymic carcinomas are characterized by a solid growth of undifferentiated cells. The diagnosis is one of exclusion with other primary sites[24].

Thymic neuroendocrine carcinomas are predominantly or exclusively composed of neuroendocrine cells and have to be distinguished by those thymic carcinomas that may contain scattered groups of neuroendocrine cells. The neuroendocrine differentiation of epithelial tumor cells can be demonstrated by immunohistochemistry when positive for chromogranin, synaptophysin NSE and CD56. These tumors are sub-classified in well-differentiated neuroendocrine carcinomas: typical and atypical carcinoid and poorly differentiated neuroendocrine carcinomas: small cell and large cells neuroendocrine carcinomas. Grossly, they are frequently invasive at the diagnosis and on the cut section are firm, grey-white or tan

with a gritty consistency. Typical carcinoids are devoid of necrotic area and exhibit a low mitotic rate (<2 mitosis in $2mm^2$); conversely to the more common atypical carcinoids that display either necrosis or 2-10 mitosis in $2mm^2$. Large cells neuroendocrine carcinomas present more than 10 mitoses in $2mm^2$; whereas, small cell neuroendocrine carcinomas are characterized by small size round, oval or spindle cells with very scant cytoplasm and high mitotic activity[24].

Finally, the 2004 WHO classification introduces the combined TETs, with at least two distinct areas each corresponding to one of the histological thymoma and thymic carcinoma types. The description and the frequency of these combined tumors underlines the morphological heterogeneity that TETs can display. Moreover, this can partially explain the limited reproducibility of histological classification and the difficulty to predict prognosis upon morphological appearance[24].

Clinical relevance of WHO classification

Difference between thymomas and thymic carcinomas is relevant for the clinical practice mainly because thymic carcinoma exhibits a more aggressive behavior and is infrequently paraneoplastic syndromes.

B2 and AB are the most common thymomas, whereas, A and B1 are less represented (Table 4). Myasthenia gravis (MG) and red pure cell aplasia have been reported in all kind of thymomas, even if, with a different frequency of association. Paraneoplastic hypogammaglobulinemia and Good syndrome were described in B tumors. For all histotypes, symptoms at the diagnosis can be either related to paraneoplastic syndromes or consequent to the presence of a mediastinal mass[24]. In type A, AB and B1 the diagnosis is frequently incidental, being the patients asymptomatic. Usually, B2 and B3 tumors manifest themselves with local symptoms such as chest pain, cough or dyspnea up to vena cava syndrome as they tend to be invasive due to their more malignant behavior. At the diagnosis, A and AB thymomas are usually circumscribed at the stage I or II (Table 1.6) and show a favorable outcome with survival reported up to 100% at 10-year[24] (Table 1.7). B1 thymomas present limited malignant behavior; more than 90% of tumors are resectable and local recurrences or late metastases occur in less than 10%[24]. Consequently, B1 thymoma 10-year survival is about 90%[24]. Conversely, B2 and B3 thymomas are more malignant tumors with reported 10-year survival between 100-50% and 70-50%, respectively[24]. 3% of B2 and 7% of B3 thymomas are metastatic at the diagnosis. 5-15% of B2 and 17-47% of B3 are not resectable at presentation. After surgery, B2 and B3 thymomas present local recurrence in 5-9% and 15-17% and metastasize in 11% and 20% of cases, respectively. Such data support a prognostic segregation of low

malignant grade tumors (A, AB and B1) and intermediate grade malignant neoplasms[24] (B2 and B3; Figure 1.5).

Micronodular thymomas are 1-5% of TETs that occur at a mean age of 58 years and are rarely associated with paraneoplastic syndromes (<5%). Micronodular thymoma outcome is usually favorable due to stage I diagnosed in more than 90% of patients. Only few cases of metaplastic thymomas have been described, none of them associated with paraneoplastic syndromes. Metaplastic thymoma diagnoses were incidental with 75% of the tumor stage I[24].

Thymic carcinomas are 10-20% of TETs; they are frankly aggressive neoplasms with a 10-year survival <50%. At the diagnosis, most tumors are stage III and IV[24]. Rare paraneoplastic polymiosites but not MG have been described in thymic carcinomas. The most frequent thymic carcinomas are those with squamous cell differentiation; 90% in Asian and 30% in western series. Undifferentiated carcinoma is the second most common and it is characterized by a more severe prognosis[24]. Basaloid carcinomas are rare with few cases described; they show a remarkable tendency to originate in multilocular thymic cysts and are characterized by a less malignant behavior[24]. The remaining subtypes of thymic carcinoma are considerably rare and their description is mainly based on case reports. Out of these tumors lymphoepithelioma-like and clear cell carcinomas present a remarkable aggressive behavior. Only 6 cases of carcinomas with the translocation t(15;19) have been described for which a thymic origin has been postulated[24]. These belong to a group of neoplasom named midline tumor, characterized by a remarkably aggressive behavior, a young age of insurgence and the fusion of NUT gene with BRD4 in 2/3 of cases and with BRD3 or with unknown partners in the reaming[24].

Neuroendocrine thymic carcinomas are 2-5% of TETs; most of them are atypical carcinoid. Rare small cell neuroendocrine carcinoma and exceptionally rare typical carcinoid and large cell neuroendocrine carcinoma have been described[24]. Outcome is more favorable for atypic carcinoid 84% and 75% at 5 and 10-year survival, respectively[24]. 30-50% of small cell neuroendocrine carcinomas are diagnosed in stage IV. Small cell neuroendocrine carcinomas present a severe prognosis with 5 and 10-year survival of 50 and 30%, respectivelly[24]. Symptoms at the presentation can be related to the mediastinal mass or to the correlated endocrine syndromes. The most frequently observed endocrine syndromes are ACTH induced Cushing, present in 17-30% of adults and >50% of children, acromegaly, hypercalcemia/hypophosphatemia whereas carcinoid syndrome is rare (<1%). 25% of thymic neuroendocrine carcinomas present a MEN1 syndrome and 8% of patients affected by MEN1 syndrome present a neuroendocrine thymic carcinoma[24].

Table 1.6: WHO histotypes and stage at the diagnosis

Histotype	Stage				Survival
	I	II	III	IV	10-year
A	80%	17%	3%		100%
AB	71.70%	21.60%	5.60%	1.10%	80-100%
B1		53-58%	24-27%		90%
B2	10-48%	13-53%	19-49%	8.90%	50-100%
B3	4.20%	15-38%	38-66%	6-26%	50-70%

Table 1.7 Histotypes' characteristics			
Histotype	Prevalence	Mean age	Myasthenia gravis
A	4-19%	61	24%
AB	15-43%	55	14%
B1	6-17%	41-47	18-56%
B2	18-42%	47-50	30-82%
B3	7-25%	45-50	30-77%

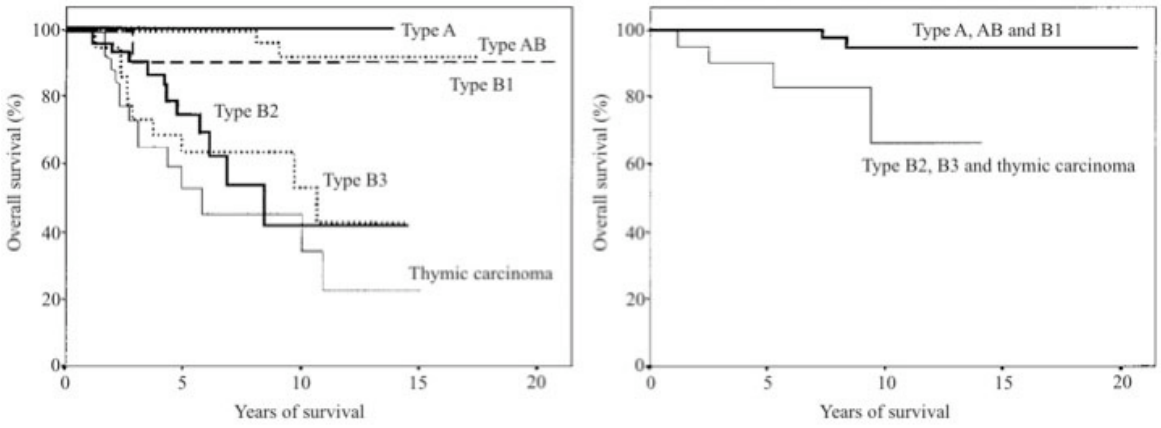

Figure 1.5: modified from Chen *et al.*[31] (A) Overall survival reported for each histological subtype. Type B2-3 and C thymomas have a significantly (P=0.001) increased risk of death. (B) Overall survival of stage I and II tumors (n 102). There were two deaths among patients with Type A, AB, and B1 thymomas (n 78), but four deaths in patients with Type B2, B3, and C thymomas (n 24). The difference is statistically significant (P =0.003)

Reproducibility of WHO classification

The 2004 WHO, as well as previous classifications, presents disputed issues regarding reproducibility and its prognostic value. The inter observer agreement has been evaluated using the material described in the chapter 3.5 and is currently under consideration for publication but do not represent a result of this dissertation. Briefly, a series of 132 TETs has been reviewed by 3 independent pathologists at 3 different institutions Humanitas Cancer Center (Rozzano-Milan, Italy), Seoul National University Bundang Hospital, Seongnam-si (Gyeonggi, Republic of Korea) and National Institute of Health (Bethesda, MD) and compared to the original diagnosis (CLAS1). The aims of this comparison were to evaluate the reproducibility of the WHO schema and determine if reproducibility can affect its prognostic value. The original histological diagnosis reported after surgery, paraffin blocks and slides, as well as clinical history were available in 129 cases. For this analysis combined thymomas were re-classified according to the more aggressive histotype (for example B2-B3, were considered B3 thymomas).

Table 1.8 summarizes histotype frequencies according to the 4 observers. The global agreement was moderated; taking into consideration all the WHO histotypes and all the pathologists at the same time: Fleiss' kappa coefficient 0.53. To compare agreement between different pathologists, Cohen's Kappa coefficient was calculated for each comparison pair (Table 1.9). The best agreement was observed between CLAS2 and CLAS1 (K coefficient: 0.84). A substantial agreement was also observed between CLAS3 and CLAS2 (K coefficient: 0.70) and CLAS3 and CLAS1 (K coefficient: 0.64). A moderate strength of agreement was observed between CLAS4 and each of the other three observers, with a Kappa correlation coefficient ranging from 0.52 to 0.53. In 63/129 (48.8%) cases there was a complete agreement among

different observers. In 43/129 (33.3%) cases three out of four pathological diagnoses were identical; in 15/129 (11.6%) cases the diagnoses were identical by pair; in 8/129 (6.2%) cases three different pathological diagnoses were reported; complete disagreement (four different diagnoses) was never observed. More frequently (9/23, 39%) the discordant diagnosis interested B thymomas, especially the discrimination of B1 and B2 (6/9). In 6/23 (26%) cases, the diagnostic discrepancy involved type AB thymomas versus B thymomas. In 7/23 (30%) cases, inconsistency regards fairly different histological subtypes: 4 cases of thymic carcinoma vs. type B3; 2 cases type B3 vs. type A; and in one case thymic carcinoma vs. type A.

The interpretations of 2 different pathologists (CLASS1 and CLASS4) were able to predict prognosis in univariate analysis of time to progression (TTP; CLAS1 p=0.001; CLAS4 p<0.001) and disease relate survival (DRS; CLAS1 p=0.039; CLAS4 p=0.027).

Previous reports have evaluated the reproducibility of WHO classification and have described an high agreement strength between pathologists interpretation (Kappa coefficient 0.9-0.87[31,32], respectively). Chen *et al.*[31] have reported inter-observer agreement between pathologists from different institutions after a training introduction from Dr. Muller-Hermelink; whereas in Riekel et al. evaluation included pathologists from the same background. Our results are in line with these reports when referred to pathologists of similar backgrounds: CLAS1 and CLAS2 were evaluated within the Humanitas Cancer Center and showed a high agreement K=0.84). Conversely, among pathologists of different backgrounds, the reproducibility was only substantial or moderate. Similarly, the evaluation of 95 TETs from 17 pathologists from UK and the Netherlands demonstrated a moderate agreement (K=0.45)[33].

These data denote the importance of a proper training for an acceptable reproducibility of the WHO classification. The most challenging diagnoses appear to be those discriminating between B1, B2 and AB thymomas in most of the reports. Consequently, more clear and defined criteria needs to be established for these histotypes. The discrimination of B2 from B1 and AB tumors is relevant for clinical practice because of their more severe prognoses; consequently, the prognostic value of WHO were, in our series, subject to variation according to pathologist interpretations.

Suster and Moran[30] proposed an exemplified classification in order to increase reproducibility and better predict prognosis. Table 1.3 summarized this classification. However, the WHO classification better highlights the morphological differences between TETs and, even if it seems to be of limited immediate clinical interest, it is remarkably important for research purpose. Thus, we are going to demonstrate that different WHO histotypes present different genomic background and may necessitate different targeted therapeutic approaches in the results section.

Table 1.8: WHO histotypes according to classification of 4 different pathologists

	A	AB	B1	B2	B3	TC
CLAS1	16.4%	21.1%	17.2%	15.6%	21.1%	8.6%
CLAS2	11.6%	20.2%	19.4%	13.9%	25.6%	9.3%
CLAS3	12.7%	19.8%	17.5%	15.9%	19.0%	15.1%
CLAS4	17.6%	19.2%	3.2%	33.6%	18.4%	8.0%

CLAS: Pathologist's classification

Table 1.9: Kappa correlation coefficient between each pathologist pair

	CLAS1	CLAS2	CLAS3	CLAS4
CLAS1		0.84 (0.77-0.91)	0.64 (0.55-0.74)	0.52 (0.41-0.62)
CLAS2			0.70 (0.61-0.79)	0.52 (0.41-0.62)
CLAS3				0.53 (0.43-0.63)

CLAS = pathologist's classification; 95%CI was reported with each coefficient in parenthesis. The agreement's strength of reputed: low: <0.41; moderate: ≥0.41<0.61; substantial: ≥0.61<0.81; high: ≥0.81.

1.7 Treatment of thymic epithelial tumors

Surgery is the mainstream of treatment for TETs and completeness of resection is the goal of the therapy, being the most relevant prognostic factor[24]. Neoadjuvant chemotherapy can improve the rate of radical resection in stage III patients who are not eligible for a complete resection[34]. If a radical resection is not achieved by surgical treatment, postoperative radiotherapy can reduce tumor recurrences. Although, the efficacy of adjuvant radiotherapy in radically resected patients is still controversial, many clinicians adopt such treatment. In patients experiencing tumor relapse, salvage surgery is often practicable but depends on the site and the number of lesions. Metastatic or not operable patients are treated by systemic chemotherapy with a palliative intent.

Surgery

A complete resection is usually practicable in stage I (100%) TETs and it is sufficient to be curative in the vast majority of patients. Conversely, the resectability rate conspicuously varies among reports in infiltrating thymomas: 43-100% for stage II, 0-89% for stage III and 0-78% for stage IV[35]. However, the reported survival is more favorable than that observed for other thoracic tumors (Table 1.10). The 15-year overall survival is 78% for stage I, 73% for stage II, 30% for stage III and 8% for stage IV[36]. The completeness of resection can not be achieved in all stage III and IV patients despite a carefully selection and a proper diagnostic workup. Relapse rate and disease free survival measure the effectiveness of surgical treatments and are summarized in Table 1.10 and Figure 1.6. Five years is the average time to recurrence, although relapses have been described up to 32 years later[36]. Stage I patients tend to recur later (mean 10 years) compared to infiltrative stages (mean time

to relapse 3 year)[36]. Among all recurrences the large majority are local (average 81%), whereas distant metastases occur in 9%. 10% of patients presented concomitantly with both local and distant relapses[36].

Table 1.10: Overall Survival of Patients With Thymic Tumors

			% 5-year Survival				% 10-year Survival			
	n	% R0	I	II	III	IV	I	II	III	IV
Kondo and Monden[28]	924	92	100	98	89	71	100	98	78	47
Regnard *et al.*[36]	307	85	89	87	68	66	80	78	47	30
Maggi *et al.*[37]	241	88	89	71	72	59	87	60	64	40
Verley and Hollmann[38]	200		85	60			80	42		
Nakahara *et al.*[39]	141	80	100	92	88	47	100	84	77	47
Wilkins *et al.*[40]	136	68	84	66	63	40	75	50	44	40
Blumberg *et al.*[41]	118	73	95	70	50	100	86	54	26	
Quintanilla-Martinez *et al.*[42]	116	94	100	100	70	70	100	100	60	
Pan *et al.*[43]	112	80	94	85	63	41	87	69	58	22
Elert *et al.*[44]	102		83	90	46					
Average		83	92	82	68	62	88	71	57	38

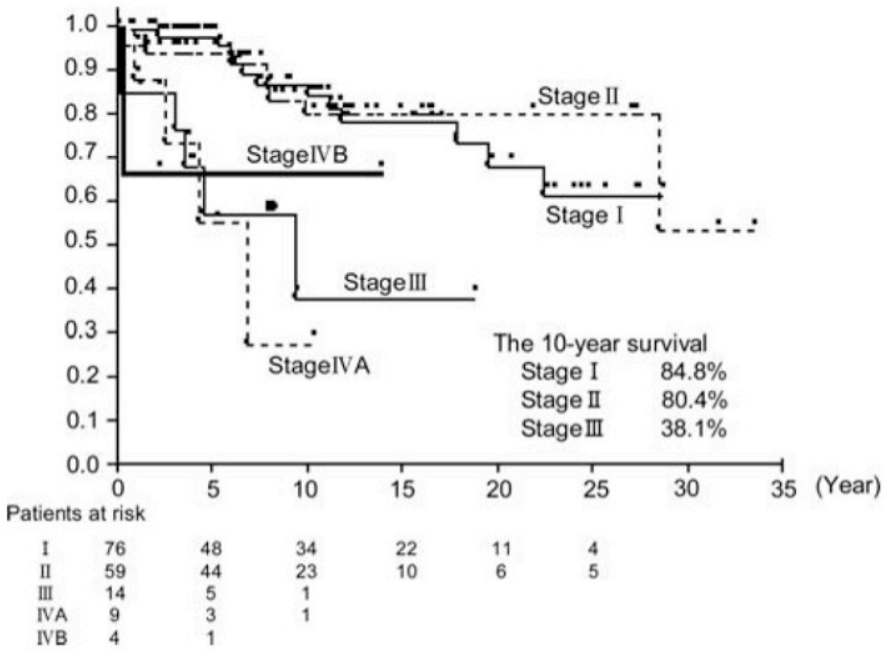

Figure 1.6: Modified from Sakamoto M, *et al.*[45]. Disease free survival reported according to Masaoka's stage after extended thymectomy. Survival for Stage III disease was significantly worse than that for Stage I (P = 0.0002) and Stage II (P = 0.002).

Subtotal resection

Despite neoadjuvant treatments, a complete resection can not always be planned. The advantages offered by a subtotal resection are still debated because of the inconsistence of reports and trial methodology limitations. Authors have reported either no advantage for debulking surgery[46,47] or an increase of 5-year overall survival about 30%[28,37,39,48]. However, a subtotal surgical resection is indicated for the relief of symptoms. Adjuvant treatments should be considered after an incomplete resection.

Salvage surgery

In those cases experiencing a relapse, the re-intervention is a valuable option because many recurrences are local and some of them can be radically removed by a salvage surgery. Increase of 5-year survival has been reported up to 40-50% beside some negative studies[41,49-53]. Although, in those cases presenting unique or few local metastases re-intervention is a valid option but it is not the standard treatment for those cases experiencing extensive pleural dissemination. The chance of resection of pleural implants is sometime feasible but has still to be considered an experimental procedure[54].

Radiotherapy

Radiotherapy has been proposed with different intent in TETs either in neoadjuvant, adjuvant, in incompletely resected tumors or as exclusive treatment. Currently, the preferred modality of administration is conformal radiotherapy with respiratory gating. The use of intensity modulated radiotherapy (IMRT) is encouraged and consists of a real-time modeling of the contours and the amount of photons delivered within the radiation beam, using a programmed movement of the blades of the collimator[55]. The dose to be delivered varies according to the purpose of the treatment. It has been suggested to deliver to the thymic area a total dose of 45 Gy in a neoadjuvant setting, 45 to 55 Gy in an adjuvant setting, and 60 to 66 Gy as an exclusive treatment using a standard fractionation scheme (one 1.8- to 2-Gy fraction per day)[55]. Patients with TETs localized in the mediastinum, but not eligible for surgery, can be considered for radiotherapy that is rarely exclusive being more frequently associated with chemotherapy[56]. Neoadjuvant radiotherapy aim is to increase the rate of complete resections. Neoadjuvant radiotherapy can induce response in up to 80% of treated patients, thus, a radical resection can be achieved in 50-75% of cases[56]. Despite its promising results, the role of neoadjuvant radiation therapy remains controversial being currently preferred neoadjuvant chemotherapy followed by adjuvant radiotherapy[55]. Because thymomas are considered radiosensitive tumors and they tend to relapse locally, postoperative radiotherapy has been evaluated in several studies.

Postoperative radiotherapy.

Postoperative radiotherapy has been offered for adjuvant treatment of completely resected tumor or to consolidate results of subtotal resections. Because stage I thymomas relapse in about 2% of cases, adjuvant radiotherapy is not recommended for these patients. The role of adjuvant radiotherapy in R0 resected stage II and III thymomas remains controversial because the rarity of the disease, reports are heterogeneous, include a limited number of cases and are not prospectively designed. In 2009, a meta-analysis evaluated the role of adjuvant radiation therapy in stage II and III radically resected tumors that were included in retrospective studies reporting a control arm of exclusively surgically treated patients. Among stage II, 273 patients received a radical surgical resection and 197 a radical resection plus adjuvant radiotherapy; relapse were observed in 11 and 8% of cases, respectively (Figure 1.7A). Out of the radically resected stage III patients, 53 received adjuvant radiotherapy and 69 did not; the relapse rate was 32% and 26%, respectively (Figure 1.7B). Significant overall survival improvement was not achieved for the patients who received adjuvant radiotherapy neither a different pattern of relapse, in favor of distant metastases, was described for treated patients[57]. The analysis of SEER database has revealed a survival advantage for those stage II and III patients who underwent adjuvant radiation therapy. However, in the same evaluation, patients completely resected did not benefit by the adjuvant radiotherapy[57]. Moreover, mediastinal radiation frequently can present both short and long term adverse events including, but are not limited to, secondary malignancies, pulmonary fibrosis, esophageal strictures, coronary disease, cardiac valvular fibrosis, and pericarditis[57]. Although, the role of adjuvant radiotherapy in stage II and III is discouraged by data,

it is currently recommended by many clinicians for stage III patients with more aggressive histotypes (B2, B3 and TC)[56].

Postoperative radiotherapy is systematically recommended after a subtotal resection[58], including the boost in areas of macroscopic invasion. Radiotherapy has consistently decreased recurrence rates from 60-80% to 21-45% after a R1 or R2 resection[28,53,59-64]. Frequently, after local recurrence salvage surgery is practicable but for those cases not operable or resectable radiation therapy could be a valuable option. Small retrospective series depicted promising response rates and 5-year survival rate of 70-80%[53].

Radiotherapy for thymic carcinoma

Peculiar considerations are appropriate for thymic carcinomas because theirs more pronunced aggressive behavior. Thymic carcinomas frequently are diagnosed when invasive and neoadjuvant chemo-radiotherapy may represent a potent approach to downstage unresectable tumors[55]. Although, the role of radiotherapy is expected to be more relevant in thymic carcinoma than in thymoma because the minor importance of the surgery, Kondo K., *et al.*[28] did not show any significant advantage for the adjuvant treatment. In the 186 thymic carcinomas underwent radical resection, 5-year survival rate was 74% after adjuvant radiotherapy and 72% after surgery alone.

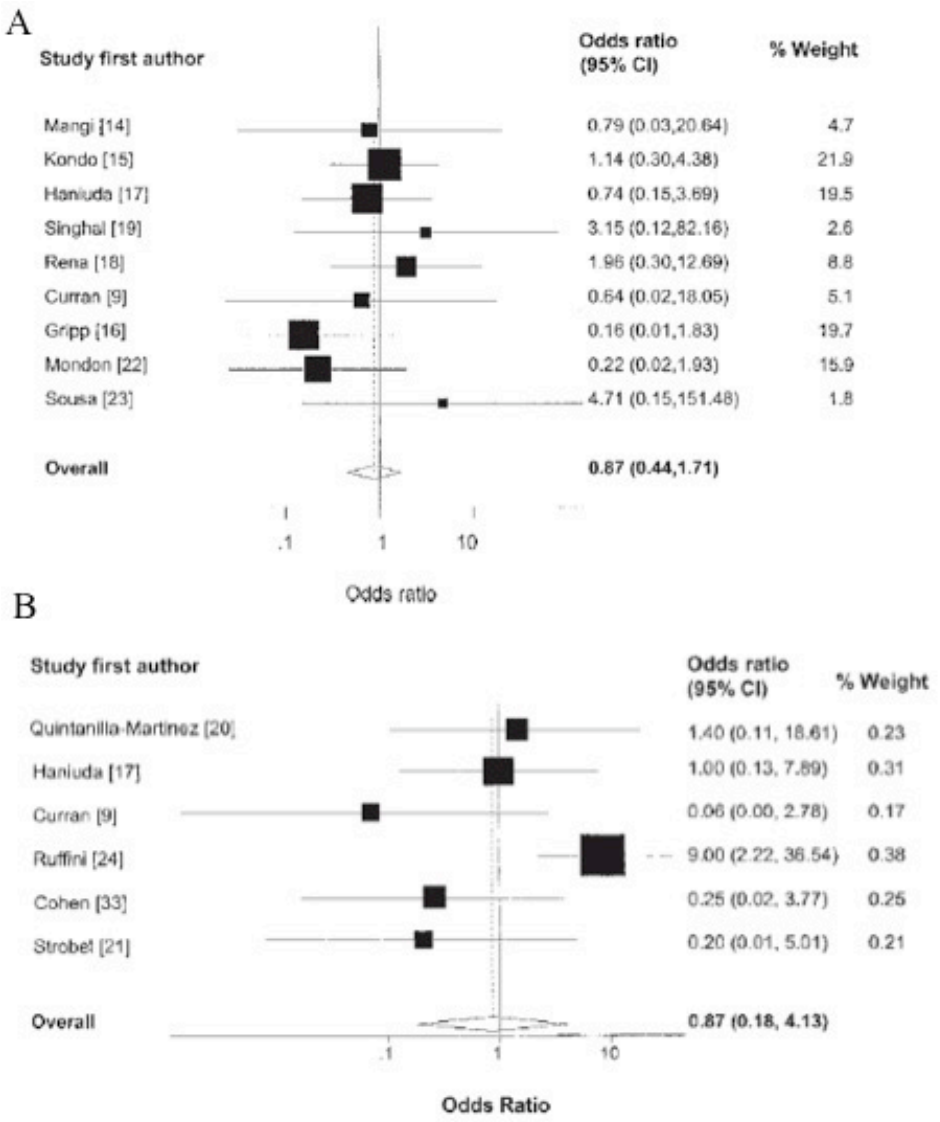

Figure 1.7: Modified from Korst RJ *et al.*[57] Forest plot generated using extracted recurrence data for patients with stage II (A) and stage III (B) TET. The squares represent the odds ratios of the individual studies, and the size of the squares reflects the calculated weight of the study in the meta-analysis. The horizontal bars running through each square represent the 95% confidence interval (CI). Studies had been weighted and the Diamond at the bottom of the plot illustrates the combined odds ratio using a fixed effects model.

Systemic therapy

Thymomas are reputed chemo-sensitive tumors. Thus, chemotherapy is indicated either with neoadjuvant or palliative intent.

Palliative chemotherapy

Chemotherapy is indeed the treatment of choice for patients with metastatic disease or with unresectable diffuse disease and recurrences. The intent of systemic treatment is to delay as much as possible tumor progression and eventually to reduce disease related symptoms. Conventional chemotherapeutic such as platinum based drugs (Cisplatin and Carboplatin), anthracyclines (Doxorubicin and Epirubicin), alkylating agents (Cyclophosphamide and Ifosfamide), vinca alkaloids, Etoposide and Pemetrexed have shown activity in TETs. Combination schedules have shown more encouraging results when adopted for the first line treatment (Table 1.11). Thus, schedules containing platinum and anthracyclines induce response rate from 50 to 92%. Since TETs, and especially thymomas, frequently present a slow rate of growth, multiple subsequent lines of chemotherapy are commonly offered to patients after disease progression. Responses to second or further chemotherapy lines are reported in up to 40% (Table 1.11). Therefore, overall survival improvement conferred by a single schedule is often difficult to understand. Although, thymomas frequently respond to chemotherapy, thymic carcinomas are much more resistant tumors. Interesting results in thymic carcinoma (response rate 30-24%) have been obtained by the combination of carboplatin and paclitaxel (Table 1.11).

Table 1.11: Chemotherapy regimes for palliative therapy of thymic epithelial tumors

References	Schedule	Line	WHO	Stage	N Pz	RR (%)	SD	Median TTP(m)	Median OS(m)
Kunitoh H[65]	Dose dense Cisplatin Doxorubicin Vincristine Etoposide G-CSF	1	T 27	IVA(22) IVB(8)	27	16PR (59%)	37%	9,5	73.2
Loehrer PJ[66]	Cisplatin Doxorubicin Cyclophosphamide	1	T 29 TC 1	III IV	30	3CR, 12PR (50%)	33%	18.4	38.4
Fornasiero A[67]	Cisplatin Doxorubicin Vincristine Cyclophosphamide	1	T 37	III (12) IV (25)	37	16CR, 18PR (92%)	5%	12	21
Grassin F[68]	Cisplatin Ifosfamide Etoposide	1	T 12 TC 4	III(8) IVA(1) IVB(7)	16	4PR (25%)	75%	13.1	nr
Loehrer PJ[69]	Cisplatin Ifosfamide Etoposide	1	T 20 TC 8	III(6) IVA(13) IVB(9)	28	9PR (32%)	61%	11.9*	31.6
Giaccone G[70]	Cisplatin Etoposide	1	T 16	III(6) IV(10)	16	5CR, 4PR (56%)	44%	39	51
Bjerrum OW[71]	Cisplatin Vincristine Lomustine Cyclophosphamide Prednisone	1		III(3) IVA(3) IVB(3)	9	1CR, 1PR (22%)	56%	Uk	Uk
Furugen M[72]	Carboplatin Paclitaxel	1	TC 16	IVA(4) IVB(9)	16	2CR, (38%)	50%	8.6	49.4
Lemma GL[73]	Carboplatin Paclitaxel	1	T 21 TC 23	III (7) IV (37)	44	3CR, 5PR 5 PR	48% 52%	19.9 6.2	nr 15
Loehrer PJ[74]	Pemetrexed	≥2	T 16 TC 11	IVA(16) IVB(11)	27	2CR, 2PR	20%	11.3	65
Bonomi PD[75]	Cisplatin	≥2	T(20)		20	2PR (10%)	40%		19
Palmieri G[76]	Capecitabine Gemcitabine	≤2	T(12) TC(3)	IVB(15)	15	3CR, 3PR (40%)	40%	11	nr

Line was 1 for naïve and ≥2 for previously treated patients. * months median duration response, T=Thymoma, TC=Thymic carcinoma; N Pz=number of patients; RR response rate, CR complete response; PR partial response, SD stable disease; TTP=time to progression in months; OS overall survival in months; Uk unknown, nr not reached.

Neoadjuvant chemotherapy

Mostly cisplatin-based regimens have been adopted for neoadjuvant down-staging of stage III and IVa TETs. The aim of neoadjuvant chemotherapy is to induce shrinkage of locally advanced tumors in order to increase the rate of complete resection. Authors have reported promising results (Table E 1.12), despite the relevant inter-trial variability. The inconsistence of the results was probably due to the different proportion of stage III and IV patients, to the presence or not of thymic carcinomas, to the aggressiveness of the surgery and to the different efficacy of chemotherapy schedules. Among the 246 patients enrolled in table E 1.12 trials 18 complete responses (CR) and 101 partial responses (PR) were observed for a response rate (PR+CR) of 48% (range 40-100%). After induction chemotherapy, 57% of tumors received a complete resection. These results appear remarkably improved compared to those reported in historical cohorts for stage III and IV patients exclusively treated by surgery[77]. Moreover, a conspicuous number of patients received a surgical resection with curative intent after neoadjuvant chemotherapy even if they initially had been considered not resectable.

Table1.12: Chemotherapy regimes for neoadjuvant therapy of thymic epithelial tumors

Reference	Yr	Schedule	Stage	N Pz	RR (%)	SD	R0	TTP 5y	TTP 10y	OS 5y	OS 10y
Kunitoh H[78]	2010	Dose Dense Cisplatin Doxorubicin Vincristine Etoposide	III 21		13PR (62%)	33%	43%	Uk	Uk	85%	Uk
Ishikawa Y[79]	2009	(CAMP) Cisplatin Doxorubicin Methylprednisolone	Iva 67		6PR (86%)	14%	29%	Uk	Uk	81%	70%
Wright CD[80]	2008	Cisplatin Etoposide Radiotherapy	III 7 IVA 3	10	4PR (40%)	60%	80%	Uk	Uk	69%	Uk
Yokoi K[81]	2007	(CAMP) Cisplatin Doxorubicin Methylprednisolone	III 4 IVA 9 IVB 4	17	1CR, 12PR (93%)	7%	12%	Uk	Uk	81%	81%
Lucchi M[82]	2006	Cisplatin Epirubicin Etoposide	III 20 IVA 10	30	2CR, 20PR (73%)	27%	77%	Uk	Uk	Uk	82%
Jacot W[83]	2005	Cisplatin Doxorubicin Cyclophosphamide	III 3 IV 5	8	6PR (75%)	13%	Uk	Uk	Uk	54%	Uk
Kim ES[83]	2004	Cisplatin Doxorubicin Cyclophosphamide Prednisone	III 11 IVA 10 IVB 1	22	3CR, 14PR (77%)	23%	76%	77%	77%	95%	80%
Berruti A[84]	1999	(ADOC) Cisplatin Doxorubicin Vincristine Cyclophosphamide	III 10 IVA 6	18	1CR 12PR (81%)	11%	50%	Uk	Uk	Uk	Uk
Shin DM[85]	1998	Cisplatin Doxorubicin Cyclophosphamide Prednisone	III 4 IVA 8	12	3CR, 8PR (92%)	8%	82%	Uk	Uk	100%	Uk
Venuta F[77]	1997	Cisplatin Epirubicin Etoposide	III 8 IVA 13	25	1CR, 9PR (40%)	Uk	80%	Uk	Uk	Uk	Uk
Rea F[86]	1993	Cisplatin Doxorubicin Vincristine Cyclophosphamide	III IVA	16	7CR 9PR (100%)	0%	31%	Uk	Uk	66%	Uk

Yr: year of publication; N Pz: number of patients; RR: response rate; CR: complete response; PR: partial response; SD: stable disease; TTP: time to progression at 5 and 10 -year; OS: overall survival at 5 and 10-year; Uk: unknown, nr: not reached.

Targeted therapy

Drugs with a designed activity against molecules responsible for the tumor growth are available for patients' treatment. These compounds have shown significant activity when appropriately administered in tumors addicted to the targeted molecules. For example the use of Imatinib in acute myeloid leukemia inhibits the product of BCR-ABL fusion genes inducing long lasting remission in the vast majority of patients[87]. Another example is the use of erlotinib and gefitinib in EGFR mutated non-small cell lung cancer able to significantly increase the patient survival[88,89]. However, the same EGFR inhibitors do not shown any or an unappreciable activities on those lung cancers without the receptor activating mutations. Similarly, many drugs have failed to show a significant effect when given outside the right subset of patients. Drugs, effective for the treatment of other neoplastic disease, have been tested in TETs after the failure of one or more chemotherapeutic regimens. Drugs targeting EGFR have been tested in TETs. In spite of the efficacy depicted in a case report[90], gefitinib induced only one partial response out of 26 tumors, whereas, none was reported for erlotinib-bevacizumab combination (Table G 1.13). Responses to cetuximab, a monoclonal antibody targeting EGFR, have been described in anecdotal case reports[91,92]. Because a case-report has described the response to Imatinib of a thymic carcinoma with c-Kit mutation[93], the drug has been tested in three small phase II trials without any evidence of efficacy (Table G 1.13). However, these trials were not selectively designed for tumors harboring the sensitizing mutations of c-KIT. As in the meanwhile, some more case-reports describing thymic carcinomas with KIT mutation sensitive to Imatinib have been described[94,95], study selectively designed for thymic carcinomas harboring KIT mutations have been advocated. Sorafenib and Sunitinib, two multikinase inhibitors,

have induced responses in case reports[96-100] and are currently evaluated in phase II trials. Because IGF1R as been shown over-expressed in thymic carcinomas and in aggressive thymomas[101] the specific monoclonal antibody Cixutumumab is under evaluation in a phase II clinical trial at NCI. The histone deacetylase inhibitor Belinostat has induced 2 partial response and 61% of disease stabilization in a phase II trial including pretreated thymoma (25 patients) and thymic carcinoma (16 patients)[102].

Because TETs, but not normal thymus or thymic hyperplasia, show indium labeled octreotide uptake, somatostatin and its analogs have been tested for therapy in combination of prednisone[103]. Among the 52 patients treated 3 experienced a complete response, 11 a partial response and 12 a disease stabilization (Table G 1.13). Finally, the use of IL-2 and SRC inhibitor did not show any efficacy[104,105].

The efficacy of biologic therapies in TETs is scant, to date. The main limitation is the lack of a robust rationale to target a specific molecule, mainly because the aberrations driving of TET growth are obscure. The aim and the results of this dissertation contribute to clarify the molecular aberration driving the tumor phenotype in thymic epithelial tumors and indicate possible new targets suitable for therapy.

Table 1.13: Targeted therapy trials for palliative treatment of thymic epithelial tumors

References	Year	Schedule	Line	WHO	N Pzs	RR(%)	SD	TTP (m)	OS (m)
Kurup A[106]	2005	Gefitinib	≥2	T(19) TC(7)	26	1PR (4%)	54%		
Bedano PM[107]	2008	Erlotinib Bevacizumab	≥2	T(11) T(7)	18	0	61%	4	
Giaccone G[108]	2009	Imatinib	≥1	T(2) TC(5)	7	0	2 0%	2	
Salter JT[109]	2008	Imatinib	≥2	TC(11)	11	0	27%	1.5	
Palmieri G[110]	2011	Imatinib	≥2	T(12)	15	0	0	3	nr
Rajan A[111]	2010	Cixutumumab	≥2	T(5)	13	0	73%		
Giaccone G[102]	2011	Belinostat	≥2	T(25) TC(16)	41	2PR (5%)	61%	5.8	19.1
Loehrer PJ[112]	2002	Octreotide Prednisone	≥1	T(31) TC(3)	36	2CR 6PR (17%)	17%		
Palmieri G[103]	2002	Somatostatin Prednisone	≥2	T(10) TC(3) NETC(3)	16	1CR 5PR (38%)	38%	14	15
Gordon MS[104]	1995	IL2	≥2	T(14)	14	0	Uk	Uk	Uk

Line: line of chemotherapy; 1 is first line metastatic disease. WHO: histotype; N Pz: number of patients; RR: response rate, CR: complete response; PR: partial response; SD: stable disease; TTP: median time to progression in months; OS: median overall survival in months; Uk: unknown, nr: not reached.

1.8 Paraneoplastic syndromes

Paraneoplastic syndromes are present in about 40% of thymomas, whereas more rarely are associated to thymic carcinomas. In thymoma paraneoplastic syndromes are often autoimmune disorders varying from systemic diseases to organ specific syndromes. Myasthenia gravis is the most frequently observed disorder in thymomas interesting about 20-30% of patients[24]. It is related to the tumor proliferation and regressions can follow tumor resection or response to radiotherapy of chemotherapy. Other frequently observed syndromes in thymomas are pure red cell aplasia and hypogammaglobulinemia[24].

The function of normal thymus is to drive thymocytes through the positive and negative selections that follow the TCR rearrangement, in order to generate functional lymphocytes (able to recognize the TCR) non reactive to self-antigens (self tolerance). Consequently many authors tend to link the neoplastic degeneration of thymic epithelial cells to the high frequency of autoimmune paraneoplastic syndromes. In order to avoid maturation of self-reactive T-lymphocytes, the epithelial cells of the thymus, especially those of the medulla, presents auto-antigens to the thymocytes. Inside the thymic epithelial cells, self-antigens are generated from the ectopic expression of tissue–specific autologous genes. Such expression is regulated by a transcription factor: the autoimmune regulator gene (AIRE)[105]. AIRE is commonly expressed in normal thymus but not in thymomas and this lack of expression may play a crucial role in the pathogenesis of autoimmune diseases by favoring the development of self-reactive T-cell clones within the thymus. Despite the suggestion that altered AIRE expression provides a fascinating link between autoimmunity and malignancy, the etiology of autoimmune disease in thymomas has

not been elucidated yet and animal models lacking AIRE genes failed to reproduce the pattern of autoimmune disorders observed in thymomas[113].

Thymic carcinomas can be associated with polymyositis, although, these autoimmune paraneoplastic syndromes are infrequent. Thymic neuroendocrine carcinomas can be associated with endocrine syndromes more commonly ACTH mediated Cushing or GH mediated acromegaly[24].

1.9 Molecular aberrations of thymic epithelial tumors

The molecular biology of TETs is poorly understood because the availability of only a few cell lines, the rarity of the disease, and the lack of specific preclinical animal models. A multistep accumulation of genetic and epigenetic aberrations in thymic epithelial cells is thought to drive the neoplastic transformation.

Cytogenetic studies have revealed chromosomal abnormalities in all histological subtypes. The recurrent abnormalities found in TETs were only t(15;19) translocation and 6p22-p25 deletion [114]. The t(15;19)(q13:p13.1) generates the fusion gene BRD4-NUT, and tumors with this translocation have been classified as a rare subtype of undifferentiated thymic carcinoma according to 2004 WHO classification. Comparative genomic hybridization studies have shown low frequency of allelic imbalance in type A thymoma[115]. B3 thymomas present frequent copy number gain of 1q and loss of 6 and 13q, whereas thymic carcinomas show frequent copy number gain of 1q, 17q and 18 and loss of 3p, 6, 16q and 17p[115]. These aberrations suggest close relatedness between B3 thymoma and thymic carcinoma[115].

The role of oncogenes and tumor suppressor genes has been studied in TETs with particular emphasis on tyrosine kinase receptors. 70% of thymomas and 53% of thymic carcinomas express the EGFR[116], which correlates with more advanced stages (III-IV) but not with WHO histotypes[95,117]. EGFR gene amplification, found in 22% of thymomas, is responsible for protein over-expression in only a subgroup of cases[118]; B3 thymomas and invasive tumors (stage II-IV) have a higher degree of amplification[118]. Only two L858R and one G863D mutations of EGFR gene have been described out of 158 cases studied[116]. Two KRAS (G12A and G12V) and one HRAS (G13V) mutations have been described in a type B2, a thymic carcinoma and a

type A thymoma, respectively. However, the frequency of RAS mutations is only 5% (3/56) of reported cases[95,117,119].

Stem cell factor receptor (KIT) expression is more frequent in thymic carcinoma (73%; 97/132) than in thymomas (2%; 10/423)[93,96,98,108,120-128]. KIT mutations have not been described in thymoma (0/67) and are infrequent in thymic carcinoma (5/59). From the observed mutations, the two V560 deletions[93,95] and the L576P substitution[127] are sensitive to imatinib[129], D820E to nilotinb, and H697Y to sorafenib[116].

. Expression of BCL2, an anti-apoptotic protein, has been evaluated in TETs. BCL2 is expressed in both type A, and the A component of type AB thymomas. Thymic carcinomas show high levels of BCL2 expression, whereas only few cases of B type thymomas express BCL2[130-140].

Transgenic mice expressing SV40 large T and small t antigen under L-pyruvate kinase promoter develop TETs[141], implicating the importance of RB and P53 during TET development. Variable expression of p53 has been reported in TETs [134-136,139,140,142-152] with p53 being more frequently expressed in invasive thymomas and thymic carcinomas. P53 expression is a poor prognostic marker in TETs[134,142,144,146] and inactivating mutations have been described with variable frequency[95,142,143,145,147,148]. In RB pathway, P16INK4 has been evaluated in TET; P16INK4, through inhibition of CDK4 and CDK6, prevents RB phosphorylation leading to G1-S block. Methylation of P16INK4 promoter has been observed in 3-13% of TETs, which correlates with p16 down-regulation only in a minority of cases[147,153]. No P16INK4 mutations have been described in TETs, but deletion of the gene locus is related to invasive phenotype in rat animal model[154].

2. Materials and Methods

2.1 Patients and tumors

Patient tumors used for these analyses were collected from four different sources:

1) Slides of FFPE tumors collected from patients enrolled in clinical trials at Medical Oncology Branch of National Cancer Institute (NCI, Bethesda, MD). Clinical data were collected prospectively during such trials. These materials were used for NUT-BRD screening.

2) Frozen tumor samples from patients treated at Medical Oncology Branch of NCI (Bethesda, MD) were collected during tumor resection and during bioptic procedure for clinical evaluation. These tumor samples were used for whole genome sequencing and transcriptome/exome sequencing.

3) Frozen samples collected during tumor resection at Pisa University Hospital (Pisa, Italy). These samples were used for transcriptome/exome sequencing.

4) Clinical data and FFPE samples were collected from a series of 132 consecutive patients who underwent surgery for TET at Humanitas Cancer Center (Milan, Italy). These samples were used for array CGH, NUT-BRD4 screening and KIT immunohistochemistry and sequencing.

Tumor diagnosis was confirmed by two independent pathologists (H.S.L. and M.R.) and histology was classified according to the 2004 WHO classification [24]. All

patients were staged according to the Masaoka staging system [155]. Completeness of resection was defined as R0 when complete, R1 when residual disease was microscopic and R2 when macroscopic [93]. These studies were conducted in agreement with the Declaration of Helsinki and were approved by the involved institutional ethical review boards (ClinicalTrials.gov ID: NCT00965627; and Pisa University Hospital Ethical Committee protocol approval No. 3141).

2.2 Construction of tissue micro array

FFPE tumor specimens were assessed for quality and adequacy of fixation and storage. A tissue microarray (TMA) block containing tissue from 132 thymoma or thymic carcinoma cases was generated. In brief, three punches of 0.36 mm^2 (0.6 mm in diameter) were taken from different intratumoral areas in each tumor sample and arranged in the recipient tissue array block. For 21 samples, peritumoral normal tissue was also available and included in the TMA. A pathologist (H.S.L.) verified the presence of tumor tissue on a hematoxylin-eosin stained TMA slide. Samples were considered adequate if tumor occupied one or more cores of three punches.

2.3 Immunohistochemistry

FFPE tissue slides and/or tissue microarrays were cut at 4 μm, deparaffinized with xylene and rehydrated in graded ethanol. Antigen retrieval was performed heating the slides at 95 ^{o}C for 20 minutes in Target Retrieval Solution (Dako, Carpinteria, CA). Endogenous peroxidase blocking solution (EnVision+ System HRP (DAB), Dako) was applied on the tissue for 10 minutes followed by incubation in

protein-free T20 (TBS) blocking buffer (Thermo Scientific, Rockford, IL) for 1 hour. Samples were then incubated with primary antibody 4^{o}C overnight in a humid chamber or for KIT 30 min at room temperature. The following reagents were used as primary antibodies: anti-NUT rabbit monoclonal antibody C52 (Cell Signaling, Danvers, MA), anti-Kit pharmDx™ Polyclonal Rabbit IgG (c-Kit pharmDx™ IHC kit, Dako) and anti-p16INK4 mouse monoclonal antibody (BD PharMingen, San Diego, CA). After 3 washes with TBST buffer, the slides were incubated for 30 min with labeled polymer-HRP as a secondary antibody and then immune reactions were visualized with 3',3'-diaminobenzidine as chromogen (EnVision+ System HRP (DAB), Dako). Slides were counterstained with hematoxylin, dehydrated, and mounted. Negative control specimens were included with related species antiserum. The following positive controls were included: normal testis for anti-NUT antibody, mouse normal pancreas for anti-KIT antibody and a xenograft of HELA cell line for p16INK4. For NUT immunohistochemistry, results were interpreted as positive if nuclear staining was present in more than 50% of cells[156]. KIT staining was graded as negative, no staining; 1+, staining <10% of tumor cells; 2+, staining ≥10% but <50% of tumor cells; or 3+, staining ≥50% of tumor cells [123,124]. Samples scored 1+ or higher were considered positive. P16INK4 results were graded according percentage of positive cells and intensity of the staining. Percentage of positive cells was ranked 0 (0-5%), 1 (6-25%), 2 (26-50%), 3 (51-75%) or 4 (76-100%). Signal intensity (1-3) was multiplied by rank of positive cells in order to get a positivity score. P16INK4, scores 0-3 were considered negative (G0), 4-6 were G1, 7-9 were G2, and 10-12 were G3.

2.4 Fluorescence in situ hybridization (FISH)

Cases positive for NUT antibody staining were processed for FISH analysis as described previously[157]. Dual-color FISH assays evaluating chromosome 19p13.1 BRD4 and 15q13 NUT break points were performed on 4-μm unstained sections from FFPE tissue blocks as previously described[157]. Probes used for the 19p13.1 BRD4 break point probes included telomeric tandem bacterial artificial chromosome (BAC) clones RP11-319o10 and RP11-681d10 (digoxigenin-labeled, FITC conjugated anti-digoxigenin-detected, green) and centromeric BAC clones RP11-207i16 and CTD-3055m5 (biotin-labeled, rhodamine-streptavidin-detected, red). BRD3 break point probes included telomeric BAC clone RP11-145e17 (digoxigenin-labeled, FITC conjugated anti-digoxigenin, green) and centromeric BAC clone RP11-2243h5 (biotin-labeled, rhodamine-streptavidin-detected, red). Probes used for the 15q13 NUT break point, flanking a 181-kb region, included telomeric BAC clones 1H8 and 64o3B (digoxigenin-labeled, FITC anti-digoxigenin-detected, green) and centromeric clones 1084a12 and 3d4 (biotin-labeled, rhodamine-streptavidin-detected, red).

2.5 DNA extraction and from FFPE material

Only samples containing >80% cancer cells were selected, as assessed by Hematoxylin & Eosin (H&E) stained slides. DNA was extracted using DNeasy kit (Qiagen, Inc., Valencia, CA) according to Genomic DNA ULS labeling kit protocol (Agilent Technologies, Inc., Palo Alto, CA).

2.6 Conventional Sanger sequencing for c-KIT

Samples were sequenced as previously described[158]. Briefly, primers were designed to cover all the coding sequences of KIT gene. Sequences were amplified by PCR using AmpliTaq Gold® PCR Master Mix (Applied Biosystems, Foster City, CA). Primers tagged with M13 sequence were used to sequence exon 1 through exon 20. A total of 40 cycles were performed using Veriti® 96-Well Thermal Cycler (Applied Biosystems) at 94 ◦C for 30 s, 60 ◦C for 45 s and 72 ◦C for 45 s. PCR products underwent ExoSAP-IT® (USB, Cleveland, OH) purification. The purified product was directly sequenced using a BigDye terminator v 3.1 cycle sequencing kit (Applied Biosystems) and 3730xl DNA Analyzer (Applied Biosystems). Data was analyzed using Mutation Surveyor v 3.23 (SoftGenetics LLC, State College, PA).

2.7 Whole genome sequencing

15 µg of patient's tumor and normal DNA were used for whole genome sequencing performed using complete genomics platform (Mountain View, CA). The methods have been previously described in detail elsewhere[159]. Briefly, genomic DNA was fragmented and cut by type IIS restriction enzymes; thereafter, directional adaptors were inserted to form DNA circles. These DNA circles were replicated by synchronized synthesis using Phi29 polymerase (RCR) 8 in order to obtain hundreds of tandem copies of genomic fragment sampling the entire genome and named DNA nanoballs (DNBs). A silicon substrate with grid-patterned arrays was used to adsorbed the DNBs. Using high-accuracy cPAL chemistry, sequencing machines were able to read up to 10 bases adjacent to each of the eight anchor insertion sites, resulting in a total of 31- to 35-base mate-paired reads (62 to 70 bases per DNB).

Data analysis was performed with dedicate in house made pipeline from Complete Genomics. The resulting mate-paired reads with a particular gapped structure were aligned to USCS hg19 reference genome in a two-stage process. First, each end of the reads was aligned independently. Then, the location of the mate pair was computed on the basis of the first aligned within the appropriate distance. For the mutation calling identification, when a candidate variation was identified, mapped reads were assembled into a best-fit, diploid sequence with a custom software suite employing both Bayesian and de Bruijn graph techniques.

2.8 Confirmation of candidate mutations

Tier 1 mutations identified using whole genome sequencing and the candidate junction sequences were confirmed using conventional Sanger sequencing. For SNV and INDELS, primers were designed across the mutation site using CLC genomics workbench 4 and tested for hairpin and heteroduplex formation using Oliogo 6.8 Carbon (MBI, Cascade, CO). All designed primers were tagged with M13 sequence. PCR Supermix High Fidelity (Invitrogen) was used for PCR amplification that was automated on Veriti® 96-Well Thermal Cycler (Applied Biosystems) according to the following steps: step 1: 94◦C for 10 minute; step 2: 35 cycles of 94 ◦C for 30 s, 60 ◦C for 45 s and 72 ◦C for 45 s; step 3: 72◦C for 7 minutes. PCR products underwent ExoSAP-IT® (USB, Cleveland, OH) purification. The purified product was directly sequenced using a BigDye terminator v 3.1 cycle sequencing kit (Applied Biosystems) and 3730xl DNA Analyzer (Applied Biosystems). Sequences from tumor and normal DNA were evaluated for the presence of the candidate mutation using Macvector (MacVector, Cary, NC).

2.9 DNA and RNA extraction from frozen material

Frozen tumors were imbedded in optimal cutting temperature (OCT) and 8 μm slides of the tumors were cut. The slides were colored by Hematoxilin and Eosin and a pathologist confirmed the presence of >80% of tumor cells. The selected tumor region was macrodissected using a razor blade. Tumor DNA and RNA were extracted from the same frozen specimen using All prep RNA/DNA kit (Qiagen, Valencia CA), according to vendor instructions. Patients' blood was collected in 5ml EDTA tubes and stored at -80C. Normal DNA was extracted from whole peripheral blood using QIAamp DNA blood maxi kit (Qiagen) according to the company protocol.

2.10 Array comparative genomic hybridization

The labeling procedure was conducted using Genomic DNA ULS labeling kit (Agilent), according to the vendor instructions. Twenty samples were hybridized on Human Genome CGH Array 105A (Agilent) and the remaining on SurePrint G3 Human CGH Array 180K (Agilent). The arrays were scanned on a laser-based microarray scanner (Agilent), and the data were extracted and normalized using Feature Extraction 10.5 (Agilent). Row data were centered to the mode using R script. CN profile was inferred using Rank Segmentation algorithm in Nexus 6 (Biodiscovery Inc., El Segundo, CA, USA). CN call thresholds were defined: high gain +0.7, gain +0.3, loss -0.3 and big loss -0.7. Sex chromosomes were excluded from the analysis. Genomic Identification of Significant Targets in Cancer (GISTIC) algorithm was applied using the online version on Gene Pattern server 2.0 [160].

2.11 Exome sequencing

Exome capture was performed using SureSelect Human All Exon 50Mb Kit (Agilent) according vendor instructions. Briefly, libraries from 1μg of genomic DNA were generated and then fragmented. DNA fragments were hybridized with biotinylated complementary exon sequences. Using magnetic beads exon sequences were enriched, then denatured and purified. Captured sequences were fragmented using TruSeq DNA Sample Preparation Kit (Illumina) and each fragmented ligated with adaptor primers according to vendor instructions. These products were denatured and amplified on a Cluster Station (Illumina). One line of Genome Analyzer II (GA-II, Illumina, San Diego, CA) flow-cell was used to generate 72 pair end sequences.

2.12 Exome sequencing data analysis

GA-II output files were converted in FASTQ format and assessed for quality of the sequencing results using FASTQC software (http://www.bioinformatics.bbsrc.ac.uk/projects/fastqc/). An average of 32.5e6 72 pair end sequences were obtained from each GA-II line. Sequences were mapped to human genome 19 (USCS) using Novoalign (Novocraft, Petaling Jaya, Selangor, Malaysia) and deduplicated by Picard (Illumina). Quality recalibration was performed using Genome Analysis Tool Kit (GATK, Broad Institute, Cambridge, MA). Single nucleotide variation (SNV) and INDELs were called in tumor and normal DNA using GATK; for INDELs, re-alignment was performed to reduce false positive mutations. Somatic mutations were identified using GATK by subtraction of the SNV and INDEL calls from normal DNA to tumor DNA. Somatic mutations were annotated using Annovar (http://www.openbioinformatics.org/annovar)

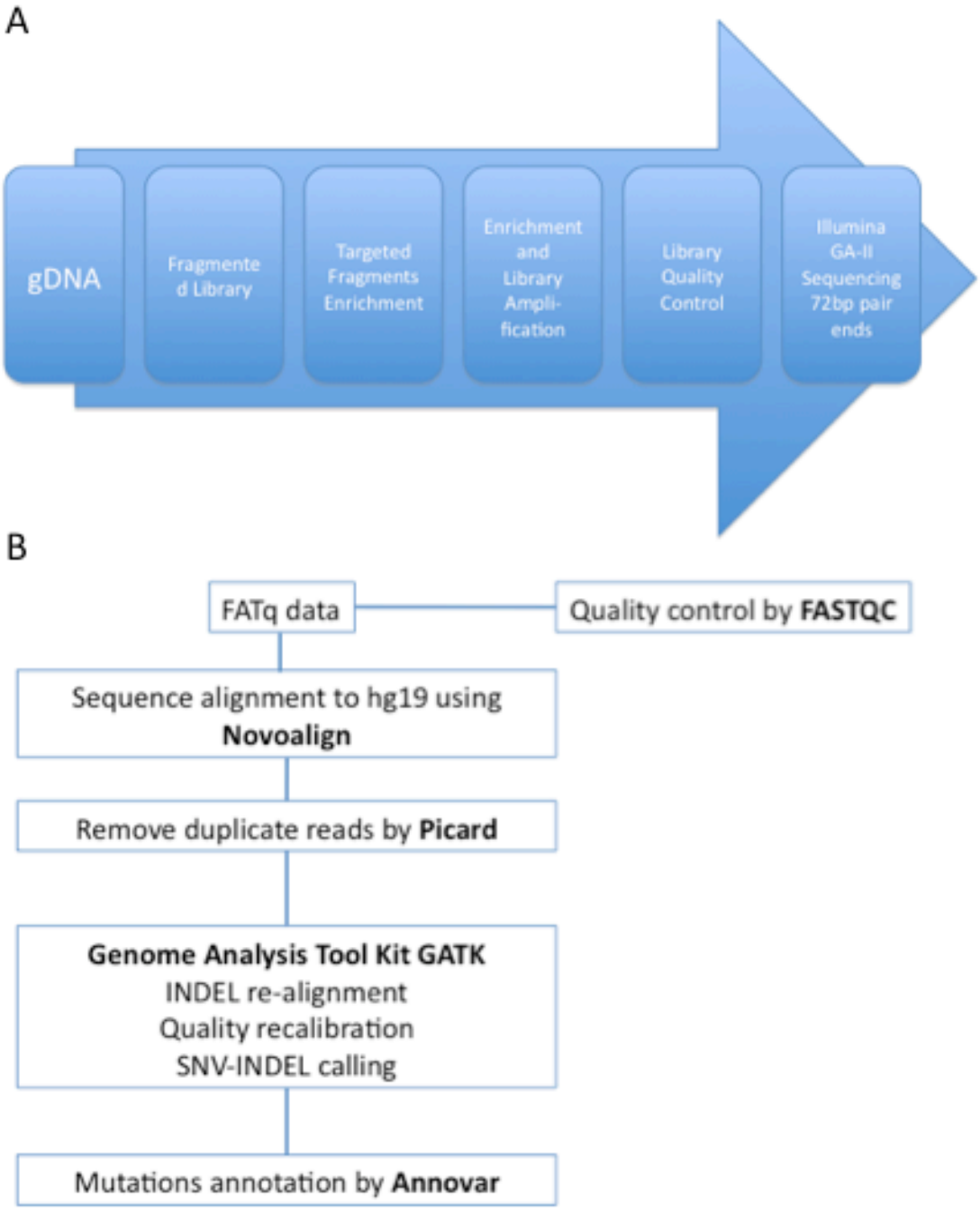

Figure 2.1: Exome sequencing procedure. (A) Workflow from genomic DNA to sequencing machine. (B) Data analysis pipeline.

2.13 RNA quality evaluation

RNA quality was tested using RNA 6000 nano kit (Agilent) and run on Agilent 2100 Bioanalyzer: only samples with a RNA integrity number (RIN) >8 were included for transcriptome sequencing. In the Agilent chip a gel electrophoresis of the total RNA was performed; the ratio between the florescent peaks corresponding to S18 and S28 rRNA bands was adopted to compute the RNA integrity through a mathematical algorithm that return a numeric value: being 1 the most degraded profile and 10 the most intact.

2.14 Transcriptome sequencing

Libraries were constructed from 3μg total RNA using TruSeq RNA Sample Preparation Kits v2 (Illumina) according to vendor instructions. Briefly, enrichment for mRNA was carried out using polyA-tail capture. The RNA was chemically fragmented and converted into single strand cDNA using random hexamer priming. Then, for each fragment the complementary sequence was generated. An adenosine base was added to each end of the fragments and adaptors were ligated with a T base overhang on 3'end. These products were denatured and amplified on a Cluster Station (Illumina). One line of Hiseq 2000 (Illumina) or GA-II (Illumina) flow-cell was used to generate 101 pair end sequences for 2 and 13 samples, respectively.

2.15 Transcriptome sequencing data analysis

GA-II and Hiseq2000 output files were converted in FASTQ format and assessed for quality of the sequencing results using FASTQC. Sequences were mapped to human genome 19 (USCS) using GSNAP (GVST, http://www.gvst.co.uk/index.htm) and deduplicated by Picard (Illumina). Gene expression was estimated using Cufflink (University of California Barkley). Bam files were visualized using IGV (Broad Institute) to supervised confirmation of the identified mutations.

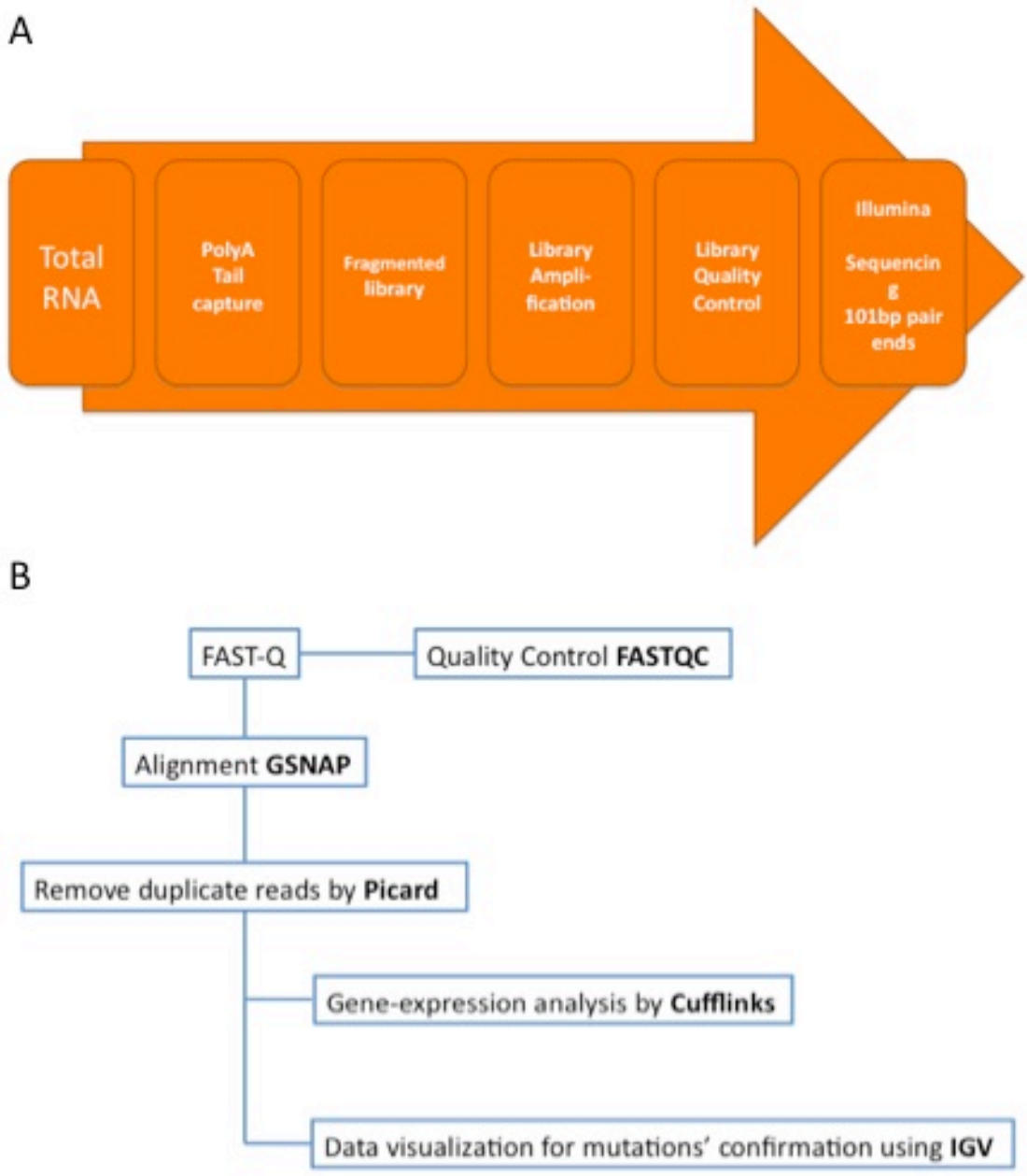

Figure 2.2: Transcriptome sequencing procedure. (A) Workflow from total RNA to sequencing machine. (B) Data analysis pipeline.

2.16 Cell lines and cell line work

Thymic carcinoma T1889 and B1 thymoma T1682 cell lines were kindly provided by Dr. Marco Breinig [161]. TY-82 thymic carcinoma cell line was purchased from Japan Health Science Foundation (Tokyo) whereas HELA, HEK-293, H157, NCI-H146 and NCI-H82 were from ATCC. All cell lines were cultured in RPMI 1640 containing 200 mM L-Glutamine (Invitrogen, Grand Island, NY), 50 U/mL penicillin, 50 U/mL streptomycin (Invitrogen) and 10% heat-inactivated calf serum (Invitrogen) and grown in a 37 ^{o}C incubator with humidified 5% CO_2 atmosphere. Protein extraction, western blot and immunoprecipitation were performed as previously described [162,163]. Anti-BCL2 antibody was purchased from DAKO (Carpinteria, CA), anti-MCL1 and anti-p16INK from BD PharMingen and all the remaining antibodies were from Cell Signaling. Activity of ABT263 and Gx15-070 (Selleck Chemicals, Houston, TX) was tested using a proliferation assay (CellTiter 96 Non-Radioactive Cell Proliferation Assay, Promega), a vitality assay (CytoTox 96 Non-Radioactive Cytotoxicity Assay, Promega) and a membrane permeability assay using TOPRO3 (Invitrogen) staining for flow cytometry (FACScalibur and Cellquest, BD), because Gx15-070 generates auto-fluorescence that interferes with propidium iodide and 7AAD. Caspase-3 activity was calculated using a colorimetric Caspase-3 Activity Detection Kit (Millipore, Billerica, MA).

2.17 ShRNA, siRNA and transfection experiments

BECN1 shRNAs (1: V2HS_23694 and 2: V2HS_241693) and RIPK1 shRNAs (1: V2HS_17422 and 2: V2HS_241668) were purchased from Open-Biosystems (Thermo Scientific, Huntsville, AL) and subcloned into pMSCV-PM-pheS retroviral expression vector (Clontech, Mountain View, CA). High titer shRNA viral particles were produced in HEK-293T packaging cells and infection of TET cell lines was carried out in the presence of 4 μg/ml polybrene (Millipore, Billerica, MA).

Anti-apoptotic BCL2 family member ON-TARGETplus siRNA pools and ON-TARGETplus Set of 4 siRNAs were purchased from Dharmacon (Lafayette, CO). Transfection was performed using PepMute siRNA Transfection reagent (SignaGen Laboratories, Rockville, MD) and 10 nM of each siRNA.

2.18 Statistical analysis

Clinical and biological characteristics were compared using the Fisher's exact test, $\chi 2$ test, Student's T-test or One-way ANOVA with Dunn test for post-hoc comparisons, when appropriate. P-values were considered significant at the < 0.05 level (two tailed). Survival curves were generated using the Kaplan-Meier method and differences tested by Log-Rank test. Multivariate analyses were performed using Cox proportional hazard model. Disease-Related Survival (DRS) was calculated from the date of surgery to the date of death; patients dead for causes other than tumor progression were censored. Time to progression (TTP) was calculated from date of surgery to relapse or progression; patients dead without any evidence of tumor progression were censored. For patients who do not undergo surgical resection TTP and DRS were calculated from tumor biopsy. All tests were performed using the SPSS version 17 (SPSS, Inc., Chicago, IL). Synergism of drug combination was calculated using CalcuSyn 2.1 (Biosoft, Cambridge, UK).

3. Results

3. Results

3.1 Overview and strategy of the performed experiments

Genomic aberrations have been studied in TETs by karyotype analysis and conventional CGH studies on a limited number of cases. Karyotype studies revealed an heterogeneous status of aberrations. Among these abnormalities only the translocation t(15;19) and deletion of part of the short arm of chromosome 6 were recurrent. Deletion of chromosome 6p was confirmed by conventional CGH in thymomas and thymic carcinomas[115]. Chromosome 6p deletion is going to be evaluated by array CGH in the following sections. KIT mutations have been described in thymic carcinoma and have been related with response to tyrosine kinase inhibitors in case-report studies[164].

NUT-BRD4 translocation and the presence of KIT mutations were evaluated because, even if they have been reported in TETs, their incidence was not know. Given the low frequency observed for both mutations, a genome wide screening approach was chose to identify those genomic aberrations driving the TET growth. We applied whole genome sequencing to a B3 thymoma cases and whole exome sequencing to 3 thymomas and 2 thymic carcinomas. In these tumors, among a relevant heterogeneity of the feature observed, the copy number (CN) aberrations identified by CGH pointed CDKN2A and BCL2 as relevant genes for TET biology. Being the CN aberrations the most common way of deregulation of these genes, CGH analysis was extended to a larger series of tumors and the function of these genes was studied in TET cell line models.

3.2 NUT-BRD4 fusion gene in thymic epithelial tumors

The translocation t(15;19) originate a fusion proteins BRD4-NUT, resulting in the ectopic expression of NUT protein. NUT rearrangement has been found in ~10% of midline carcinomas[165] in children and young adults. Approximately two thirds of NUT rearrangements on 15q14 in NUT midline carcinomas (NMCs) occur in a balanced translocation with BRD4 (bromodomain containing protein 4) gene on 19p13.1 creating BRD4-NUT fusion protein, and the remaining one third (NUT fusion variants) either with BRD3 on 9q34 or with some unknown partners. NUT, a testis specific protein, is highly expressed in normal testis and does not contain any known functional domain[166], whereas BRD4 is ubiquitously expressed in somatic cells[166,167]. The fusion proteins retain both bromodomains of BRDs and almost the entirety of the NUT coding sequence[168]. BRD3 and BRD4 belong to a specific family of transcription/chromatin regulators known as BET. They are double bromodomain-containing proteins, which preferentially associate with acetylated histones[169,170]. BRD4 binds mitotic chromosomes and may stimulate RNA polymerase II dependent transcriptional elongation post mitotic silencing[171-173], whereas the function of BRD3 is less characterized. Although the molecular mechanisms of BRD-NUT fusions in NMC development is unclear, knockdown of the fusion proteins in NMC cells induces cell cycle arrest and squamous differentiation[168]. There are only a few sporadic reports of t(15:19) translocations in thymic carcinomas[174-177].

Clinical Features of studied thymic epithelial tumors

The 2004 WHO tumor classification system denotes this subgroup of thymic carcinomas as t(15;19) carcinomas. A total of 148 TETs were included in this study, 111 of which were thymomas and 37 thymic carcinomas. The median age of our TET cases was 55 years ranging from 20 to 87 years. The median survival rate of the TETs was 192 months (95% CI 65.3 – 318.7). Twenty-one of the 37 thymic carcinoma patients (57%) were diagnosed as stage IV carcinomas according to the Masaoka staging system, 16 of which were in stage IVB with metastatic tumors (Table 3.1). The median age of our thymic carcinoma series (n = 37) was 54 years ranging from 28 to 72 years. The median survival was 48 months (95% CI 30.6-65.4; Figure 3.1A). Histologically, most of the thymic carcinomas were squamous (n=17) or undifferentiated subtypes (n = 8). In agreement with previous reports [178,179], immunohistochemistry analysis of p63, one of the two p53 homologues, revealed that p63 was positive in most (17/19) of the thymic carcinomas studied (Table 3.1).

Table 3.1. Case characteristics of thymic carcinomas

Case	Age	Sex	Stage*	Histology	P63 IHC	Survival (months)
1	56	F	IVB	Squamous cell	+	14
2	33	M	IVB	Non-papillary adenocarcinoma (mucinous)	+	41
3	65	M	I	Squamous cell	+	146+
4	49	M	IIA	Mucoepidermoid	ND	67+
5	53	M	IVB	Squamous cell	+	75+
6	32	M	IIIB	Neuroendocrine	-	103+
7	64	M	IIIA	Squamous cell	+	50+
8	72	F	I	Squamous cell	+	125+
9	64	M	IIIA	Squamous cell	ND	28+
10	55	M	IIB	Neuroendocrine	ND	71
11	67	M	IIIA	Non-papillary adenocarcinoma (mucinous)	+	59+
12	61	M	IVB	Undifferentiated	+	1
13	61	M	IVA	Undifferentiated	+	32+
14	63	M	UK	Squamous cell	ND	48
15	69	M	IVA	Squamous cell	ND	51
16	64	F	IVA	Undifferentiated	ND	34
17	39	M	IVB	Basaloid	-	9
18	59	M	IVB	Undifferentiated	ND	23
19	28	M	IVA	Neuroendocrine (large cell)	ND	56
20	59	M	UK	Undifferentiated	+	12
21	53	F	IVB	Undifferentiated	+	20
22	37	M	IVB	Squamous cell	ND	20+
23	38	F	IIIB	Squamous cell	ND	19
24	32	F	IVB	Squamous cell	+	8
25	52	F	IVB	Squamous cell	+	18
26	61	M	IIIB	Undifferentiated	ND	20
27	54	M	IVB	Squamous cell	+	36
28	47	M	IVB	Neuroendocrine (large cell)	ND	61
29	46	M	IVB	Squamous cell	+	30
30	40	F	IVB	Undifferentiated	ND	29
31	30	M	IVB	Basaloid	+	26
32	55	M	IVB	Neuroendocrine	ND	40
33	44	F	IIIA	Squamous cell	+	49
34	31	F	I	Neuroendocrine (atypical carcinoid)	ND	55
35	45	M	IVA	Squamous cell	ND	61
36	67	F	IIIB	Lymphoepithelioma-like	ND	62
37	61	F	IIIA	Squamous cell	ND	12+

*Stages were determined according to the Masaoka staging system; IHC, immunohistochemistry; UK, unknown; ND, not done.

The overall survival of thymic carcinomas (10-year OS rate 20%) was poorer than thymomas (10-year rate 72%; p<0.001) in our series including 37 thymic carcinomas and 111 thymomas. It is interesting to note that among the 37 thymic carcinomas analyzed in this study overall survivals were significantly poorer in undifferentiated (median survival: 23 months; 95%CI 14.3 – 31.8) than differentiated carcinomas (median survival: 55 months; 95%CI 44.5 – 65.5; Figure 3.1B) and in metastatic (median survival: 26 months; 95%CI 15.2 – 36.8) than non-metastatic tumors (median survival: 56 months; 95%CI 45.3 – 66.7; Figure 3.1B and C; LogRank p = 0.001 and p = 0.002 respectively).

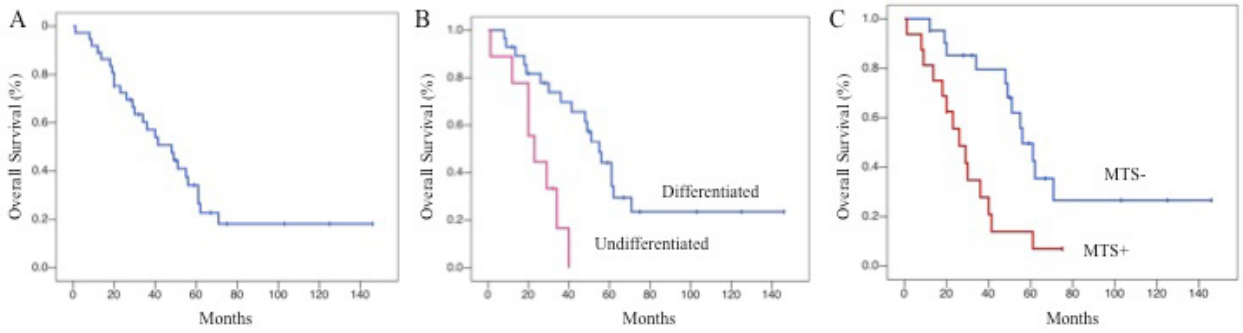

Figure 3.1: Survival analysis of thymic carcinoma patients. (A) Overall survival curve of thymic carcinoma patients (median: 48 months). (B) Overall survival by differentiation status. (C) Overall survival by metastasis status. Survival curves were generated using the Kaplan-Meier method. MTS: metastasis.

NUT rearrangement in thymic carcinomas is uncommon

Clinicopathological features of previously reported thymic carcinomas with t(15;19) resulting in constitutive BRD4-NUT fusion gene expression are summarized in Table 3.2. They appear to be undifferentiated and very aggressive tumors with remarkably poor survival. Taking advantage from the specificity and accuracy of NUT antibody in identifying NMCs[156], NUT expression was screened in 148 TETs by immunohistochemistry. All of the 148 cases were found negative for NUT expression with the exception of one thymic carcinoma that exhibited speckled nuclear NUT staining (Figure 3.2 A), a typical NUT staining pattern found in other NMCs[156]. To determine if the NUT-positive tumor carries BRD3- or BRD4-NUT rearrangement, we performed FISH analysis using split-apart NUT, BRD3 and BRD4 probes respectively as described previously[157]. The tumor showed an evident NUT but not BRD3 or BRD4 rearrangement (Figure 3.2 B), indicating this is a variant NUT rearrangement tumor. The patient was a 30 year-old male diagnosed with stage IVB thymic basaloid carcinoma according to the Masaoka staging system and WHO histology classification. Computed tomography of the chest and abdomen showed bulky mediastinal mass suggestive of thymic origin, and enlarged left supraclavicular and para-aortic lymph nodes (Figure 3.2 C).

Table 3.2: Features of reported thymic/mediastinal carcinomas with t(15:19)

Features \ Cases	1	2	3	4	5
Age/Sex	22/F	11/F	5/M	15/M	30/M
Tumor Origin	anterior mediastinum, thymus	intrathorax, thymus, lung, nonseminomtous germ cell, mediastinal teratocarcinoma	disseminated anterior mediastinum, thymus	anterior mediastinum, thymus	mediastinum, thymus
Pleural effusion	yes	-	yes	yes	-
Metastasis	lung, bone,	bone	bone	bone	lymphnode, bone
Survival (mo)	3.5	4.5	1.5	6	26
Pathology*	undiff. ca	undiff. ca	undiff. ca	poorly diff. squamous ca	basaloid ca
EMA	+	?	+	+	
CK	+/-†	+	+	+	+
CEA	-	+	+	+	
CD5					+
NUT	+	+	not done	+	+
NUT partner	*BRD4*[166]	*BRD4*[168]	*BRD4*‖	*BRD4*[168]	UK
Karyotype¶	t(15;19)(q15;p13)	t(15;19)(p12;q13)	t(15:19)(q12;p13.1)	t(11;15;19)(p15;q12;p13.3)	ND
References	Kubonishi et al[174,175]	Kees et al[180]	Lee et al[177]	Toresky et al[176]	present

*Cases were also diagnosed as: malignant lymphoma, diffused large cell type (case 1); lung undifferentiated carcinoma (case 2); mediastinal carcinoma of mucoepidermoid type (case 3).
†Keratinizing foci within tumors were positive, but the cell line (Ty82) derived from the tumor was negative for cytokeratin.
‖ Presumed *BRD4-NUT* rearrangement based on cytogenetics.
¶Karyotypes were quoted from the original publications.
EMA, epithelial membrane antigen; CK, cytokeratin; CEA, carcinoembryonic antigen; CD5, cluster of differentiation 5; undiff, undifferentiated; diff, differentiated; ca, carcinoma; ND, not done; UK, unknown.

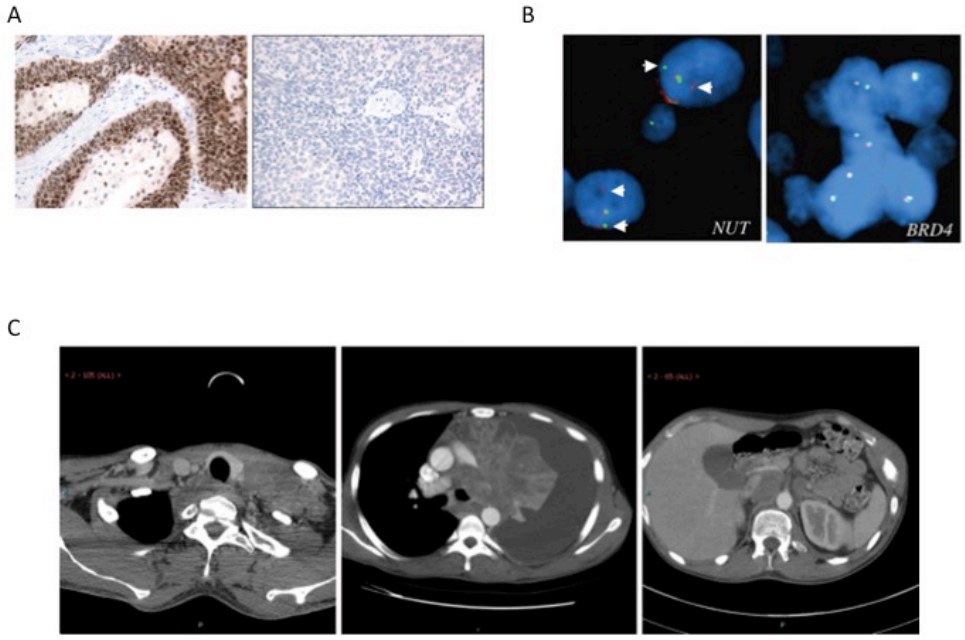

Figure 3.2: NUT in thymic carcinoma. (A) NUT immunohistochemistry. NUT-positive (left) and –negative (right) thymic carcinomas. Note that in the thymic carcinoma with NUT rearrangement the speckled NUT expression was mainly restricted in the undifferentiated cell nuclei and much less NUT was in the differentiated squamous cell area. (B) NUT gene rearrangement in a thymic carcinoma. Dual-color split-apart FISH was performed with probes flanking 5' centromeric (red) and 3' telomeric (green) of NUT, BRD3, and BRD4 respectively as described previously. Arrows (left panel) marked split-apart NUT signals (red/green signals were split apart due to NUT rearrangement), whereas no BRD3 (not shown) or BRD4 split-apart signal (right panel) was detected in the same tumor sample indicating that the NUT rearrangement did not involve BRD3/4. (C) Computed tomography of the thymic carcinoma patient with NUT rearrangement: left supraclavicular lymph nodes, primary bulky mediastinal mass, and para-aortic lymph nodes.

Core needle biopsy of the primary mediastinal mass at the time of diagnosis showed a squamous cell carcinoma with a basaloid component (Figure 3.3 A). Immunostaining was positive for p63, CD5, cytokeratin AE1/AE3 (Figure 3.3B-D) and c-KIT (data not shown), confirming the diagnosis of thymic carcinoma. Metastases were found in lymph nodes and bones at the time of diagnosis. Later in the disease course, fine needle aspirate of a supraclavicular lymph node showed atypical cells in a necrotic background suspicious for a metastasis from a thymic carcinoma. The patient underwent thoracocentesis to relieve a left-sided pleural effusion following which he received two cycles of multi-drug chemotherapy consisting of cisplatin, doxorubicin and cyclophosphamide. A restaging CT scan did not show any significant changes. Two and a half months later the patient presented to the National Cancer Institute where he first underwent thoracocentesis. The patient was enrolled onto the ongoing clinical trial with anti-insulin-like growth factor-1 receptor antibody, cixutumumab and received three cycles of treatment every three weeks following which he was taken off treatment due to disease progression. He then received a course of palliative radiation therapy to control painful tumor deposits in the left chest cavity and supraclavicular fossa, following which he opted to receive supportive care only. The patient passed away 2 months later, which was 26 months after initial onset of symptoms. Given that the NUT immunostaining is highly accurate in NUT rearrangement prediction and NMC identification [156], and that only one of the 148 TETs was found positive for NUT expression and rearrangement, we conclude that NUT rearrangement is rare in TETs.

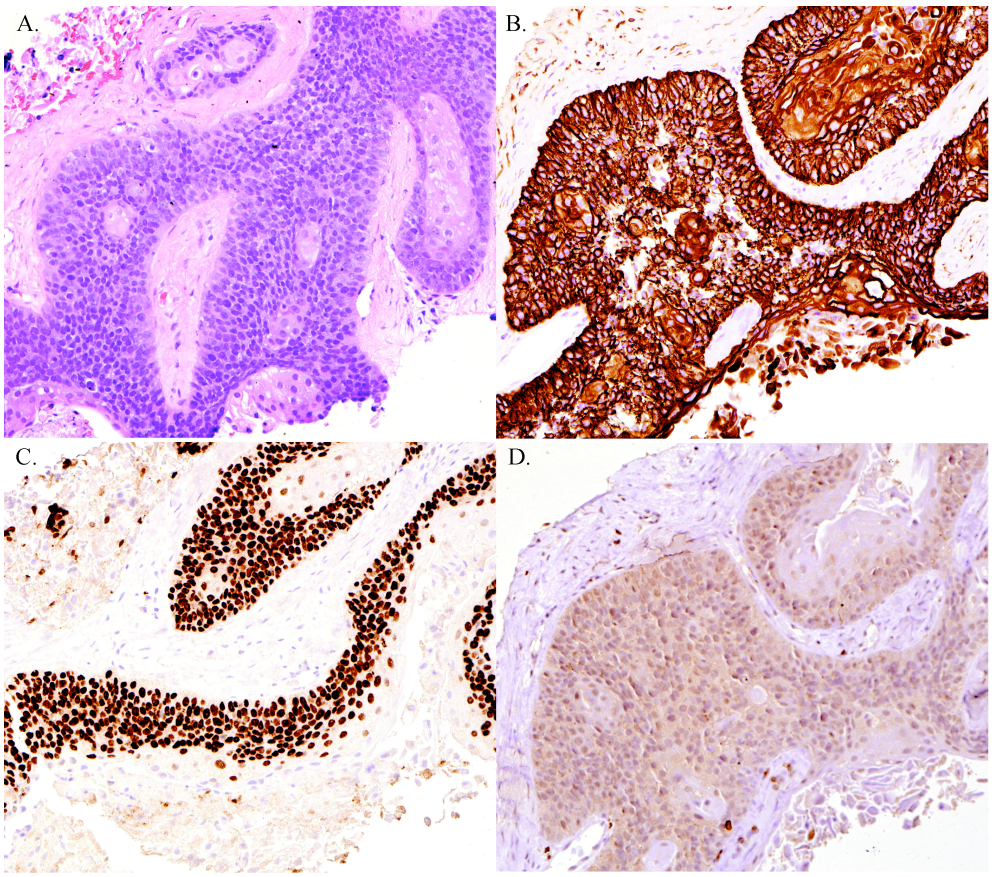

Figure 3.3: Thymic carcinoma with a basaloid component. (A) Mediastinal tumor cells with NUT rearrangement infiltrate in the fibrous stroma. Keratinization is seen (H&E; x20). (B) Keratin immunohistochemistry. Tumor cells are strongly and uniformly positive (AE1/AE3 immunostain; x20). (C) p63 shows positive staining mainly in the basaloid component (p63; x20). (D) Epithelial cells also express CD5 (CD5; x20).

3.2 Expression and mutational status of c-Kit in thymic epithelial tumors

c-Kit is a type III cytokine receptor expressed on the membrane of hematopoietic stem cells, mast cells, melanocytes and interstitial cells of Cajal[181]. Stem cell factor binds to c-Kit inducing homodimerization of the receptor and phosphorylation of downstream intracellular molecules, regulating cell proliferation, differentiation, adhesion and apoptosis[182]. Overexpression of c-KIT is observed in a spectrum of human malignancies, primarily gastrointestinal stromal tumors (GISTs), chronic myeloid leukemias (CML), mast cell neoplasms, melanomas, and seminomas[183]. c-KIT mutations have also been described in several of these tumors[182,184]. In GISTs the most common mutations affect exons 11, 9, 13 and 17[182] and the site of mutation has prognostic implications in this disease. Responsiveness of GISTs to treatment with the kinase inhibitor Imatinib depends largely on the exonic location of the c-KIT mutation[182]. Higher objective response rates to Imatinib have been described in patients with mutations of exon 11 compared to patients with wild type receptor or with mutations of exon 9[185]. Mutations have been also described in patients with negative c-Kit expression, evaluated by immunohistochemistry (IHC)[186]. Durable responses to Imatinib treatment were observed in GIST patients with a very low expression of c-Kit but showing exon 11 mutations[187].

In TETs, c-Kit expression has been reported between 50-88% in thymic carcinoma but it is rare in thymomas (0-5%)[95,121,123,124,183]. In thymic carcinoma, few mutations have been described in the literature[93,95,124,183]. Recently Girard et al. reported 2 c-Kit mutations, out of 7 thymic carcinomas analyzed[95]. One of these mutations (H697Y) was novel and found in exon 14, a region not sequenced in previous studies.

In 2004 Stroebel et al. reported a case of poorly differentiated epidermoid carcinoma with V560del Kit mutation who responded to Imatinib[93]. In 2009 another case of thymic carcinoma with D820E Kit mutation was reported that responded to Sorafenib, a multitarget tyrosine kinase inhibitor, with weak c-Kit inhibitory activity[96,188]. Three small phase II trials have been performed with Imatinib in patients with no evidence of response[108-110].

c-KIT immunohistochemistry

A tissue microarray was generated from a series of 132 thyic epitelial tumors. This series is going to be described in detail in chapter 3.5. Examples of positive and negative samples are shown in Figure 3.4 A and B. There was no c-Kit expression by IHC in the normal residual thymus of 9 evaluable patients. Ten (8.3%) out of 120 evaluable samples were positive for c-KIT expression. This included 6 of 13 thymic carcinomas tested (46%) and 4 of 107 thymomas (4%). c-KIT expression was significantly more frequent in thymic carcinomas than in thymomas (Fisher exact test $p<0.0001$). There was no difference in c-KIT expression between early vs advanced stages, level of completeness of resection, and primary vs relapsed tumors. However, c-KIT positive samples were all found in primary (98 cases) and none in relapsed tumors (22 cases). All patients with tumors showing c-Kit expression were older than the median age of 55 years (Fisher exact test $p=0.001$). c-KIT expression was associated with a worse DRS (Log Rank $p=0.028$; Breslow $p=0.002$). The 10-years DRS was 90% for c-KIT negative and 71% for c-KIT positive patients (Figure 3.4 C). A statistically significant worse TTP (TTP) was observed using the Breslow test ($p=0.001$) but not using the LogRank test ($p=0.061$). The 10-year TTP was 70% for c-KIT negative patients and 50% for c-KIT positive patients (Figure 3.4 D).

Patients with thymic carcinoma showed a statistically significant worse DRS than thymomas (Log-Rank p=0.002; Breslow p=0.003). Median survival was not reached for both groups. The 10-year DRS was 60% for thymic carcinomas and 91% for thymomas (Figure 3.4 E). Also the TTP was significantly worse for thymic carcinomas (Log-Rank p=0.021; Breslow p=0.002). The estimated median TTP was 69.4 months for thymic carcinoma (95%CI 0-142.7) and 147 months for thymomas (95%CI 121.7-172.4). The 10 year TTP was 43% for thymic carcinoma and 72% for thymomas (Figure 3.4 F). By multivariate analysis, c-KIT expression was neither an independent prognostic factors for DRS (p=0.67 and 0.22, respectively) nor for TTP (p= 0.79 and p=0.23, respectively). However, the small number of cases limts the possibility to draw definitive conclusions on the prognostic value of KIT expression expecially because the multivariate analysis was not significat, being KIT usually positive in thymic carcinomas.

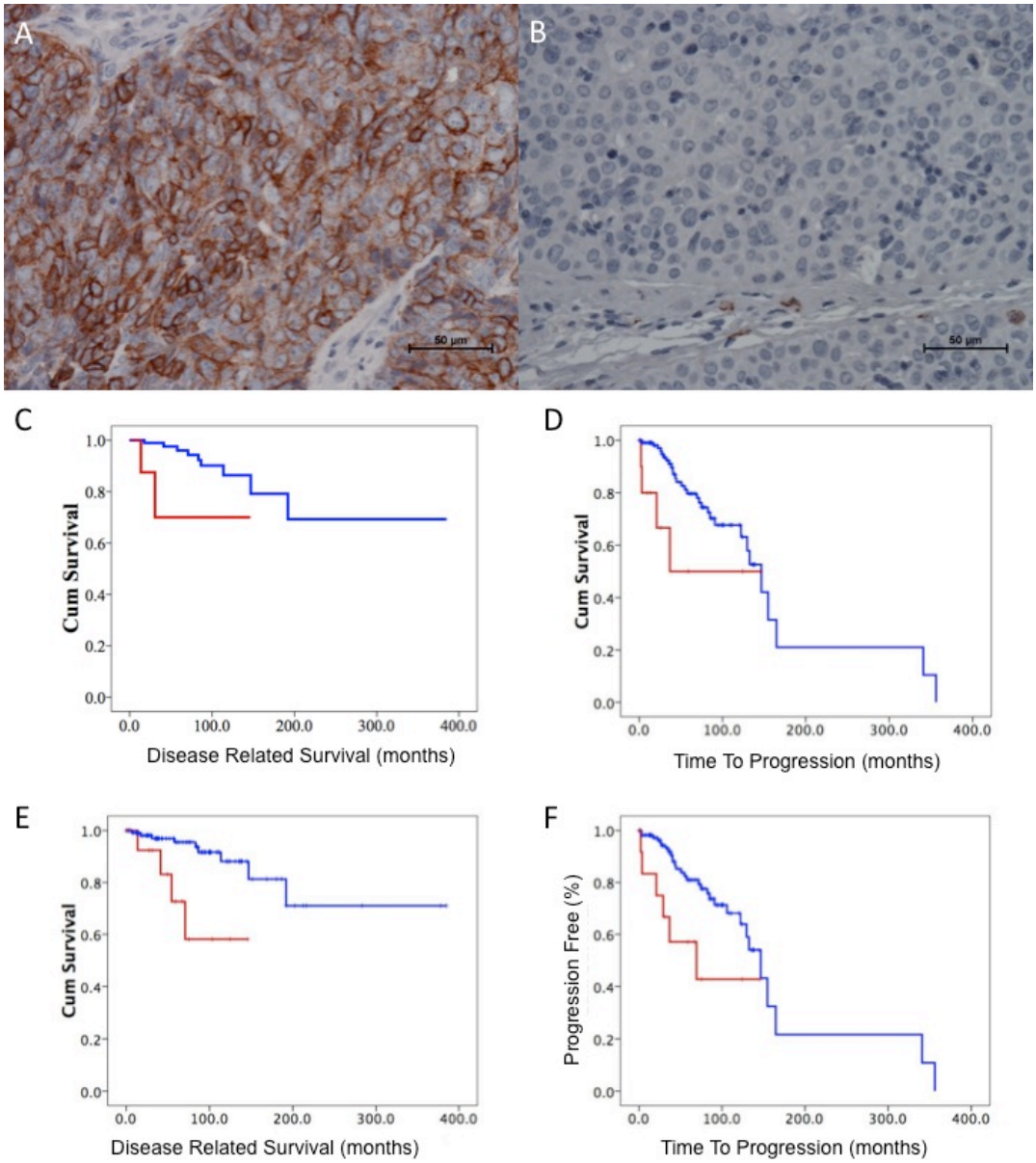

Figure 3.4: KIT staining results (A) Membrane c-Kit positive staining 40x original magnification; (B) c-Kit negative staining 40x original magnification; Kaplan Meier plot for (C) disease-related survival of patients positive or negative for c-Kit expression; (D) time to progression related to c-Kit expression; (E) disease-related survival of thymoma and thymic carcinoma patients; (F) time to progression of thymoma and thymic carcinoma patients.

Sequencing analysis of KIT

We sequenced all the exons of KIT in 8 thymic carcinomas and 5 thymomas from FFPE samples with a success rate of 77.5%. Histological characteristics of the tumors that underwent sequencing are reported in table 3.3. We did not detect mutations in any of the tumor samples and in the T1889 thymic carcinoma cell line, previously reported to be negative for c-Kit expression[161]. We observed the previously reported single nucleotide polymorphism (SNP) corresponding to M541L in one type A thymoma and in one thymic carcinoma[189].

Table 3.4 summarizes the studies that have investigated c-Kit mutations in TETs. Only a few c-Kit mutations have been reported and those were exclusively detected in thymic carcinomas. No KIT mutations were reported in thymomas among 88 cases sequenced. In thymic carcinoma only 5 mutations have been described among the 59 cases studied (9%).

Table 3.3: Thymic carcinoma and thymoma histology, mutation and c-Kit immunohistochemistry

Sample	Histotype	c-Kit IHC	KIT mutation
I-Thy 1	Squamous cell carcinoma	+3	No
I-Thy 2	Mucinous adenocarcinoma	0	No
I-Thy 3	Squamous cell carcinoma	+2	-
I-Thy 4	Mucoepidermoid carcinoma	0	No
I-Thy 5	Squamous cell carcinoma	0	No
I-Thy 6	Neuroendocrine carcinoma	0	-
I-Thy 7	Squamous cell carcinoma	+1	-
I-Thy 8	Squamous cell carcinoma	+3	No
I-Thy 9	Squamous cell carcinoma	+2	No
I-Thy 10	Neuroendocrine carcinoma	0	No
I-Thy 11	Mucinous adenocarcinoma	+3	No
I-Thy 12	Undifferentiated carcinoma	0	-
I-Thy 13	Undifferentiated carcinoma	0	-
I-Thy14	Thymoma type A	+1	No
I-Thy 15	Thymoma type B3	0	No
I-Thy 16	Thymoma type AB	+1	No
I-Thy 17	Thymoma type A	+1	No
I-Thy 18	Thymoma type B3	0	No
T-1889	Undifferentiated carcinoma cell line	0[161]	No

Table 3.4: Summary of published reports of c-Kit expression and mutation in TEMs

Reports	Samples	IHC -	IHC +	Mutation -	Mutation +	Described mutations
Retrospective studies						
Henley 2004[121]	Thymoma	19	1 (5%)			
	TC	4	11 (73%)			
Pan 2004[122]	Thymoma	110	0			
	TC	3	19 (86%)	21		
Nakagaua 2005[123]	Thymoma	48	2 (4%)			
	TC	4	16 (80%)			
Tsuchida 2008[124]	Thymoma	20	0			
	TC	6	11 (65%)	9		
Yoh 2008[127]	Thymoma	24	0	22		
	TC	2	15 (88%)	10	1	L576P
Girard 2009[95]	Thymoma	33	0	38		
	TC	3	3 (50%)	5	2	V560del H697Y
Phase II trial						
Salter 2008[190]	TC	2	9			
Giaccone 2009[191]	Thymoma	2	0	2		
	TC	1	1	1		
Case reports						
Stroebel 2004[93]	TC		1		1	V560del
Bisagni 2009[96]	TC		1		1	D820E
Li 2009[98]	TC		1			
Vasamiliette 2009[192]	TC		1			
This series						
	Thymoma	103	4 (4%)	5		
	TC	7	6 (46%)	8		
Total						
	Thymoma	359	7 (2%)	67	0	
	TC	32	95 (75%)	54	5	

3.3 Complete genome sequencing of a B3 thymoma

Patient's clinical history

In April 2007, a 55 years old Caucasian female presented whit shortness of breath and fatigue. A computed tomography (CT) revealed a left side anterior mediastinal mass of 12.3x7.9cm infiltrating the pericardium, the diaphragm and the left lung but without evidences of distant metastases. The patient underwent a mediastinoscopy with curative intent but during the procedure the tumor was judged unresectable and a biopsy was performed. The pathological diagnosis was B3 thymoma in stage IIIA. She did not show any paraneoplastic or immunological syndrome possibly associated with the disease. The patient received 6 cycles of chemotherapy according to the ADOC schema (Cisplatin, Doxorubicin, Vincristine and Cyclophosphamide) reaching a minor response. After 6 months, the tumor progressed and the patient received 3 cycles of ifosfamide obtaining a disease progression. Thereafter, she received prednisone therapy for 5 months up to a minor response of disease. In April 2009, she has been referred to NCI (Bethesda, MD), where the restaging of the tumor did not showed any evidence of progressive disease nor distant metastases. The patient received an extended resection of the tumor, part of the diaphragm, part of the pericardium, part of left chest wall and a left pneumonectomy without evidence of macroscopic residual disease. The pathology report confirmed the diagnoses of B3 thymoma infiltrating the pericardium the lung and the diaphragm but the absence of infiltrating margins. The patient refused adjuvant radiation therapy and did not present any evidence of disease for 26 months. Then the patient developed fatigue, dyspnea (New York Heart Association grade 3) and chest pain associated with exertion and relieved by rest. The cardiologic follow up demonstrated absences of coronary disease, a left ventricle ejection fraction of 55% and the presence of

pericardial nodules and effusion. The CT demonstrated local relapse in the site of left lung ileum and in the cardiac root region with encasement of the pulmonary artery. The patient was treated by radiation therapy, utilizing IMRT modality with 6MV photons to a total dose of by 6300 cGy in 180 cGy fractions, obtaining relieve of symptoms. Currently, after 10 months the patient is still asymptomatic without any further evidence of disease progression.

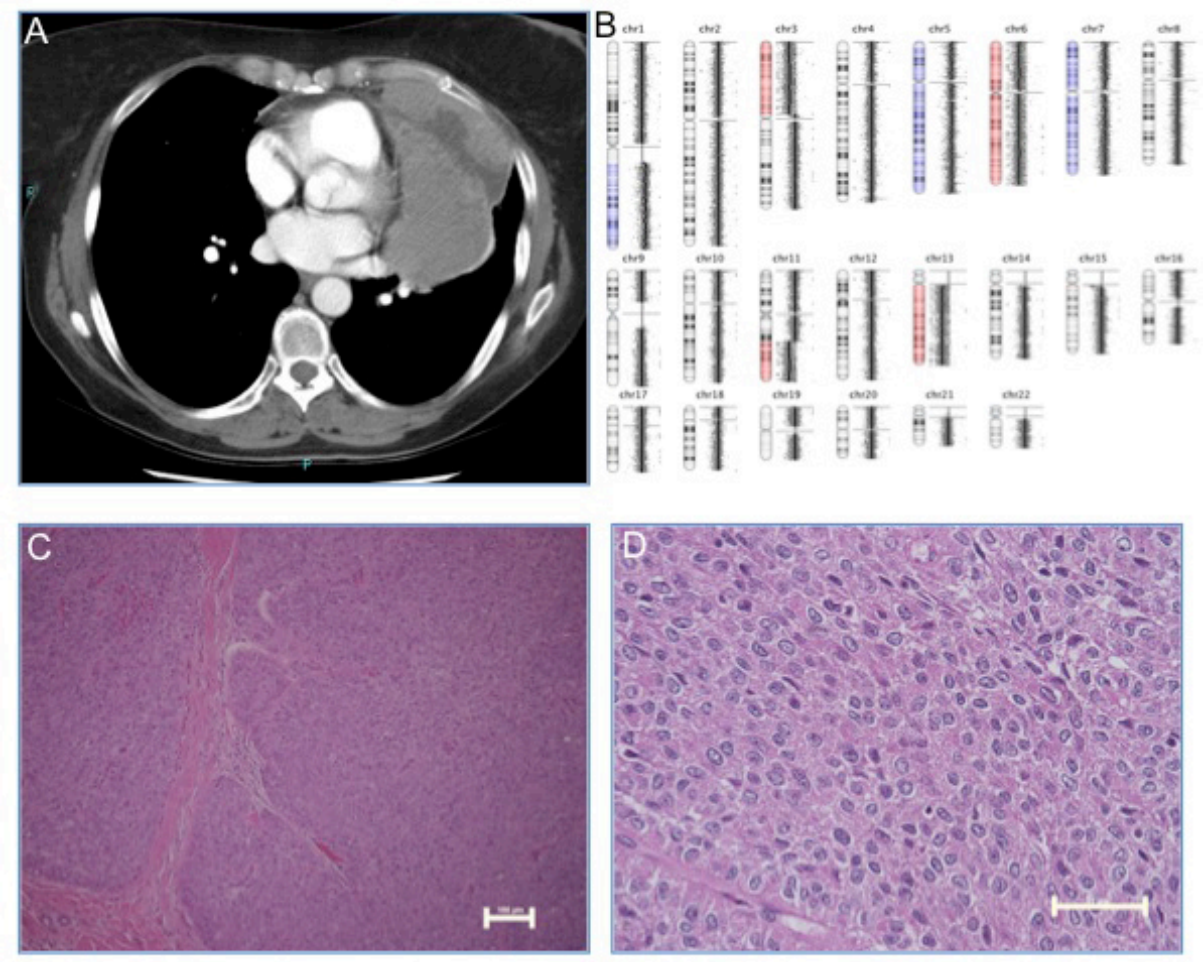

Figure 3.5: KSA tumor features. Panel A depicts the CT scan results performed before the surgical resection showing the cardiac root, the tumor occupying large part of the left hemithorax and invading the chest wall. (B) Summary of array CGH results for autosomal

chromosomes: in red are reported regions of CN gain and in blue of CN loss. Panel C and D report histology results for the resected sample showing 10x and 40x magnification, respectively. The tumor is organized into large nets of epithelial cells separated by fibrous bans; to be note the round-polygonal shape of the thymic epithelial cells in almost complete absence of lymphocytes. Scale-bar is 100μm in C and 50μm in D.

Preparation and validation of tumor material

Part of the tumor resected at NCI was snap frozen in liquid nitrogen and preserved at -180^{o}C. The frozen tumor was imbedded in optimal cutting temperature (OCT) and 8μm slides of the tumors were cut. The slides were colored by Hematoxylin and Eosin and a pathologist confirmed the presence of >80% of tumor cells and histological features compatible with the diagnosis of B3 thymoma. Tumor DNA and RNA were extracted from the same frozen specimen using All prep RNA/DNA kit (Qiagen, Valencia CA). Array CGH was performed using tumor DNA and normal human male DNA from Promega (Madison, WI) as reference. The array CGH analysis revealed copy number (CN) gain of chromosome 1q, 5 and 7 and CN loss of chromosome 3p, 6, 13 and part of chromosome 11q in the autosomal chromosomes. These data are compatible with those reported for B3 thymomas by Zetel A, et al. by conventional CGH[115] and by Girard N, et al. by array CGH[95], confirming the presence of a large proportion of tumor cells in the sample. Patient's normal DNA was extracted from 5 ml of whole peripheral blood using QIAamp DNA blood maxi kit (Qiagen).

Whole genome sequencing results

High throughput sequencing generated 222.2 and 234.53 Gb of mapped sequences against reference genome for tumor and normal DNA, respectively. More than 95% of the genome was fully covered in tumor and normal DNA being able to call variation in each allele. A total of 3,096,049 of single nucleotide variations (SNVs) were observed in tumor DNA whereas a total of 3,314,611 in the normal DNA. The presence of extended regions of CN loss in tumor DNA could explain the higher number of SNV observed in normal than in tumor DNA. Similarly an increased number of INDEL was observed in normal DNA Table 3.5.

Table 3.5: summary of whole genome sequencing results

	Tumor	**Normal**
Mapped sequence yield (Gb)	222.02	234.53
Fully called genome fraction	95.3%	96.4%
SNV total count	3,096,049	3,314,611
Novel SNV	133,662	145,929
SNV Transitions/transversions	2.14591	2.14218
INS total count	158,681	173,448
DEL total count	174,697	192,178
INDEL total count	333,378	365,626
Insertion/deletions ratio	90.8%	90.3%
Novel INDEL	67,163	74,562

Complete genomics analysis (CGA) tool was adopted to call tumor specific variations (somatic). 6530 candidate somatic SNVs were observed together with 2776 insertions, 1600 deletions and 1570 substitutions. The somatic SNVs and INDELs were disperse in the genome and have been organized in 4 groups:

Tier 1: mutations affecting exons with the following characteristics: (n=47)

a) Not synonymous (the nucleotide change results in a triplet coding for a different amino-acid.

b) SNV not previously described in dbSNP135 except those mutations concomitantly described in COSMIC database.

Tier 2: mutations affecting splicing sites (n=6) and RNA genes (n=24) or highly conserved regions in non-repeat masked regions in USCS (n=153; degree of conservation was calculated using phastCons44way tables: phastCons is an algorithm that generates similarity scores from the multiple alignments of 44 vertebrate genomes to the human genome. PhastCons score >500 discriminates highly conserved regions[193]).

Tier 3: mutations affecting not repeated regions (n=1881)

Tier 4: all other mutations (n=10365)

The 47 candidate mutations from tier 1 were validated using Sanger sequencing; 8 of them were confirmed (table 3.6), the WDR70 G1823A mutation was identified in tumor and normal DNA and consequently classified as germ line variation. An higher confirmation rate (25%) was observed for SNVs than for INDELs (4%) being confirmed only that interesting BCOR locus.

Table 3.6: confirmed INDELS and SNVs

Gene symbol	Genomic location	NCBI reference sequence	Nucleotide modification	Amino acid change
VN1R5	chr1:247419950	NM_173858	C577T	R193W
PHF15	chr5:133914340	NM_015288	T1706A	L569Q
PION	chr7:76978720	NM_017439	A1493	E498G
PPP1R3A	chr7:113517959	NM_002711	G3188C	G1063A
SFXN3	chr10:102795325	NM_030971	T245C	F82S
PCNXL3	chr11:65385813	NM_032223	C980A	P327Q
SRGAP1	chr12:64491096	NM_020762	G1754A	R585H
BCOR	chrX:39930263	NM_001123385	3201_3202insGA	Frame-shift

Genomic position is related to hg19; nucleotide modifications and amino acid change positions are related to the specified NCBI Reference sequence.

Junction sequences

Junction sequences are those resulting from the joint of two sequences normally not adjacent or in the same orientation in the reference genome. These sequences can originate from either the same or a different chromosome. Thus, junction sequence can be the result of structural variations (SV) such as deletions, duplication, inversions, and translocations (Figure 3.6).

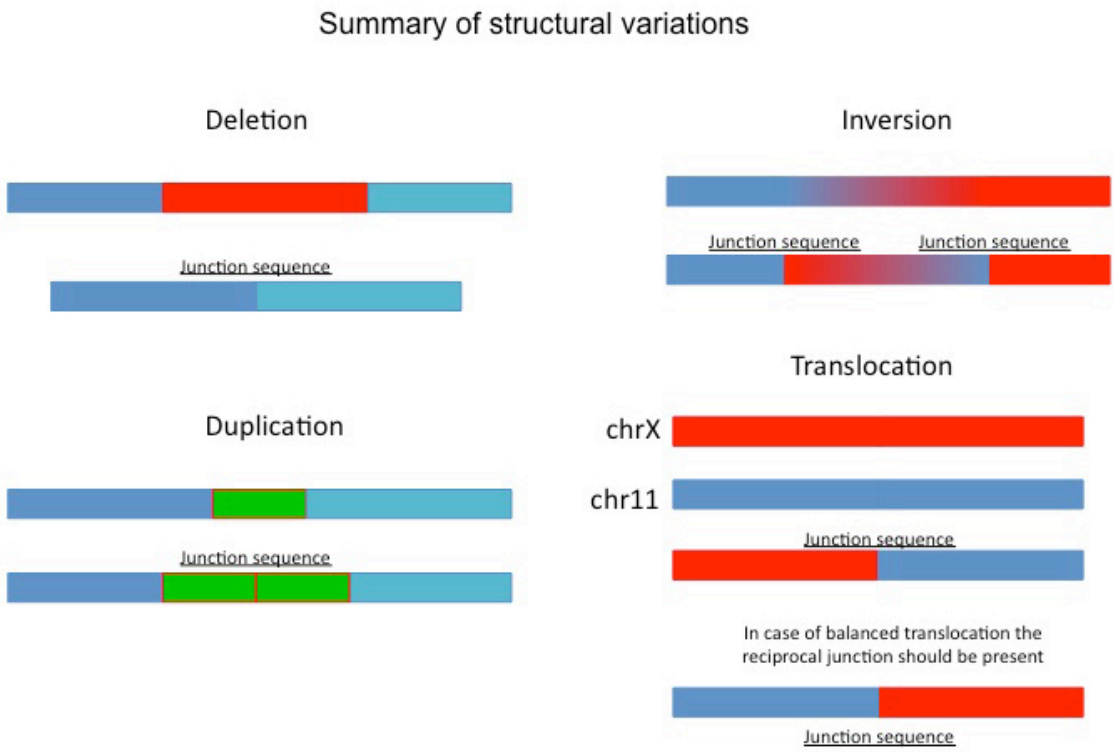

Figure 3.6: schematically summary junction sequences consequence of frequent DNA rearrangements.

Using junctiondiff (CGAtool) a list of 97 predicted tumor specific junctions was generated by subtracting normal from tumors junctions. Fillers were applied excluding SVs not supported by a sufficient number of discordant paired-ends (pair count < 20) and with small span size (span< 5kb). Six variations met these criteria but 3 of them have been also described in a dataset of structural variation generated by sequencing 52 genomes of normal persons (disease free) using complete genomic platform, thus these shared junction sequence highlight regions of the genome that are difficult to call or are heterogeneous within individuals or have been not mapped in the reference genome yet. Thus, only 3 tumor specific junction sequences were robust candidates (Table 3.7)

Table 3.7: candidate structural variation (junction sequences)

Variation	Left position	Left strand	Right position	Right strand
1	chr11:49883579	-	chrM:16083	+
2	chr11:86017394	+	chrX:123645300	+
3	chr1:158725872	+	chr2:148952671	-

Primers for left and right position were designed and PCR performed on the tumor and normal patient DNA in order to detect the presence of the aberration and evaluate its tumor specificity. Moreover, an unrelated reference male genome DNA (Promega) was introduced as negative control. Figure 3.7 reports PCR results; the candidate variation 1 was present in patient's tumor, normal and unrelated normal DNA and probably it is related to a normal genomic sequence not already mapped in the current version of the human genome (hg19). The variation 2 was present only in the tumor DNA, thus it was considered validated. The junction 3 resulted a sequence proper of the normal patient genome but not common to the unrelated genome, therefore it was not considered tumor specific and confirmed. Sanger sequencing of PCR products and their predicted size confirmed the specificity of the amplified segments.

The sole confirmed variation is a translocation between chromosome 11 and X interesting the coding region of exon 2 of C11orf73 and the intronic region of ODZ1 between exon 19 and 18 (Figure 3.10).

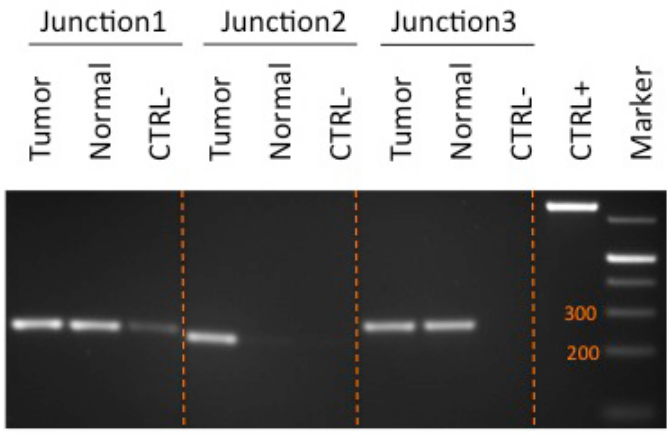

Figure 3.7: Gel electrophoresis of PCR products generated using primer designed on the two sides of the junction sequences. Primers for junction 1,2 and 3 were used for amplify the candidate junction sequences in tumor and normal DNA from the studies patient and from an unrelated male human genome. A positive control provided with PCR amplification kit was included. Marker size confirmed the expected size of PCR products.

Copy number aberrations

Copy number aberrations were evaluated using array CGH and estimated from whole genome sequencing data using CGA tool. These results were remarkably similar, except for small discordant regions possibly related to CN variation that has been subtracted by NGS sequencing but not from array CGH data (Figure 3.8). Figure 3.10 summarizes the results of whole genome sequencing.

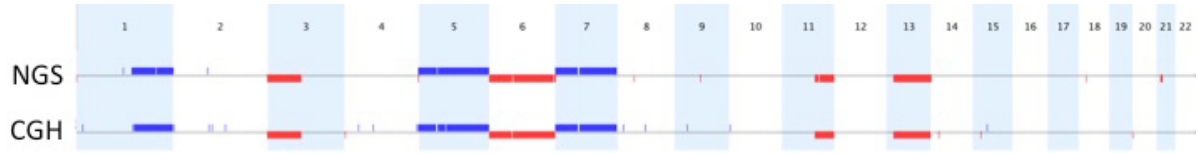

Figure 3.8: CGH estimated by CGA tool from whole genome sequencing data (NGS) and from array CGH are compared. Region of CN gain (blue) and CN loss (red) are reported for the autosomal chromosomes 1-22. Each chromosome is reported with the short arm on the left.

Expression of mutated genes in patient's tumor

The 47 mutations predicted by whole genome sequencing affect 42 genes that has been evaluated by RNA sequencing. Transcriptome sequencing results were sufficient to evaluate highly and moderate expressed genes. Less expressed genes did not have an enough number of copies of mRNA to be captured from this analysis. The expression of a gene is directly related to the number of reads (short sequences generated by high throughput sequencing) able to map to its genomic position. Reads, generated by transcriptome sequencing, were aligned to the reference genome (hg19) using GSNAP and gene expression estimated by FPKM value calculated using Cufflink[194]. Figure 3.9 summarizes the results of gene expression analysis. The predicted mutations were observed only in PHF15, WDR70, PCNXL3, BCOR and SFXN2. For the other gene, the predicted mutation was not identified in the expressed RNA. For the remaining mutations confirmed by Sanger sequencing, VN1R5 and PPP1R3A were not captured by this analysis because not enough expressed. Whereas, SRGAP1 and PION, even if expressed, did not have reads coverage in the mutation

locus, thus they can not be confirmed or excluded using RNA sequencing data. Expression data estimated for this patient were in line to those identified using the same technology from a group of 11 TETs (7 thymomas and 4 thymic carcinomas) and 3 TET cell lines. 26 of the candidate mutate genes were annotated in COSMIC database as they have been previously described mutated in cancer patients.

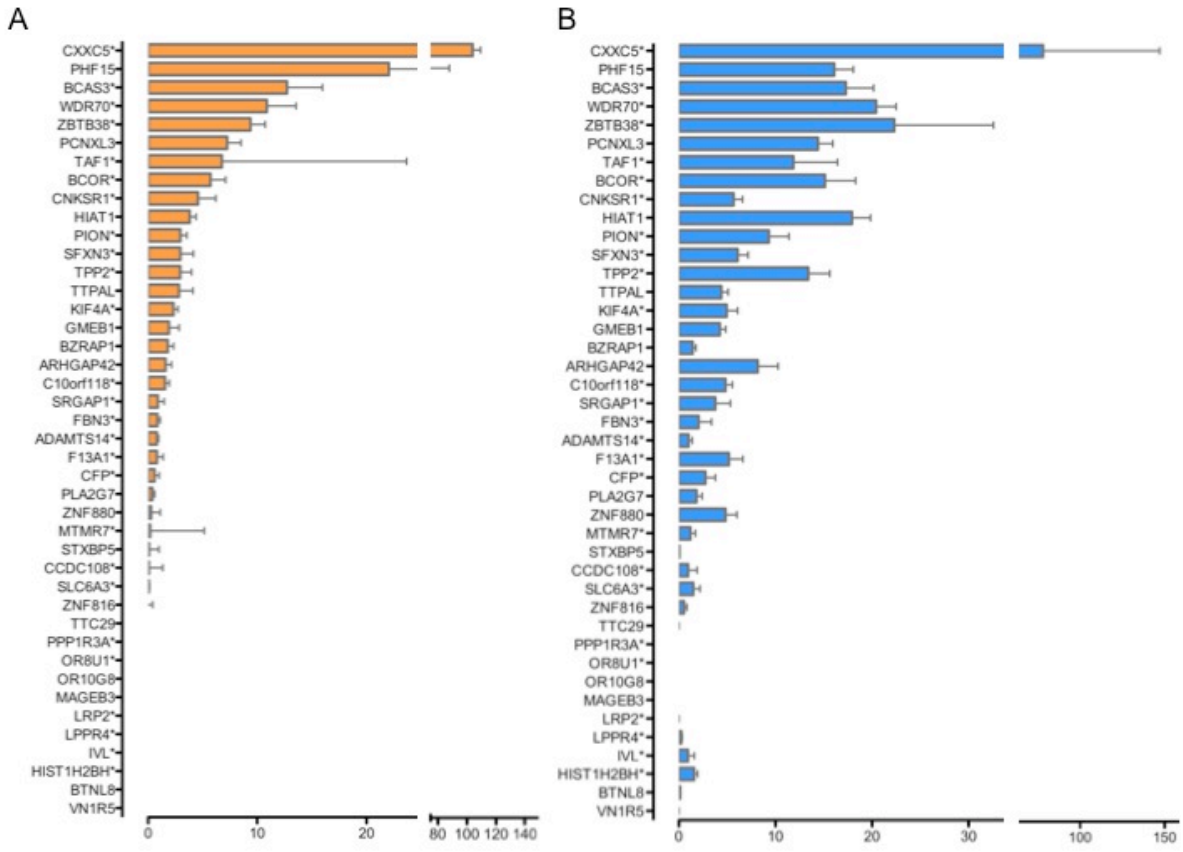

Figure 3.9: Expression of candidate mutated genes using transcriptome-sequencing data. (A) For each candidate mutated gene, FPKM value was calculated using cufflink; error bars report the 95%CI related to the prediction of gene expression. Genes labeled by * are those reported mutated in COSMIC database. (B) Average expression of candidate mutated genes in a series of thymic epithelial tumors: 11 patients neoplasm and 3 cell lines. Error bars represent the standard deviation of gene FPKM values obtained in the 14 transcriptomes.

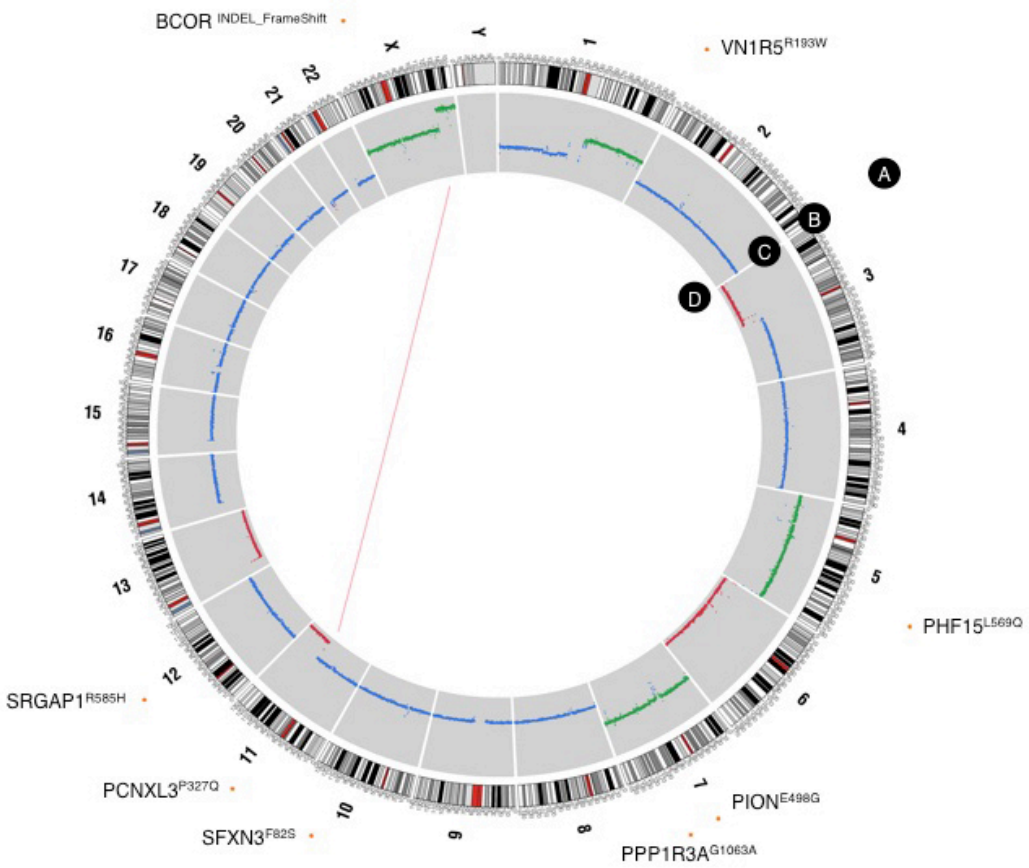

Figure 3.10: summary of confirmed mutations in thymoma B3 patient's genome. (A) Confirmed single nucleotide variations and INDEL. (B) Genomic coordinates: chromosomes and their bands, crentromeres are marked in red. (C) CN aberrations: CN gain are reported in green and CN losses in red, whereas diploid regions in blue. (D) Junctions' track reports the t(11;X).

Function of mutated genes and their relevance in cancer

Limited data are available on the role in tumor growth of the genes identified mutated by whole genome sequencing. The normal biological activity of VN1R5, SFXN3, PCNXl3 and SRGAP1 is only marginally elucidated. PION is involved in amyloid beta production and it has been reported mutated in cancer in cosmic database, however its relevance to cancer growth is undetermined.

PHF15 known also as JADE2 belongs to a family of more than 100 proteins characterized by the Plant Homo Domain (PHD) finger. Very limited data are available for this gene. Several of the PHF proteins are localized in the nucleus, and are involved in chromatin-mediated gene regulation. Other members of PHF family are ASH1L, MLL and AIRE. The function of JADE2 is largely unknown; however, more details are available on the junction of JADE1 (PHF17) that presents tumor suppressor activity in kidney cancer. JADE1 is normally stabilized by VHL protein and prevents tumor growth by inducing apoptosis[195]. When over-expressed, JADE1 can increase histone H4 acetylation in vivo[196].

PPP1R3A encoded for the regulatory subunit of a protein phosphatase glycogen-associated presents in skeletal muscle. Mutations for this gene have been described in cosmic for different type of tumors. A possible relation between PPP1R3A mutations and colon cancer metastases was described[197] as well as a reduced expression in breast tumors[198].

BCOR is corepressor of several transcription factors, firstly discovered for its ability to inhibit BCL6 through the BCOR-BCL6 binding domain[199]. BCOR is an essential transcriptom repressor for hemopoiesis, mesenchymal stem cell and early embryo development[200,201]. Germline BCOR mutations cause the Oculofaciocardiodental syndrome, an inherited X-linked syndrome characterized by cardiac defects and dysmorphic

appearance[202]. BCOR has been recently described to be mutated in a subset of acute myeloid leukemia patients[203]; about 50% of them present both BCOR and DNMT3A mutations suggesting a possible cooperation of the two genes, possibly through interference with epigenetic mechanisms[203]. BCOR may increase its transcriptional repression interacting with epigenetic regulators such as class I and II HDACs or the polycomb group protein.

Of the genes involved in the translocation t(11;X), C11orf73 codes for a protein relevant for lung development such as demonstrated in knockout mice that present severe emphysema at birth and disorganization of Golgi apparatus in Clara cells[204]. ODZ1 belongs to the tenascin family and teneurin subfamily. It is a transmembrane protein type II and may function as cellular signal transducer forming dimmers with the other members of teneurin family. It is predominantly expressed in the developing nervous system[205]. The role of C11orf73 and ODZ1 in cancer is unknown.

A more precise characterization of the function of the mutated genes is necessary to understand their relevance to thymoma growth. Moreover, it is useful understand the frequency of these mutations in TETs to eventually identify those that are recurrent and may be relevant to disease pathogenesis. Because any of these genes is an obvious oncogene or tumor suppressor gene, an high throughout approach was adopted to evaluated mutations in a cohort of 26 patients.

3.4 Exome sequencing and transcriptome sequencing

Whole exome sequencing, transcriptome sequencing and array CGH were performed on frozen material from 26 patients, in order to identify which tumor specific mutations are recurrent in TETs and, therefore, may drive the cancer growth. Moreover, the identification of recurrent mutations could offer druggable targets for therapy. From a series 55 TETs, 8μm frozen sections were cut, colored by H&E and reviewed by a pathologist: only tumors presenting more than 80% of cancer cells on histological grounds were included in this study. Part of the frozen tumor was scraped and RNA and DNA were extracted from the same specimen using All prep RNA/DNA kit (Qiagen). The tumor DNA was further tested to estimate the presence of tumor cells by array CGH. Because CN aberrations are only in tumor cells, the ability to detect aberration with a mean Log2Ratio higher than 0.3 supported the presence of a sufficient low normal cell infiltration. An exception was type A thymomas that usually do not show any CN aberration; however these tumors do not present a significant normal thymocyte infiltration. Considered the expected depth of coverage of exome sequencing, a restricted infiltration of normal cell was required to have chance to identify tumor mutations.

CGH results

Figure 3.11 depicts the frequency of CN aberrations in the 26 tumors that passes the previously stated filters.

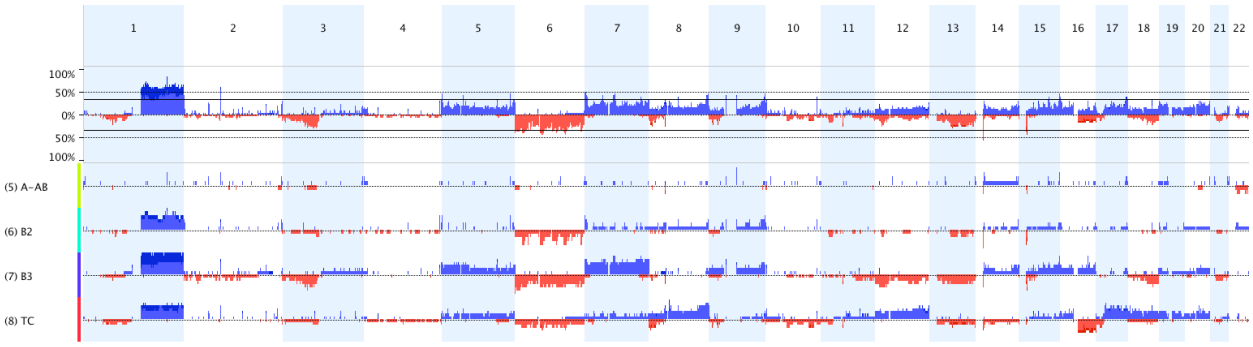

Figure 3.11: Frequency of CN gain was reported in blue and CN loss in red across the 22 autosomic chromosomes. Frequency of aberration according to WHO histotype was reported on the bottom of the figure. There were 4 type A and 1 type AB that have been grouped together because the small numbers.

Concordantly with previously reported CGH data, a more quiet patter of aberrations was observed in type A thymomas. In B3 thymomas and thymic carcinomas a more complex karyotype was appreciated. To be noted that all the samples were hybridized against the same male normal genome DNA (Promega) therefore CN variations are famished to tumor specific CN aberrations. CN variations are defined as increases or decreases in CN of a genomic region between persons. Thus, such CN variations are a recently discovered and pervasive form of inter-individual genomic variability and depending on their frequency can be considered in the same way as polymorphisms. Variations interesting genomic regions long less than 1kb are named INDELS; whereas, CN variations are those longer than 1kb. 99% of

CN variations interest a region shorter than 2.8kb[206]. CN variation affect about 10% of human normal genome[207] and may be associated with the susceptibility to develop neoplasms[207]; however, they are not tumor specific being present in the germeline DNA. Even if interesting, CN variations are not the topic of our research and this evaluation has not the power and was not designed to draw reliable conclusions on CN variations. Databases list described CN variations; therefore, such data can be used to interpret CGH results.

CN aberrations candidate to drive the cancer grow were evaluate by the systematic statistical algorithm called GISTIC[208]. This test scores the frequency and amplitude (Log2 ratio) of CN aberrations across the sample set. To assess chromosomal regions that significantly associate with CN aberrations, GISTIC identifies regions with scores above the random aberrations simulated by null distribution. The generated p-values were corrected for multiple hypotheses testing by Benjamini-Hochberg FDR procedure to obtain q-values[208]. Q-value < 0.25 was considered significant, as previously described[209]. Table 3.8 reports the significant peaks individuated using GISTIC.

Table of GISTIC results				
Region	**Extended Region**	**Type**	**Q-Bound**	**G-Score**
chr1:206,045,902-206,516,047	chr1:198,331,518-211,496,273	CN Gain	1.84E-10	12.7
chr2:91,057,122-91,270,370	chr2:91,057,122-91,270,370	CN Gain	1.52E-04	8.3
chr2:201,422,144-201,439,344	chr2:201,407,033-201,659,352	CN Gain	1.65E-01	5.2
chr4:186,791,937-186,840,903	chr4:186,791,937-186,914,612	CN Gain	1.01E-01	5.4
chr5:168,379,349-168,559,373	chr5:168,105,568-173,214,961	CN Gain	1.22E-03	7.5
chr5:1,069,130-1,406,444	chr5:210,598-2,087,107	CN Gain	7.66E-02	5.6
chr5:53,209,574-53,640,485	chr5:53,173,269-54,236,049	CN Gain	9.69E-02	5.5
chr7:1,418,833-1,592,579	chr7:0-3,055,777	CN Gain	2.62E-02	6.1
chr7:150,805,324-151,211,689	chr7:148,308,057-151,988,867	CN Gain	1.23E-01	5.3
chr8:48,886,756-49,012,099	chr8:47,062,622-49,012,099	CN Gain	2.79E-08	11.3
chr8:39,349,089-39,487,965	chr8:37,553,512-43,515,933	CN Gain	3.26E-04	8.0
chr9:138,486,659-138,586,250	chr9:137,381,974-139,651,033	CN Gain	2.62E-02	6.1
chr9:67,859,114-68,483,948	chr9:67,859,114-68,483,948	CN Gain	3.41E-02	6.0
chr9:43,626,920-44,199,460	chr9:43,626,920-44,199,460	CN Gain	9.37E-02	5.5
chr10:126,294,198-126,341,050	chr10:126,280,557-126,416,088	CN Gain	4.33E-02	5.9
chr10:1,634,251-1,758,787	chr10:1,534,055-1,773,310	CN Gain	7.53E-02	5.6
chr12:9,536,233-9,615,714	chr12:9,492,374-9,615,714	CN Gain	7.80E-02	5.6
chr12:131,709,394-131,716,529	chr12:131,195,008-132,009,052	CN Gain	1.55E-01	5.2
chr15:48,637,396-48,766,096	chr15:48,043,931-50,757,915	CN Gain	5.55E-02	5.8
chr16:541,204-1,538,513	chr16:268,079-5,074,779	CN Gain	1.26E-01	5.3
chr16:69,424,613-69,748,994	chr16:69,400,497-69,758,575	CN Gain	2.09E-01	5.0
chr17:36,921,402-36,938,175	chr17:30,354,578-46,424,631	CN Gain	6.36E-02	5.7
chr18:58,944,656-59,130,723	chr18:58,916,038-59,130,723	CN Gain	1.00E-03	7.6
chr20:61,190,572-61,707,182	chr20:60,945,331-62,435,964	CN Gain	2.09E-01	5.0
Region	**Extended Region**	**Type**	**Q-Bound**	**G-Score**
chr1:72,537,679-72,585,332	chr1:68,716,597-77,798,533	CN Loss	3.59E-07	12.8
chr2:34,548,116-34,588,943	chr2:33,705,609-36,503,080	CN Loss	8.25E-02	6.2
chr3:76,932,507-77,232,003	chr3:76,246,296-78,291,688	CN Loss	1.09E-01	5.6
chr4:68,990,434-69,405,506	chr4:57,726,480-70,668,797	CN Loss	1.95E-01	4.3
chr6:385,685-936,412	chr6:0-1,772,372	CN Loss	7.76E-02	6.3
chr6:66,235,602-66,365,606	chr6:63,016,584-70,893,508	CN Loss	1.03E-01	5.8
chr8:39,487,965-39,502,789	chr8:39,349,089-39,502,789	CN Loss	1.79E-08	14.3
chr9:22,034,292-23,081,796	chr9:20,681,145-25,336,492	CN Loss	7.33E-02	6.4
chr11:55,216,250-55,245,355	chr11:55,108,013-55,256,788	CN Loss	2.15E-02	7.1
chr13:56,546,551-56,777,534	chr13:52,298,749-70,391,446	CN Loss	1.25E-01	5.1
chr14:18,446,762-19,490,547	chr14:18,446,762-19,490,547	CN Loss	4.85E-04	9.2
chr15:19,671,527-19,839,771	chr15:19,482,222-20,188,556	CN Loss	1.50E-03	8.6
chr16:59,324,764-62,176,251	chr16:57,420,242-64,216,572	CN Loss	1.28E-01	5.0

Table 3.8: for each peak are listed the top region of the peak (region) and the peak boundaries (Extended region). Peak boundaries were determined so that the change in the GISTIC score from peak to boundary had < 5% likelihood of occurring by random fluctuation. G-Score (>1) and Q-bound (<0.25) summarized the GISTIC statistics.

Among the peaks identified by GISTIC two presented CN aberrations with peculiar characteristics. The peak of CN loss interesting chromosome 9p21.3 was constituted by 5 tumors with CN loss, two of them showed a remarkably low Log2ratio compatible with homozygous CN loss. Different breakpoints defined these 2 regions, thus, the probability that they were related to CN variation was limited. Moreover, these CN losses interested a limited region of the genome; therefore, it was easy to point out CDKN2A and CDKN2B, two well-characterized tumor suppressor genes. Tumors with CDKN2A/B CN loss were 1 B2, 1 B3 thymoma and 1 thymic carcinoma plus 2 thymic carcinomas with the lower intensity CN loss. Similarly, the peak of CN gain of 18q21.33 was constituted by CN aberrations from 9 tumors; 4 of them showed a remarkably high Log2Ratio related to the high number of copies predicted for this region.

The chance that these CN aberrations were related to CN variations was limited because they did not showed breakpoint in the same position. The 9 regions of CN gain differed in the breakpoint positions reducing the chance to be related to common CN variations. Moreover, these aberrations interested a narrow region of chromosome 18 containing only BCL2 locus. Patients carrying BCL2 CN gain were 1 type A, 2 B2, 1B3 and 5 thymic carcinomas 4 of them with gene amplification at very high Log2Ratio.

CN variations sharing the same breakpoints to these CN aberrations have not been described in literature, to date. Any CN variation for BCL2 locus has been described, whereas the presence of CN variations, interesting CDKN2A/B loci, has been reported in subjects with familiar melanoma syndrome.

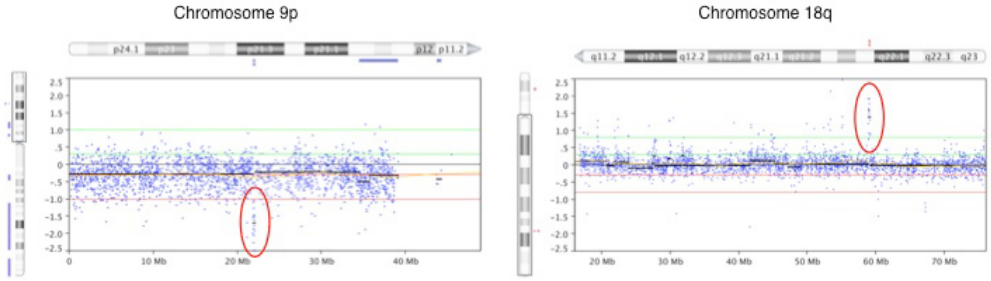

Figure 3.12: depicts circled in red (A) CDKN2A/B CN loss in the short arm of chromosome 9 and (B) BCL2 amplification in chromosome 18. To be noted the remarkable deviation from the baseline copy number of these aberrations (low and high Log2ratio, respectively) and the small extension in base pairs.

Exome sequencing results

Among these tumors we selected 5 cases: 2 TC, 2 B3 and 1 B2 thymoma to perform whole exome sequencing. Paired normal DNA for these patients was extracted from peripheral blood using QIAamp Blood Maxi kit (Qiagen). Mutations were classified in SNVs and INDELS. Among the INDELS those interesting <5bp are confidently called using GATK tool kit (Broad Institude, Cambridge MA) on reads aligned by Novoalign (Novochraft) to hg19, INDELS 5<x<10bp can be called sometime, whereas INDELS 10-1000kb are of difficult identification with the adopted technology. Only mutations affecting the coding exons with nonsynonymous amino acid modification were evaluated. Mutations previously described as SNP in dbSNP132 were excluded by the analysis with the exception of those mutations also described in cancer and reported in COSMIC database.

Table 3.9: Somatic Mutations in Thymic epithelial tumors

Thymoma			Thymic Carcinoma	
B2	B3	B3	TC	TC
P-Thy016	P-Thy001	P-Thy015	N-Thy011	P-Thy003
ID2 K1N	ABTB A748V	ACAT1 I52T	ADAMTS9 S1479N	ASH1L M1427T
ADAMTS9 S1479N	AC099759.1 A183V	AMPD2 E279G	C13orf31 A86T	C10orf112 R195K
	DCHS1 L460V	C20orf186 R69*	CYLD Q493*	C6orf221 Q204*
	GABRA1 Y196C	JMJD1C D779V	EXOG G146E	COL15A1 G856*
	MYOCD R402*	LRBA I275T	GABBR2 L252V	DNAH3 Y3008S
	PRSS12 N507D	MYO5A Y263C	GIMAP8 R164*	EPB41L4B D371N
	RNF103 R590K	NETO1 R206Q	GLI2 R103C	EXOC1 Q26R
	USP17 S23P	TMEM50A W37G	ITGB2 *410G	GRM8 M27K
	SMG6 Y623*	UBR1 P181T	KIAA1609 R265H	HRAS Q61R
	SPATA16 N105K	ZNF479 R11*	LRP2 R2336W	JPH3 V253I
	TBC1D26 C328S		NEFM R54C	KLC2 W491*
	TCTEX1D1 R54H		NLRC5 R400*	LDB3 T425S
	TRIML1 P433L		PAXIP1 P755S	MEF2C F109Y
			PBRM1 R1675W	MRPL53 L17F
			PCDH12 R498H	NAT10 K1017E
			PEX1 V429I	NIPBL W2107G
			TMEM2 T276M	SHISA6 R256*
			TMX4 C326R	SLC34A2 R623H
			ZNF521 R185K	SLC4A2 A463T
				TEAD4 A54T
				TP53 R342*
				TTN D24617H
	AL445989.1 18_SUB_CGYGSGYGY/Y		DNMT3B R420_Frameshift	CDKN2A A106_Frameshift

The exome sequencing results revealed a remarkable heterogeneity of mutations between tumors, without any recurrent mutation identified. Probably, the small number of cases evaluated, together with the tumor heterogeneity, limited the chance do identified recurrent events. In this small group a trend through a more complex pattern of mutation was observed from B2 to thymic carcinomas. Interestingly, one thymic carcinoma presented TP53, HRAS SNVs and CDKN2A insertion of a cytosine into the codon 107 with consequent frame shift mutation of the protein. KIT mutations were not detected.

Transcriptome sequencing results

Expression analysis of mutated genes enables data confirmation together with a functional interpretation of the observed changes. Transcriptome sequencing is a powerful method to evaluate expression of genes and the presence of known mutations on genomic scale. Table 3.10 summarized these expression results for the mutations identified from exome sequencing.

Table 3.10: Confirmed mutations by transcriptome sequencing

Thymoma			Thymic Carcinoma	
B2	B3	B3	TC	TC
P-Thy016	P-Thy001	P-Thy015	N-Thy011	P-Thy003
ID2 ^{K1N}	ABTB ^{A748V}	ACAT1 ^{I52T}	ADAMTS9 ^{S1479N}	ASH1L ^{M1427T}
	GABRA1 ^{Y196C}	AMPD2 ^{E279G}	C13orf31 ^{A86T}	HRAS ^{Q61R}
	PRSS12 ^{N507D}	JMJD1C ^{D779V}	CYLD ^{Q493*}	MRPL53 ^{L17F}
	RNF103 ^{R590K}	LRBA ^{I275T}	ITGB2 ^{*410G}	NAT10 ^{K1017E}
	TCTEX1D1 ^{R54H}	MYO5A ^{Y263C}	KIAA1609 ^{R265H}	NIPBL ^{W2107G}
			PAXIP1 ^{P755S}	SLC34A2 ^{R623H}
			PBRM1 ^{R1675W}	SLC4A2 ^{A463T}
			PEX1 ^{V429I}	TEAD4 ^{A54T}
			TMEM2 ^{T276M}	TP53 ^{R342*}
			TMX4 ^{C326R}	CDKN2A $^{A106\_FS}$

The expression of the mutated genes suggests their possible role in cancer growth. However, it remains do be determined if the identified mutations can affect the function of the translated protein. The INDEL affecting CDKN2A modify its structure introducing a frame shift mutation. This mutation and interests the ankyrin repeat domain (30-130AA) of p16INK4 necessary for CDK4 inhibition[210]. For alterative splicing, p14ARF can be translated from CDKN2A gene; in this sequence the INDEL occupies 118AA and affects the carboxyl-terminal domain necessary for nucleolar localization but not for MDM2 binging[211]. For SNVs, Sorting Tolerant From Intolerant (SIFT) algorithm was adopted to predict the effect of the mutation on protein structure[212]. Briefly, SIFT assumes that important positions in a protein sequence are conserved throughout related species and, consequently, substitutions at

these positions can affect protein function[212]. SIFT scores and predicted effects are reported in table 3.11.

Table 3.11: Prediction of mutation of protein function

Patient	Gene	Protein ensembl ID	Substitution	Prediction	SIFT Score
P-Thy016	ID2	ENSP00000379585	K1N	N/A	N/A
P-Thy001	ABTB2	ENSP00000298992	A748V	TOLERATED	0.14
P-Thy001	GABRA1	ENSP00000023897	Y196C	DAMAGING	0
P-Thy001	PRSS12	ENSP00000296498	N507D	TOLERATED	0.18
P-Thy001	RNF103	ENSP00000237455	R590K	TOLERATED	0.93
P-Thy001	TCTEX1D1	ENSP00000282670	R54H	TOLERATED	0.3
P-Thy015	ACAT1	ENSP00000265838	I52T	TOLERATED	0.16
P-Thy015	AMPD2	ENSP00000256578	E279G	TOLERATED	0.18
P-Thy015	JMJD1C	ENSP00000382195	D779V	DAMAGING	0
P-Thy015	LRBA	ENSP00000349629	I275T	TOLERATED	0.2
P-Thy015	MYO5A	ENSP00000348693	Y263C	DAMAGING	0
P-Thy015	UBR1	ENSP00000290650	P181T	TOLERATED	0.55
N-Thy011	ADAMTS9	ENSP00000295903	S1479N	TOLERATED	0.32
N-Thy011	C13orf31	ENSP00000317619	A86T	DAMAGING	0
N-Thy011	CYLD	ENSP00000308928	Q493*	N/A	N/A
N-Thy011	ITGB2	ENSP00000303242	*410G	N/A	N/A
N-Thy011	KIAA1609	ENSP00000343635	R265H	TOLERATED	0.1
N-Thy011	PAXIP1	ENSP00000319149	P755S	TOLERATED	0.3
N-Thy011	PBRM1	ENSP00000296302	R1675W	DAMAGING	0
N-Thy011	PEX1	ENSP00000248633	V429I	TOLERATED	0.42
N-Thy011	TMEM2	ENSP00000366243	T276M	TOLERATED	0.06
N-Thy011	TMX4	ENSP00000246024	C326R	TOLERATED	0.48
P-Thy003	ASH1L	ENSP00000357330	M1427T	TOLERATED	0.19
P-Thy003	HRAS	ENSP00000309845	Q61R	DAMAGING	0.02
P-Thy003	MRPL53	ENSP00000258105	L17F	N/A	N/A
P-Thy003	NAT10	ENSP00000257829	K1017E	TOLERATED	0.14
P-Thy003	NIPBL	ENSP00000282516	W2107G	TOLERATED	0.33
P-Thy003	SLC34A2	ENSP00000371483	R623H	TOLERATED	0.11
P-Thy003	SLC4A2	ENSP00000311402	A463T	TOLERATED	0.2
P-Thy003	TEAD4	ENSP00000351184	A54T	DAMAGING	0
P-Thy003	TP53	ENSP00000269305	R342*	N/A	N/A
P-Thy003	CDKN2A	ENSP00000307101	A106_FS	Frameshift	N/A

SIFT results need to be carefully interpreted because the specificity and sensitivity of the method: 69% and 81%, respectively; and mainly because it represents only a prediction of function.

Transcriptome sequencing data were available only for one patient with possible homozygous CN loss of CDKN2A that expressed low level of mRNA (FPKM 0.804; 95%CI 0-0.804) compared to the mean of the other 10 tumors evaluated by RNA sequencing average FPKM 38.63 (95%CI 7.838-69.42). Transcriptome sequencing data for BCL2 expression were available for 3 patients with BCL2 amplification and for 8 without. Three tumors with BCL2 amplification present an increased expression of BCL2 mRNA (p=0.0121; Figure 3.13) and for 2 of them we had enough material to prove an increase of BCL2 protein expression.

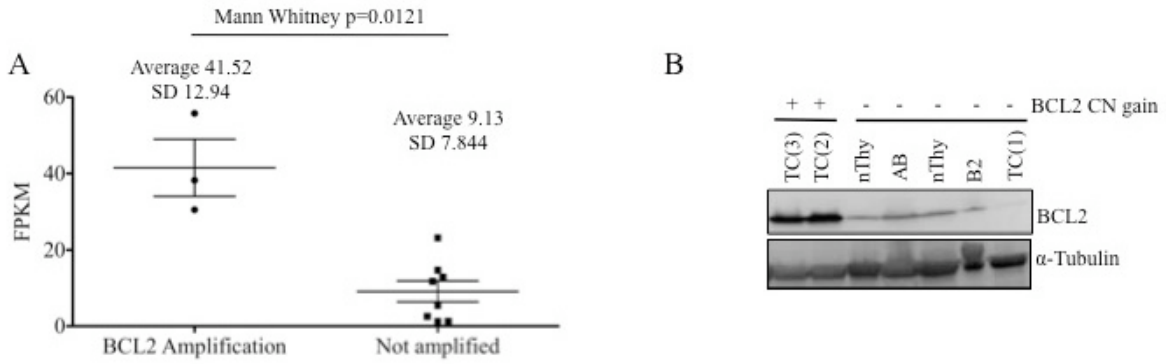

Figure 3.13: overexpression of BCL2 in tumor with BCL2 amplification. (A) BCL2 expression estimated from transcriptome sequencing data was significantly higher in tumors with BCL2 amplification than those without. (B) BCL2 protein was expressed at increased level in the two thymic carcinomas with BCL2 amplification TC(3) and TC(4) than in the sample without: 1 thymic carcinoma TC(1) 1 AB and 1 B2 thymoma or in 2 samples of normal thymus (nThy).

An overall remarkable heterogeneity of SNV and INDEL was observed in the studied samples, whereas common patterns of CN aberrations were observed. Interestingly, CDKN2A was mutated in different ways, INDEL in 1 case and focal very low intensity Log2ratio CN loss in 2 cases. Because BCL2 and CDKN2A are more likely to be mutated by CN aberrations we evaluated by array CGH a series of 59 FFPE TETs.

3.5 CGH evaluation of a series of formalin fixed paraffin embedded thymic epithelial tumors.

FFPE material is a valuable repository of tumor DNA stored for several years. Because the rarity of these tumors, the chance to evaluate archive material is necessary to correlate molecular aberrations with patients outcome. Several years are necessary to reach a mature follow up for these tumors. The newly available Agilent ULS labeling kit enables us to perform array CGH using FFPE tumor tissue.

A series of 132 patients affected by TETs were consecutively operated at the Istituto Clinico Humanitas (Rozzano, Milan, Italy) between 1996 and 2008. Clinical data were retrospectively collected. The main patient and tumor characteristics are summarized in Table 3.12. The median age was 55 years and the male:female ratio was of 1:1. Most of the patients had an early stage of the disease (68% stage I and II) and underwent a radical resection (R0, 71%). Survival was assessable in all patients, and median follow up was 7 years (84.5 months; 95%CI 72.1-96.9). Thirty-one patients (23.5%) were reported to be dead at the update performed in June 2009. The median overall survival (OS) was 31.5 years (377.8 months; 95%CI 112.5-634.2) with a 10-year OS of 70% (Figure 3.14A). Only 13 patients (9.8%) died because of disease progression, 2 patients died because of myasthenia gravis and 4 because of a secondary cancer (3 hepatocellular carcinomas and 1 non-small cell carcinoma of the lung). The median Disease-Related Survival (DRS) was not reached after 32 years follow-up. The 10-year DRS was 87% (Figure 3.14B). Considering the median age of 55 and the indolent clinical behavior of most tumors, DRS was chose over OS for further survival analyses.

A total of 131 patients were evaluable for TTP; for 1 patient no updated data on the progression date were available. Thirty-six patients developed progression during the period of study. The median TTP was 12.3 years (147 months; 95%CI 121.6-172.4), and the 10-year TTP rate was 69% (Figure 3.14C).

In the univariate analysis for DRS, stage (I-II vs III-IV; Logrank p=0.017, Figure 3.14D) and WHO classification (A-Ab-B1 vs the other; p=0.087) but not completeness of resection (R0 vs R1-R2; p=0.388) were significant. In the multivariate analysis any independent prognostic factor was observed. The univariate analysis for TTP revealed stage (p=0.0027), completeness of resection (p0.025) and WHO classification (p=0.0001) to be prognostic factors in TETs. However, the Cox hazard model demonstrated that only WHO classification was an independent prognostic factor in this series (p=0.0099). Data regarding paraneoplastic syndromes were available in 125 patients: 32 (25.6%) developed myasthenia gravis during the course of the disease, one patient developed autoimmune encephalopathy and one patient autoimmune glomerulonephritis. Paraneoplastic syndromes did not have a significant impact on survival. An haematoxylin and eosin stained slide from each tumor sample was revised by a pathologist and regions with >80% of tumor cells were selected for macro-dissection. DNA was extracted and used for CGH analysis.

Table 3.12: Patient characteristics			
		Total (132)	**aCGH (59)**
Median Age (range), years		55 (20-86)	57 (20-86)
Sex	Male:Female	67 : 65	28 : 31
Tumor sample	Primary tumor	108 (82%)	46(78%)
	Relapsed	24 (18%)	13(22%)
Stage	I	35/114 (31%)	15/49 (31%)
	II A	26/114 (23%)	9/49 (18%)
	II B	17/114 (15%)	5/49 (10%)
	III A	16/114(14%)	7/49 (14%)
	III B	3/114 (3%)	2/49 (4%)
	IV A	5/114 (4%)	3/49 (6%)
	IV B	12/114 (11%)	8/49 (16%)
	Na*	18	10
Completeness of resection	R0	79/112 (71%)	33/47 (70%)
	R1	23/112(21%)	7/47 (14%)
	R2	10/112(9%)	7/47 (14%)
	Na*	20	12
WHO histotype	A	15/132 (11%)	12/59 (20%)
	AB	28/132 (21%)	14/59(24%)
	B1	24/132 (18%)	0
	B1/B2	6/132 (5%)	0
	B2	8/132 (6%)	1/59 (2%)
	B2,B3	11/132 (8%)	5/59 (8%)
	B3	24/132 (18%)	20/59 (34%)
	C	14/132 (11%)	7/59 (12%)
	Other#	2/132 (2%)	0
Paraneoplastic Syndromes	MG	32/125 (26%)	17/58 (29%)
	Other+	2/125 (2%)	1/58 (2%)
10-year DRS		87%	83%
10-year TTP		69%	65%

Table 3.12: patients' characteristics. Na*, patients for whom data are not available at diagnosis. Other#, 1 micronodular and 1 cystic thymoma. MG: Myasthenia Gravis. Other+, 1 autoimmune glomerulonephritis (in the array CGH analysis) and 1 autoimmune encephalopathy. TTP, Time to progression. DRS, disease-related survival.

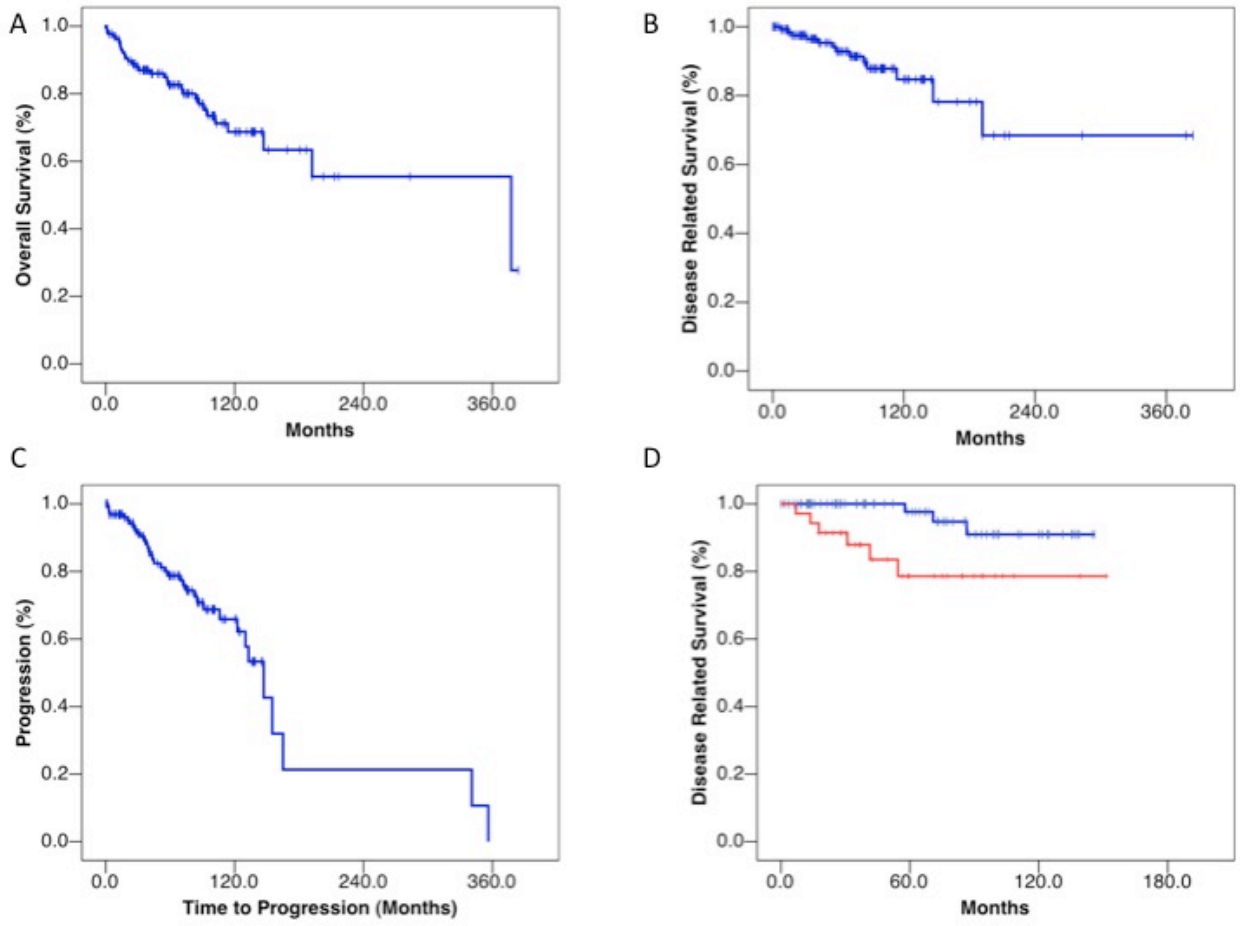

Figure 3.14: Kaplan-Meier survival estimate curves for A) Overall Survival, B) Disease-Related Survival, C) Progression-Free Survival, D) Disease-Related Survival for patients with stages I and II versus stages III and IV.

Correlation between chromosome arm-level aberrations and thymic epithelial tumor histotypes

The distribution of CN aberrations was calculated according to their length, which was expressed as percentage of the CN aberrations in relation to the respective chromosome arm. Small CN aberrations (0-10% of a chromosome arm length) were the most common (Figure 3.15A; n=3665). The number of CN aberrations progressively decreased in inverse proportion to their length up to 80% of their respective chromosome arms, and then rose again reaching a second peak at 90-100%. Based on the equation of the CN aberration distribution observed for up to 80% of chromosome arm-length, the number of 90-100% arm length CN aberrations was much higher than expected (90 instead of 7; χ^2 $p<0.001$). This observation suggests that small (focal) and long arm-level aberrations might represent distinct types of CN aberrations and therefore they need to be analyzed separately.

Figure 3.15B depicts the frequency of arm-level CN aberrations and their distribution according to TET histotypes. Only CN aberrations cumulatively covering more than 80% of an arm were defined as arm-level CN aberrations. Hierarchical cluster analysis of histotype profile indicated a close relatedness between B3 and TC. B2+B2/B3, AB and A types were incrementally dissimilar to TCs (Figure 3.15B). Type A thymoma showed occasional chromosome arm-level CN aberrations. On the contrary, types B3 and TC shared frequent arm level CN gains of 1q, as well as losses of chromosomes 6 and 13q. In addition, TC presented frequent losses of 16p and 17q. Although the potential continuum with A subtypes is impossible to evaluate due to excess of non-neoplastic thymocytes in the intermediate histotypes, our results support the presence of a continuum of genomic aberrations between B2/B3, B3 and TC histotypes (Figure 3.15B).

Chromosome arm-level CN loss of 13q is a candidate marker of poor prognosis

Loss of 13q was associated with a poorer TTP (log rank p=0.013; Figure 3.15C) and DRS (p=0.063; Figure 3.15D). Arm-level CN loss of 13q was found only in more aggressive histotypes (B3 and TC). Deletions of the whole or parts of chromosome 13 have been shown to have survival implications in other tumors, such as multiple myeloma (whole chromosome 13) [213] and breast cancer (13q12-13) [214]. The limited number of tumors carrying chr13 arm level CN loss limits the possibility to draw definitive conclusion on this candidate prognostic marker. Thus, confirmation in an independent series is recommended.

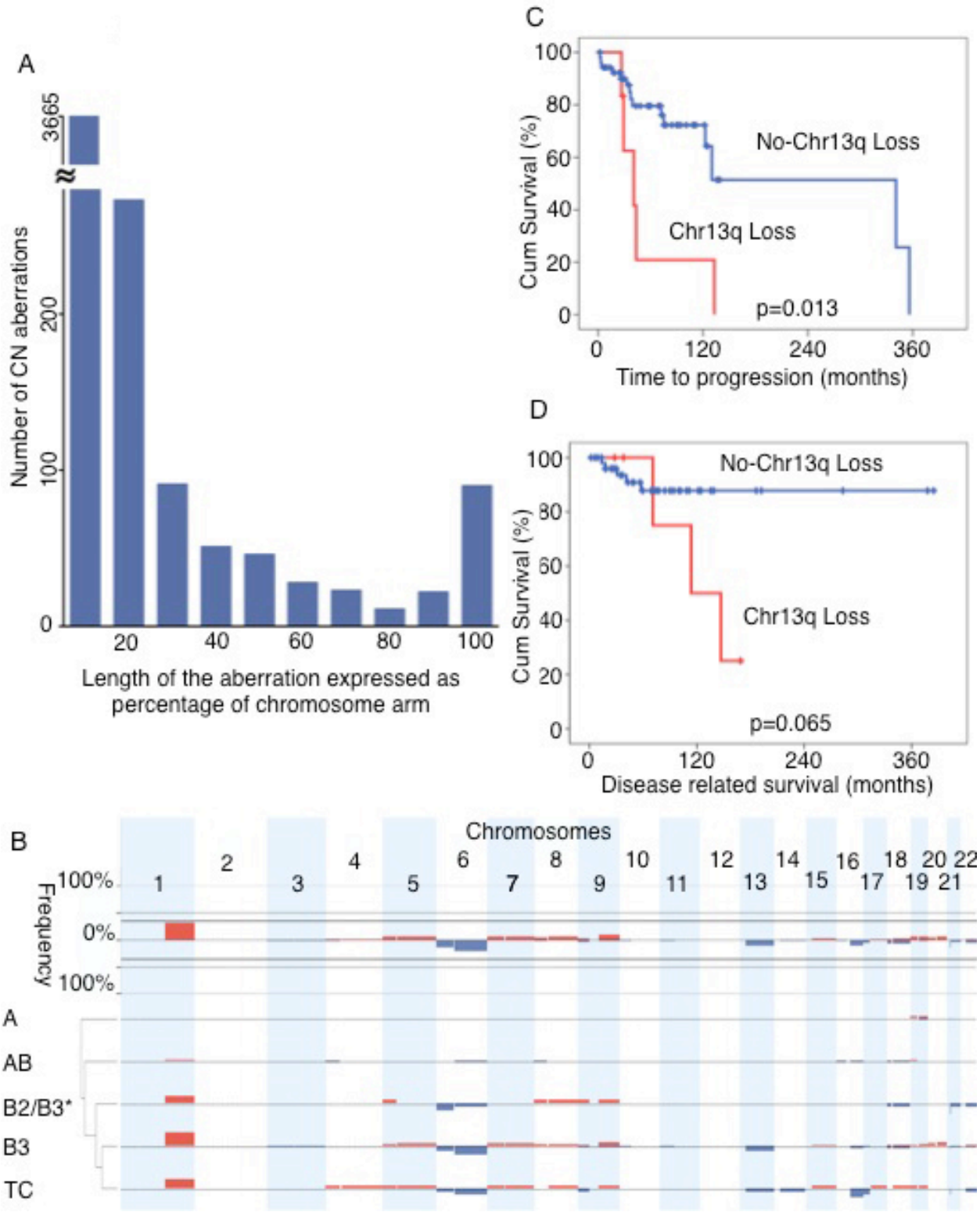
A
3665
Number of CN aberrations
200
100
0
20
40
60
80
100
Length of the aberration expressed as percentage of chromosome arm
C
Cum Survival (%)
100
80
60
40
20
0
No-Chr13q Loss
Chr13q Loss
p=0.013
0
120
240
360
Time to progression (months)
D
Cum Survival (%)
No-Chr13q Loss
Chr13q Loss
p=0.065
Disease related survival (months)
B
Chromosomes
1
2
3
4
5
6
7
8
9
10
11
12
13
14
15
16
17
18
19
20
21
22
Frequency
100%
0%
100%
A
AB
B2/B3*
B3
TC

Figure 3.15: Arm-level CN aberrations in thymic epithelial tumors identified by array CGH. (A) Arm-level CN aberrations were divided into 10 categories according to their cumulative lengths covering the percentage of their respective mapping chromosome arm. The number of CN aberrations cumulatively covering <10% of the chromosome arm-length were the most abundant. The power function $y=6.5636x^{-2.546}$ summarizes the distribution of CN aberrations based on chromosome arm-length from 0 to 80%, and based on this equation the expected number of 90-100% arm length CN aberrations was 7 instead of 90 observed ($\chi 2$ $p<0.001$). (B) Arm level CN gains (red) and losses (blue) of autosomal chromosomes. The top panel depicts the overall summary of frequency of arm level CN aberrations. The arm level CN aberrations grouped by histotype (A, AB, B2+B2/B3, B3 and TC) are summarized in the bottom panel. * indicates B2 and B2/B3. Thymic carcinomas and B3 thymomas exhibit similar patterns of arm level CN aberrations. Only few arm level CN aberrations were observed in A thymomas. (C) Time to progression curves in relation to 13q CN loss. (D) Disease related survival curves in relation to 13q CN loss.

Identification of significant CN aberrations in thymic epithelial tumors by GISTIC algorithm

In order to identify CN aberrations driving the cancer phenotype, we applied the GISTIC algorithm [208] to TET array CGH data. Q-value < 0.25 was considered significant. We identified 72 peaks of CN gain (817 genes + 23 miRNAs) and 54 of CN loss (155 genes + 3 miRNAs) (Figure 3.16A and B).

Of the genes mapped into GISTIC peaks, known cancer-related genes were selected and depicted in Figure 3.16A and 3.16B based on the following criteria: (1) those present in focal GISTIC peaks (< 5Mb), (2) recurrent (occurred in at least 2 tumors) and (3) and in peaks containing few genes (<15 genes). CN aberrations of CDK4, CDKN2A/B and IKBKB have been previously reported in other tumors [209]. Other known cancer-related genes identified in our analysis include HRAS and AKT/mTOR pathway signal transduction genes (PIK3CD and ATK1), or belong to FGF receptor family (FGFR3). Interestingly many genes regulating programmed cell death were also found in GISTIC peaks (BCL2, BCL-XL, PDCD1, CRK) suggesting an important role of apoptosis in TET pathogenesis. Moreover, CN loss of a DNA damage repair gene FANCF suggests a link with BRCA/ATM pathway and uncontrolled cell cycle progression [215].

To further narrow down candidate genes potentially relevant to TET biology, we evaluated the implication of CN aberrations on survival. The CN status of each gene locus was assessed in relation to DRS. A total of 418 genes (373 in CN gain; 45 in CN loss) and 15 miRNAs (11 in CN gain and 4 in CN loss) were found to be associated with DRS ($p<0.05$). Thirty-eight genes and two miRNAs were located in 6 GISTIC significant peaks (Figure 3.16C). We then assessed which of the 40 loci were also significantly associated with TTP (p

< 0.05). Only two loci significantly correlated with both poor DRS and TTP: CN gain of BCL2 and homozygous loss of CDKN2A/B loci (Figure 3.16C). The results of this exploratory analysis allowed us to pinpoint candidate genes relevant for tumor biology, to be further experimentally validated. The presence of other important genes for cancer growth was not excludible because the relative small number of tumor limited the statistical power of this analysis. However, this is larger series of array CGH in TETs to date.

CDKN2A CN loss correlates with low p16INK4 expression and poor prognosis

Cases carrying homozygous 9p21.3 CN loss (2 B3 thymomas and 2 TCs) had a significantly worse DRS (Log Rank p=0.021) and TTP (Log Rank p=0.019). Focal deletion of 9p21.3 is a frequent event in cancer (40% overall and 16% focal CN loss) [209], and poor outcome for patients carrying 9p21.3 deletion has also been described in lymphoblastic leukemia [216]. This region contains two known tumor suppressor genes, CDKN2A and CDKN2B. We confirmed array CGH CN loss of CDKN2A locus by CN-PCR. Copy number losses of CDKN2A locus were evaluated in 5 samples without and 4 samples with CDKN2A CN loss identified by CGH, and CGH results were confirmed in all samples (Fisher exact test p= 0.008).

We evaluated p16INK4 expression in TET samples using a tissue microarray containing 132 TET tumors, which include those evaluated by array CGH. None of the 5 tumors carrying 9p21.3 CN loss expressed p16NK4. Out of 119 evaluable cases, 34 were positive for p16INK4, which correlated with better DRS (Figure 3.16D and E; log rank p=0.041). These data suggest p16INK4 as a potential prognostic factor in TET. Interestingly, 61% of the primary TETs (34/56) and the three TET cell lines showed no detectable

p16INK4 expression in the absence of CDKN2A CN loss (Figure 3.16F) indicating that negative p16INK4 expression was not exclusively due to CDKN2A CN loss. The loss of p16INK4 expression in those tumors could be related to p16INK4 promoter methylation [147,153] or miR-24 deregulation [217].

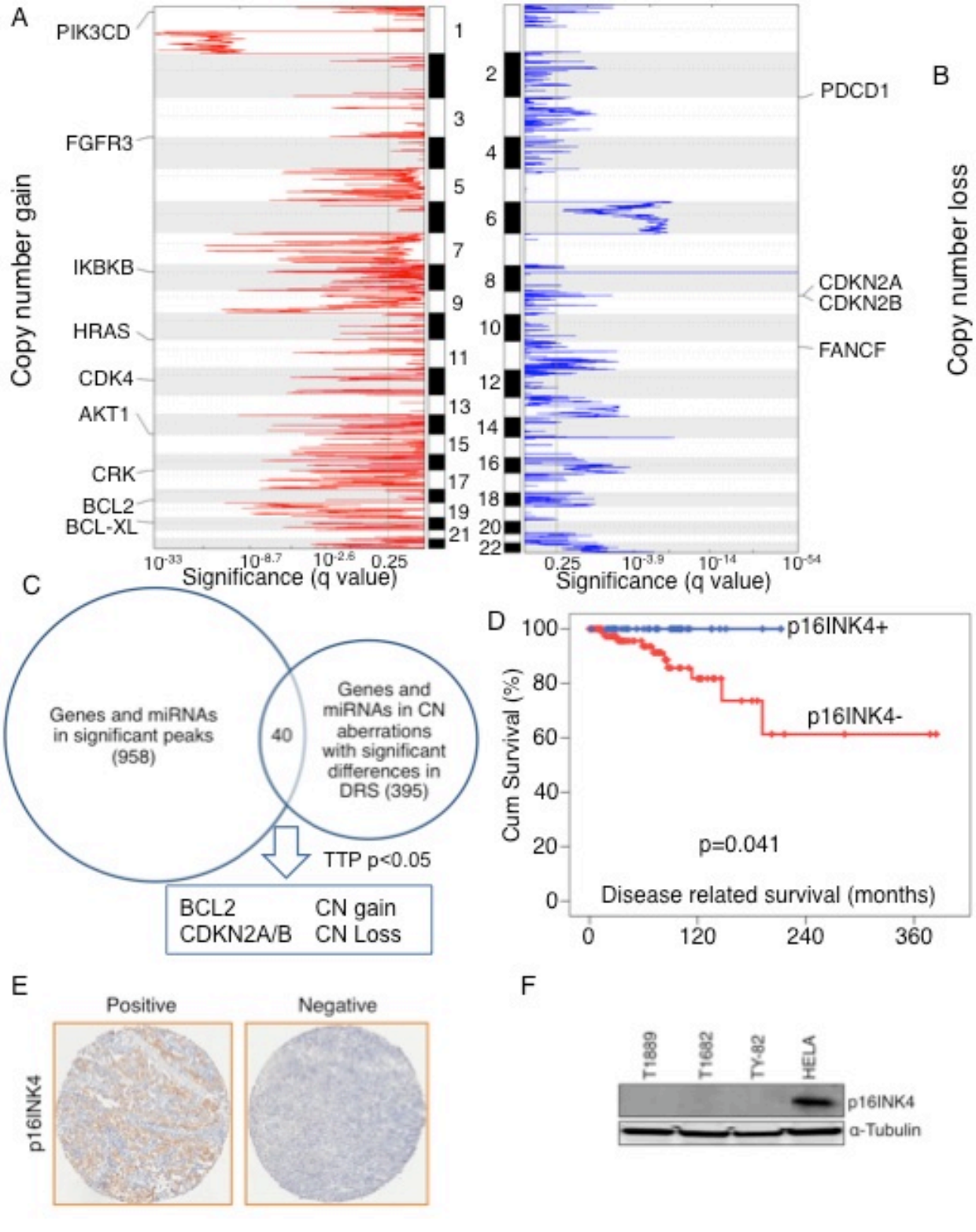
A
PIK3CD
FGFR3
IKBKB
HRAS
CDK4
AKT1
CRK
BCL2
BCL-XL
Copy number gain
Significance (q value)
B
PDCD1
CDKN2A
CDKN2B
FANCF
Copy number loss
Significance (q value)
C
Genes and miRNAs in significant peaks (958)
40
Genes and miRNAs in CN aberrations with significant differences in DRS (395)
TTP p<0.05
BCL2 CN gain
CDKN2A/B CN Loss
D
p16INK4+
p16INK4-
Cum Survival (%)
p=0.041
Disease related survival (months)
E
Positive
Negative
p16INK4
F
T1889
T1682
TY-82
HELA
p16INK4
α-Tubulin

Figure 3.16: Identification of significant CN aberration peaks with survival implications. (A) Peaks of CN gain and (B) CN loss identified by GISTIC algorithm. GISTIC q-values (x-axis) are plotted across the genome (y-axis). q value of 0.25 was used as cut-off value for significance (blue line). 13 cancer-related genes were identified in the GISTIC peaks. (C) Venn Diagram summarizes significant CN aberration peaks identified by GISTIC (left circle) and genes that were related to significant differences in disease-related survival (right circle). There were 40 shared-genes between the two groups. Only two genes were also significantly related to time to progression. TTP, time to progression; DRS, disease-related survival. (D) Disease-related survival in relation to CDKN2A expression evaluated by immunohistochemistry. (E) Representative p16INK4 positive and negative cases out of 119 thymic epithelial tumor samples evaluated by immunohistochemistry staining on tissue microarray. (F) p16INK4 expression in thymic epithelia tumor cell lines by Western blot. α-tubulin was used as loading control.

Table 3.13: Immunohistochemistry results for CDKN2A

		p16INK4			
	Total	**G0**	**G1**	**G2**	**G3**
Total	132	85	25	8	1
Female	65	43	15	3	1
Male	67	42	10	5	0
Tumor samples					
Primary	108	69	19	7	1
Relapse	24	16	6	1	0
Stage					
I	35	26	7	0	0
IIA	26	15	6	5	0
IIB	17	10	2	2	0
IIIA	16	7	4	1	0
IIIB	3	2	1	0	0
IVA	5	3	0	0	1
IVB	12	8	1	0	0
Na*	18				
Completeness of resection					
R0	79	50	14	5	1
R1	23	15	5	2	0
R2	10	6	1	0	0
Na	20				
WHO histotype					
A	15	6	5	1	0
AB	28	17	6	3	0
B1	24	18	5	0	0
B1/B2	6	4	0	1	0
B2	8	6	1	0	0
B2/B3	11	6	2	1	1
B3	24	16	5	1	0
C	14	10	1	1	0
Others	2				
Paraneoplastic syndromes					
No	91	60	15	7	1
Yes	34	21	10	0	0

Deregulation of BCL2 family genes in thymic epithelial tumors

BCL2 locus presented CN gain in 10% (6 out of 59) of the TET samples, including 1 type A, 2 B3 thymomas and 3 TCs.

Consistently with previous reports, MCL1 and BCL2 were frequently co-expressed in thymic carcinomas [131] and MCL1 CN gain is a frequent event in several cancers [209] We observed MCL1 CN gain in 51% of all TET cases especially in B3 (70%) and TC (57%). However, this CN gain was mainly the result of the whole 1q gain rather than focal MCL1 CN amplification.

To evaluate the significance of BCL2 and MCL1 CN aberrations in TETs, we studied the expression of BCL2 family genes in three TET cell lines. BCL2 expression was higher in TY82 and T1682 than in T1889 (Figure 3.17A), in agreement with the array CGH results showing that T1889 but not T1682 or TY82 carries CN loss of the BCL2 locus. In TET cell lines, BCL2 is co-expressed with other anti-apoptotic BCL2 family members (Figure 3.17A). While all TET cell lines expressed BAK, BAX expression was prominent only in T1682 (Figure 3.17A). To further dissect the significance of BCL2 family genes in TETs, BCL2, MCL1, BCL-XL, BCL-W and A1 were depleted in T1889, TY82 and T1689 cells by siRNA approaches, one by one (Figure 3.17B). Four siRNA plus the pull of them were used to knock down protein expression; a scramble siRNA was used as control. The extent of knock down and MTS assay results were correlated using a linear regression model. BCL2 knockdown significantly correlated significantly with the reduction of proliferation in all 3 cell-lines whereas MCL1 played a role only in T1889 and TY82 cells (Figure 3,17B). The results suggest that these cells may be addicted to BCL2 and MCL1 for growth (Figure 3.17D).

Taken together, these data suggest that BCL2 family genes are deregulated in TET cells and may play important roles in maintaining TET cell growth/survival.

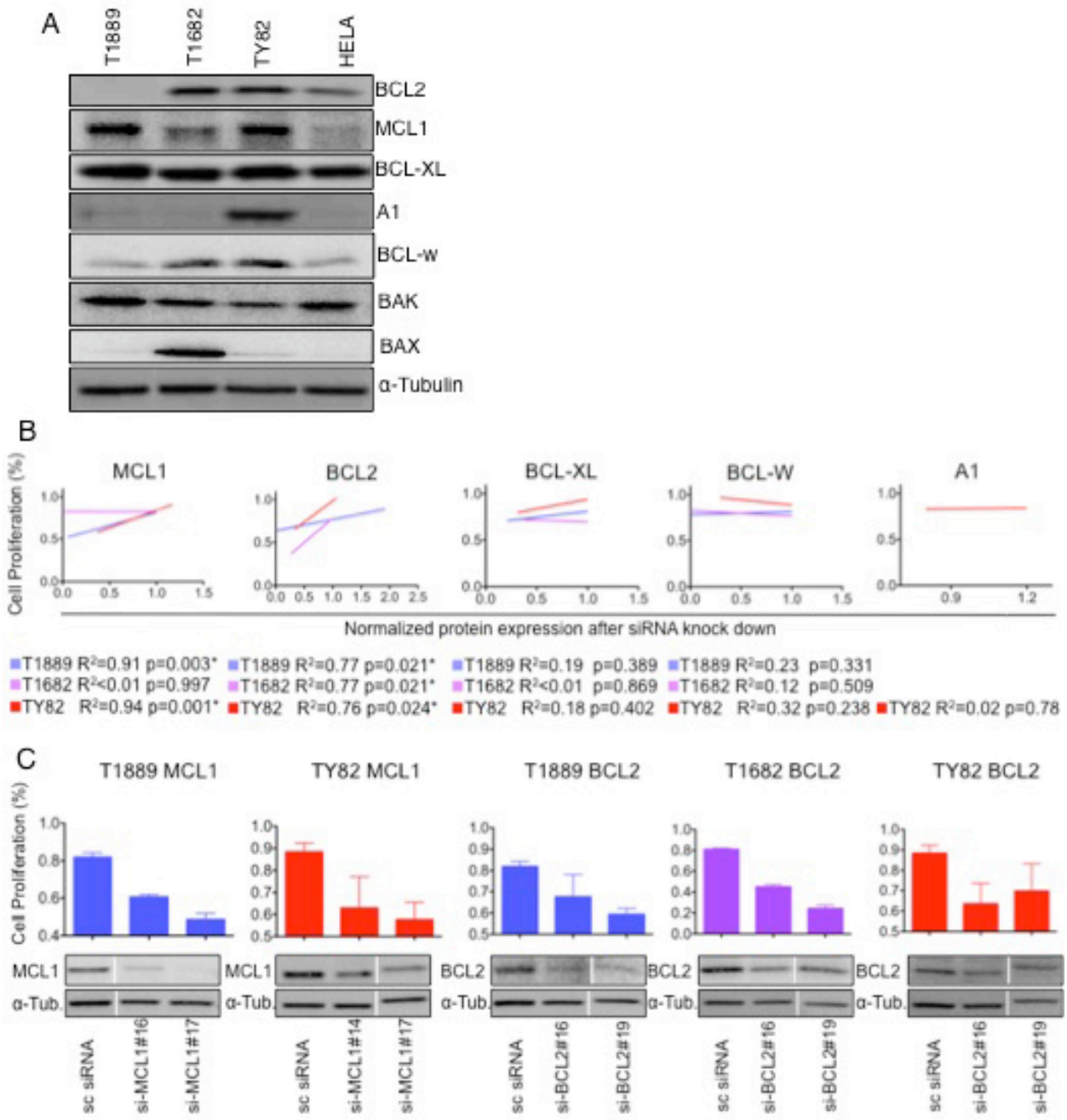

Figure 3.17: Deregulation of Bcl-2 family member genes in thymic epithelial tumors. (A) Expression of BCL2 anti-apoptotic and pro-apoptotic family members in thymic epithelial tumor cell lines. (B) Correlation between protein expression after siRNA knockdown of anti-apoptotic BCL2 family proteins (X axis) and inhibition of thymic epithelial tumor cell proliferation (Y axis). After 48 hours protein expression was evaluated by western blot in untreated cells and after transfection of siRNA pool, 4 individual siRNAs or scrambled siRNA (scRNA) as control. After 72 hours proliferation was tested by MTS assay in mock-transfected and transfected cells. MTS results were normalized to those of untreated cells, whereas protein expression to Tubulin-α and reported as percentage of protein expression in scRNA transfected cells. scRNA refers to scramble siRNA transfected cells; R2 indicates the determination coefficient and * denotes those p values <0.05 considered significant. (C) Results on proliferation of thymic epithelial tumor cell lines of the 2 most effective siRNA in knockdown of anti-apoptotic BCL2 family proteins. Data are normalized to untreated cells.

Thymic epithelial tumor cell lines are resistant to ABT263 treatment but sensitive to the combination with sorafenib

The dependence of TET cell growth on BCL2 and MCL1 (Figure 3.18B and C) prompted us to evaluate the potential application of these targets for treatment. For this purpose, we analyzed the sensitivity of the three TET cell lines to ABT263, a small-molecule BH3 mimetic that inhibits the anti-apoptotic proteins Bcl-2, Bcl-x_L and Bcl-w [218]. All TET cell lines were relatively resistant to ABT263 (Figure 3.18A), similar to an ABT263-resistant small cell lung cancer cell line (H82) that does not express BCL2 [218]. Resistance to ABT263 treatment has been linked to MCL1 expression [218]. Although T1682 expressed low level of MCL1, T1682 cells (IC50 = 2.52 uM) were highly resistant to ABT263 in MTS assay as compared to ABT263-sensitive H146 small cell lung cancer cells (IC50 = 33 nM) (Figure 3.10A), which may be attributed to the observation that ABT263 induced MCL1 expression in T1682 cells (Figure 3.18C). Sorafenib significantly attenuated MCL1 expression in MCL1 expressing TY82 and T1889 cell lines (Figure 3.18D). Sorafenib has recently been shown to be able to reduce MCL1 expression in cancer cells [219]. Intriguingly, the combination of sorafenib with ABT263 was highly synergistic in preventing cell proliferation in TET cell lines for most of the concentrations tested (Figure 3.18E). Our study suggests that TETs with BCL2 family gene deregulation may be highly sensitive to sorafenib/ABT263 combination therapy.

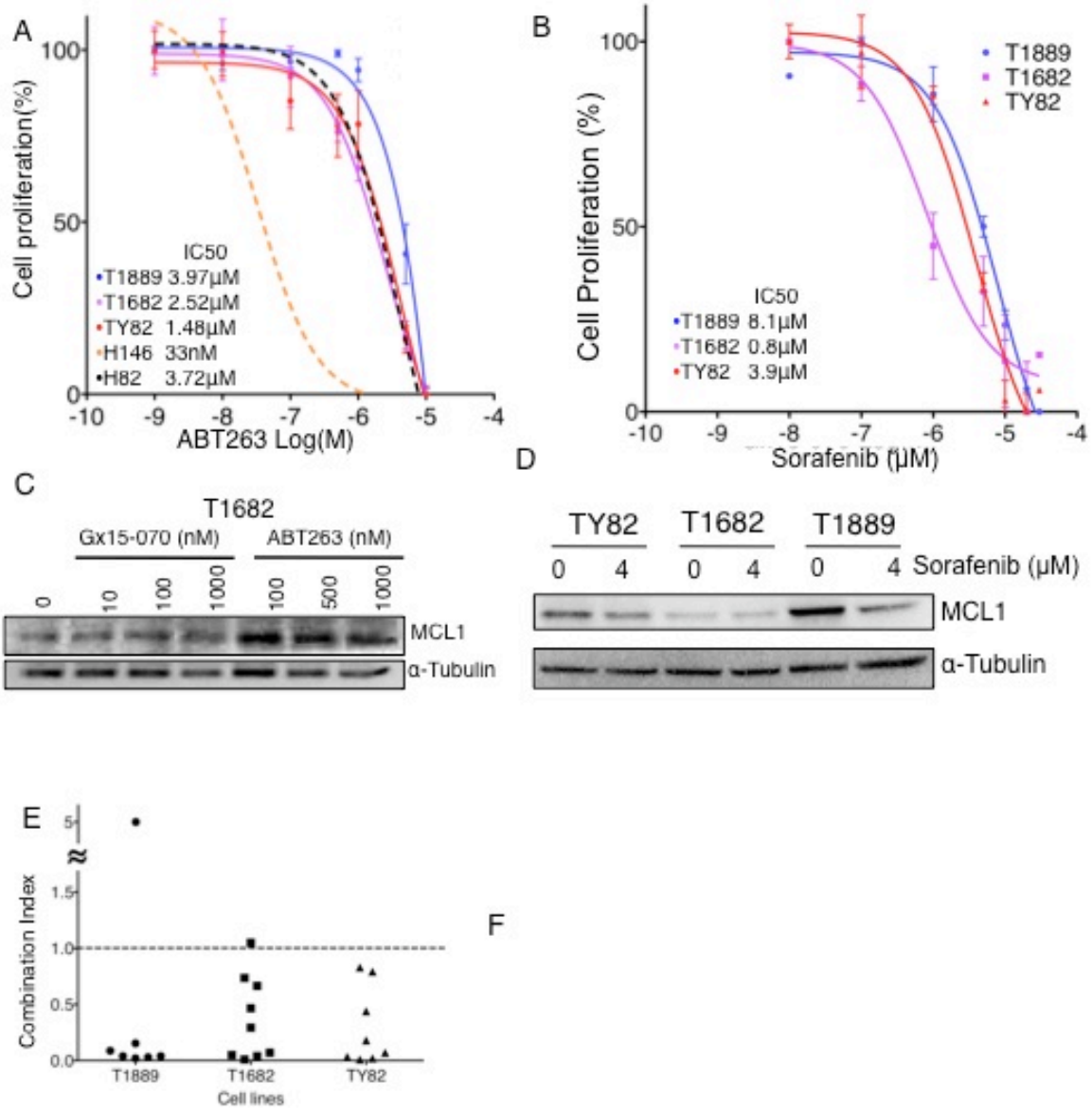

Figure 3.18: Effect of two Bcl-2 inhibitors, ABT263 and Sorafenib, in thymic epithelial tumor cell lines. MTS assay of (A) ABT263 and (B) Sorafenib in thymic epithelial tumor cell lines and control cell lines. H146, H82 small cell lung cancer cell lines were used as references in ABT263 experiments [218]. (C) In T1682 cells, ABT263 treatment increases MCL1 level compared to untreated cells or Gx15-070 treatment. (D) Treatment with 4μM sorafenib for 48h reduced expression of MCL1 in those thymic epithelial tumor cell lines with higher basal levels of MCL1 (T1889 and TY82). (E) Combination index computed by

Calcusyn for ABT263-sorafenib combination in three thymic epithelial tumor cell lines. Values <1 were considered synergistic. Detailed results are reported in table 3.14.

Table 3.14: Combination Index for ABT263 plus Sorafenib treatment.

T1889			T1682			TY82		
ABT263 (μM)	**Sorafenib (μM)**	**CIx**	**ABT263 (μM)**	**Sorafenib (μM)**	**CIx**	**ABT263 (μM)**	**Sorafenib (μM)**	**CIx**
1	1	5.893	0.1	0.1	0.293	0.1	0.1	0.439
3.49	5.58	0.03	0.5	0.5	0.465	1	1	0.792
3.97	6.98	0.04	1	1	0.665	1.3	2.77	0.83
5	5	0.087	2.22	1.21	0.07	1.48	3.46	0.18
5.96	10.47	0.04	2.52	1.51	0.05	5	5	0.034
7.94	13.96	0.02	5	5	1.05	2.22	5.19	0.02
10	10	0.153	3.78	2.27	0.04	2.96	6.92	<0.01
			5.04	3.02	0.01	10	10	0.07
			10	10	0.736			

List the results of the combination treatment for ABT263 and sorafenib, calculated using Calcusyn. Several doses of the two drugs were used for thymic epithelial tumor cell lines. CIx= combination index; Most values constitute synergistic combinations (CI < 1)

Gx15-070 inhibits thymic epithelial tumor cell growth through autophagy and necroptosis

To further explore the role of the deregulated BCL2 family proteins in TET cells, we assessed the sensitivities of TET cell lines to Obatoclax (Gx15-070, a small molecule pan-BCL2 family inhibitor) [220]. All TET cell lines were remarkably sensitive to Gx15-070 with IC50s ranging from 36 to 100 nM (Figure 3.19A). Gx15-070 significantly suppressed the growth of TY82 xenografts in nude mice (Figure 3.19B). To understand the mechanism of action of Gx15-070 in TET cells, we studied whether Gx15-070-induced cell death is caspase-3 dependent after 48-h treatment (Figure 3.20A). Although upon exposure to 1000 nM Gx15-070, 60% of T1682 cells underwent cell death, whereas at 100 nM ABT263 only 25% of the cells were dead (Figure3.19D), western blot analysis revealed that cleavage of PARP and caspase-3 was predominantly observed in T1682 cells treated with ABT263 but not with Gx15-070 (Figure 3.19C).

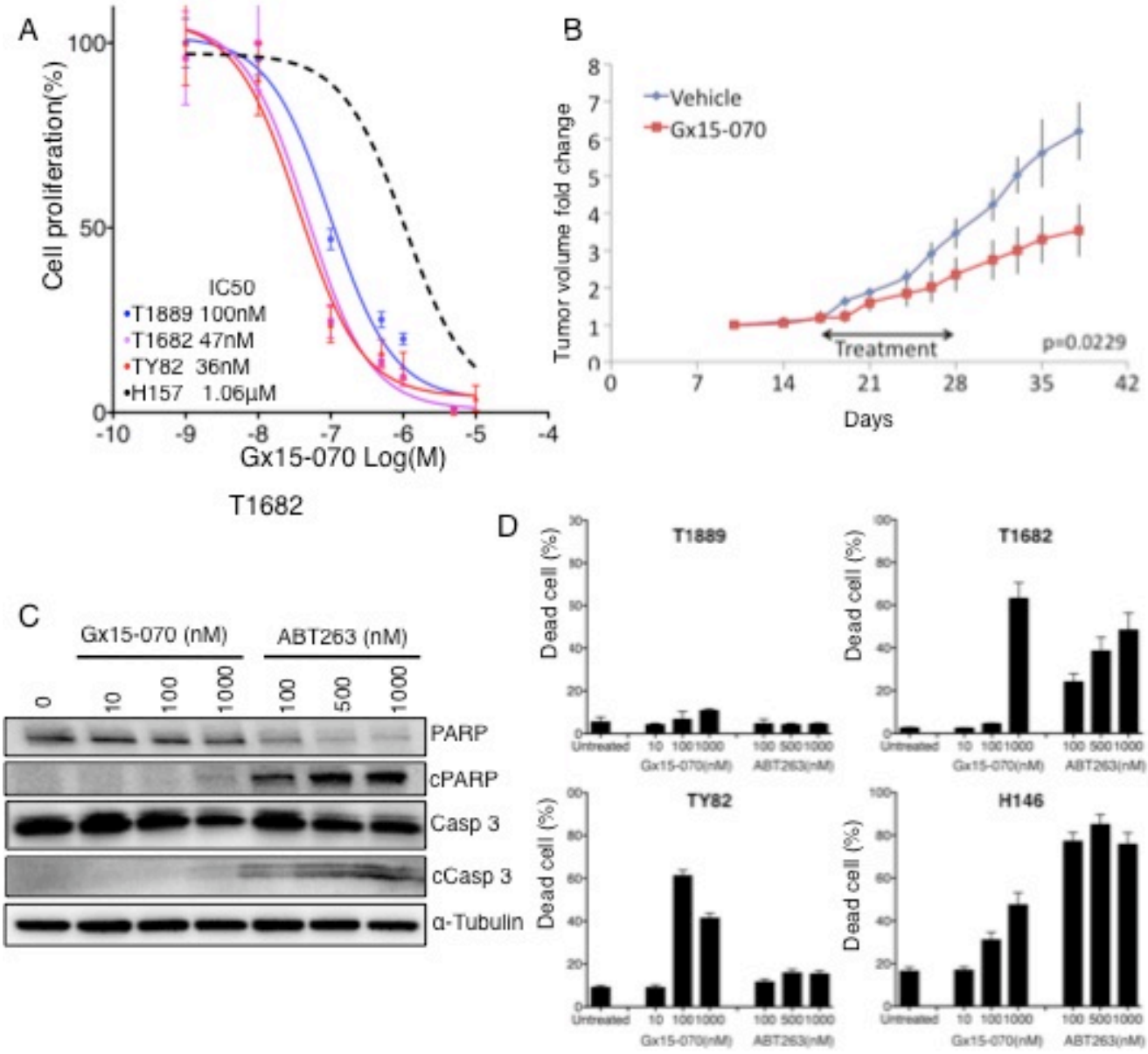
A
Cell proliferation(%)
IC50
T1889 100nM
T1682 47nM
TY82 36nM
H157 1.06μM
Gx15-070 Log(M)
T1682
B
Tumor volume fold change
Vehicle
Gx15-070
Treatment
p=0.0229
Days
C
Gx15-070 (nM)
ABT263 (nM)
PARP
cPARP
Casp 3
cCasp 3
α-Tubulin
D
T1889
T1682
TY82
H146
Dead cell (%)
Untreated
Gx15-070(nM)
ABT263(nM)

Figure 3.19: Effect of GX15-070, (A) in thymic epithelial tumor cell lines MTS assay of ABT263 and Gx15-070 in thymic epithelial tumor cell lines; H157 non-small cell lung cancer cell line was used as negative control because reported resistant[218]. (B) Gx15-070 suppressed the growth of TY82 xenografts. Average fold change of tumor volume of 10 mice treated by Gx15-070 and 10 by vehicle alone were reported. The black arrow delimitates the timing of treatment. (C) Cleavage of PARP and caspase-3 was assessed by western blot after 48-hour treatment with various concentrations of GX15-070 and ABT263 in T1682 cells. (D) Cell death induced by Gx15-070 and ABT263 was expressed as percentage of dead cells over total number of cells (cell death %). Cells were treated with the indicated concentrations of Gx15-070 and ABT263 for 48 hours, stained with TOPRO3 followed by flow cytometry analysis.

Moreover, Gx15-070 treatment did not enhance caspase-3 activity in TET cell lines (Figure 3.20). In contrast, induction of caspase-3 activity was clearly observed in ABT263-treated BCL2-positive TET cells (Figure 3.20). Together these findings suggest that Gx15-070-induced cell death is caspase-3 independent. This notion was further supported by the finding that the pan-caspase inhibitor ZVAD-FMK was not able to restore cell proliferation after Gx15-070 treatment in TET cell lines (Figure 3.22A).

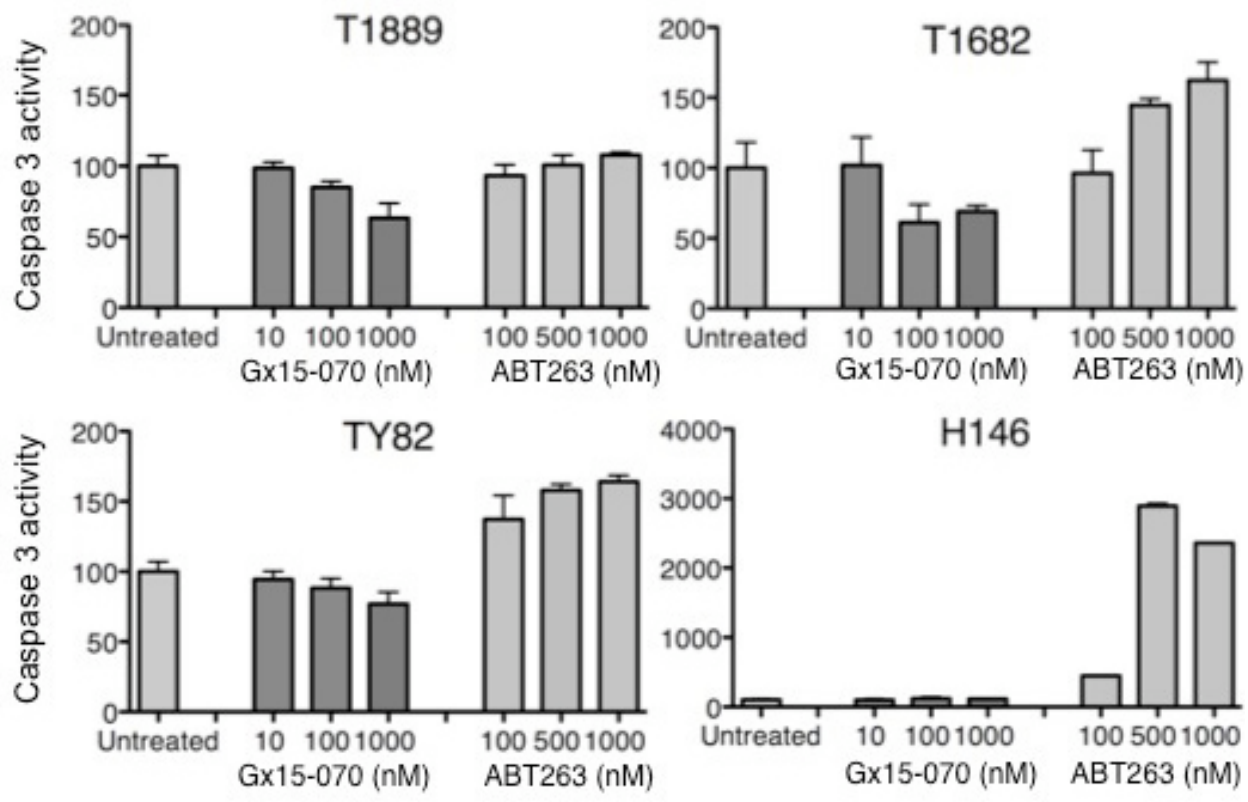

Figure 3.20: Caspase 3 activity in thymic epithelial tumor cell lines treated with Gx15-070 or ABT263. Caspase 3 activity was determined by colorimetric activity assay kit according to the manufacturer's instructions. H146 was used as a control. Activities were expressed as percentage of untreated cells.

As Gx15-070 only elicited minimal cell death in T1889 cells (Figure 3.19D), we examined the effect of Gx15-070 on cell proliferation. Though no sign of cell cycle arrest was found (data not shown), a dramatic increase of cell doubling time was observed in all Gx15-070-treated TET cell lines (Figure 3.21A-C). Together, our data suggest that Gx15-070 treatment of TET cells leads to both growth inhibition and cell death.

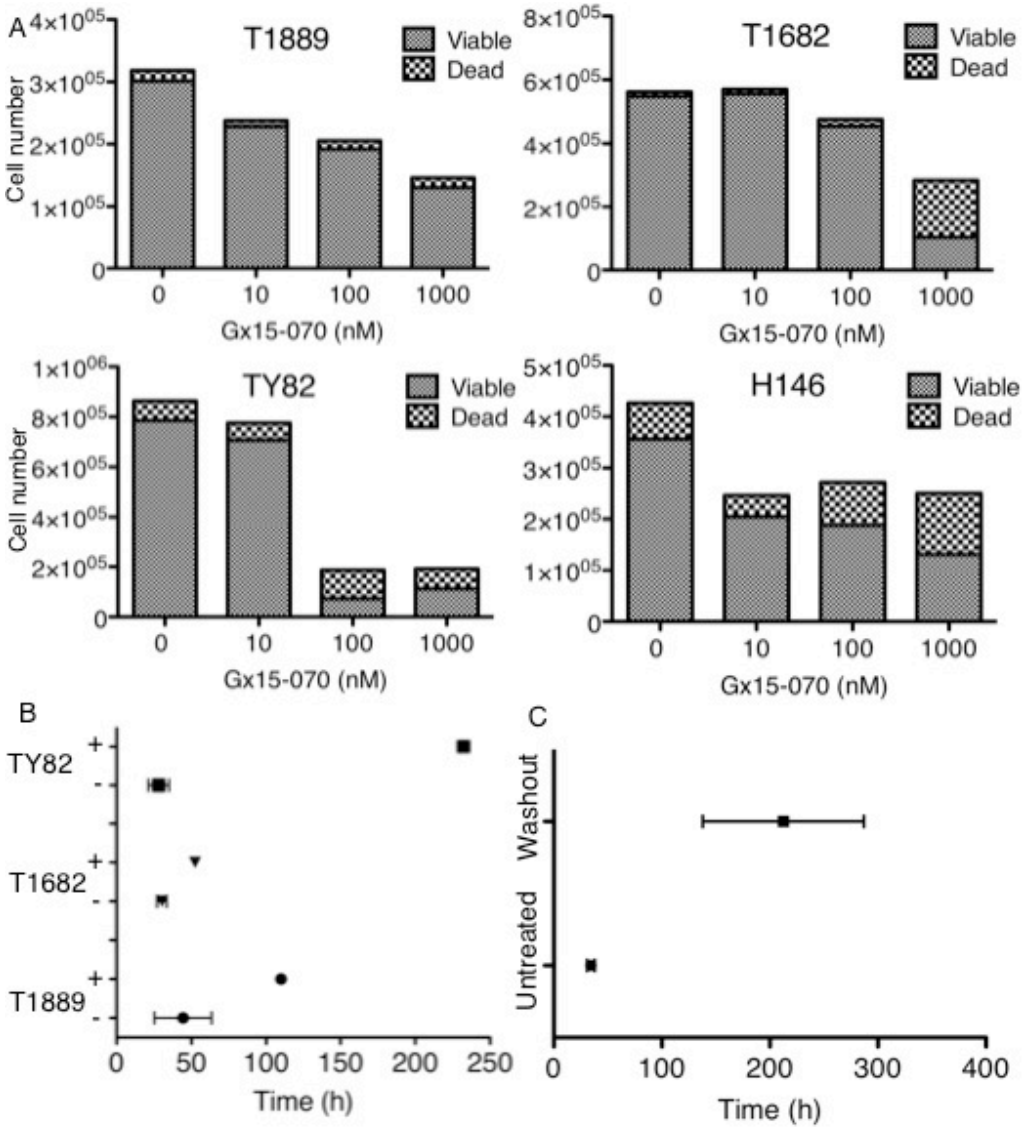

Figure 3.21: Gx15-070 induces arrest of cell proliferation in thymic epithelial tumor cell lines. (A) The number of viable cells and dead cells was reported for thymic epithelial tumor cell lines and H146 after 48-hour treatment with the indicated doses of Gx15-070. Number of viable and dead cells was calculated using TOPRO3 to evaluate membrane permeability by flow cytometry. (B) Gx15-070 increases doubling times of thymic epithelial tumor cells. Doubling time was determined by counting the cells every 24 hours for a period of 120 hours in the presence (+) or absence (-) of 250nM Gx15-070. (C) Even after 48-hour drug washout the mean doubling time of thymic epithelial tumor cell lines was still increased for treated cells. Cells were exposed to Gx15-070 for 48 hours. Data were reported as mean ± standard deviation.

Because recent studies suggested that Gx15-070 induces autophagy-dependent necroptosis in acute lymphoblastic leukemia cells [221], we performed electron microscopy in TET cells: changes in mitochondrial structure were demonstrated as early signs of autophagy after 1h Gx15-070 treatment (Figure 3.22B). After 6-hour treatment, cytoplasm vacuolization and mitochondrial swelling with early signs of necroptotic cell death were evident. Intriguingly, cytoplasmic vacuolization, late-stage necroptotic or autophagic cell death were the main features 48h after Gx15-070 (1μM) treatment. Electron microscopy showed no sign of apoptotic cell death; consistent with the observation that caspase-3 was not involved in Gx15-070-induced cell death. We also examined accumulation of the autophagy marker LC3B-II, after Gx15-070 treatment. As shown in Figure 3.22C, LC3B-II accumulation was detected in all Gx15-07-treated TET cell lines and occurred as early as 1h after Gx15-070 treatment, suggesting that Gx15-070 activates the autophagy pathway in TET cells. To further determine if the Gx15-070-induced cell death is necroptotic cell death and the death is autophagy-dependent, we evaluated the effect of necrostatin 1 (Nec1; necroptosis inhibitor) and chloroquine (CQ; autophagosome maturation inhibitor) in Gx15-070-treated TET cells and demonstrated that Gx15-070-induced growth inhibition (Figure 3.22A) and cell death (Figure 3.23) could be effectively rescued by necroptosis and autophagy inhibition. More importantly, depletion of Beclin 1 (BECN1), a key regulator of autophagy pathway, and RIPK1, a key regulator of necroptotic pathway (Figure 3.22D) recapitulated the results obtained with Nec1 and CQ (Figure 3.22A). In line with previous reports, our results suggest that Gx15-070-induced necroptosis and autophagy [221].

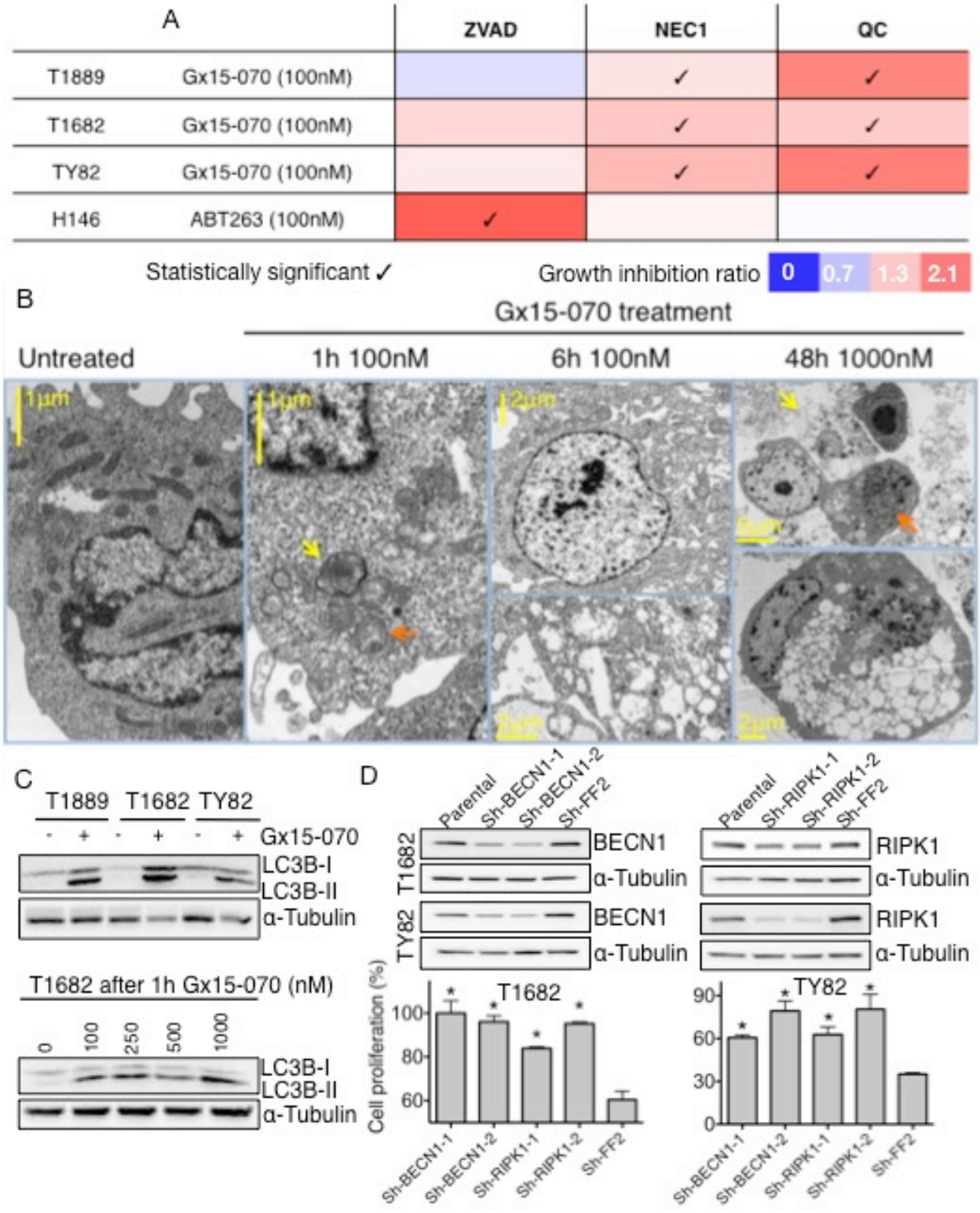
A
ZVAD
NEC1
QC
T1889
Gx15-070 (100nM)
T1682
Gx15-070 (100nM)
TY82
Gx15-070 (100nM)
H146
ABT263 (100nM)
Statistically significant ✓
Growth inhibition ratio
0
0.7
1.3
2.1
B
Gx15-070 treatment
Untreated
1h 100nM
6h 100nM
48h 1000nM
1μm
1μm
2μm
5μm
2μm
2μm
C
T1889
T1682
TY82
Gx15-070
LC3B-I
LC3B-II
α-Tubulin
T1682 after 1h Gx15-070 (nM)
0
100
250
500
1000
LC3B-I
LC3B-II
α-Tubulin
D
Parental
Sh-BECN1-1
Sh-BECN1-2
Sh-FF2
T1682
BECN1
α-Tubulin
TY82
BECN1
α-Tubulin
Parental
Sh-RIPK1-1
Sh-RIPK1-2
Sh-FF2
RIPK1
α-Tubulin
RIPK1
α-Tubulin
Cell proliferation (%)
T1682
100
80
60
TY82
90
60
30
0
Sh-BECN1-1
Sh-BECN1-2
Sh-RIPK1-1
Sh-RIPK1-2
Sh-FF2

Figure 3.22: GX15-070 induces autophagy and necroptosis in thymic epithelial tumor cells. (A) Heatmap summarizes the rescue effects of caspase (50 μM ZVAD-FMK), necroptosis (30 μM NEC1), and autophagosome maturation (25 μM CQ) inhibitors on GX15-070-induced growth inhibition. Percentage of reduction in cell growth induced by 100nM Gx15-070 was calculated from the MTS data in the presence or absence of the indicated inhibitors. Value >1 (red): rescue of GX15-070 effect; Value = 1 (white): no effect; Value <1 (green): enhanced Gx15-070 effect. (B) Time-course electron microscopic morphology of T1682 cells treated with Gx15-070 at the indicated concentrations. After 1-hour treatment, lamellar bodies (yellow arrow) consistent with early signs of autophagy and mitochondrial structural changes with loss of cristae (orange arrow) were evident. After 6-hour treatment, early signs of necroptosis with intact nuclear envelope (top panel), and mitochondrial swelling with loss of mitochondrial matrix and cytoplasm vacuolization were observed (bottom panel). After 48-hour treatment, late stages of necroptotic cell death (yellow arrow) and advanced stages of autophagy (orange arrow) were evident. The bottom panel depicts advanced stage of autophagic cell death with cytoplasmic vacuolization and lamellar bound structures consistent with autophagosomes. (C) GX15-070 (1μM) induced LC3BII accumulation after 48 hours treatments in thymic epithelial tumor cells (top blot). LC3BII accumulation was observed in T1682 cells 1-hour after GX15-070 treatment at a concentration as low as 100nM (bottom blot). (D) shRNA knock-down of Beclin1 (sh-BECN1-1 and sh-BECN1-2) and RIPK1 (sh-RIPK1-1 and sh-RIPK1-2) in T1682 and TY82 cell lines. Western blot shows protein expression in parental cells , cells treated with the target shRNAs , and with a vector control (sh-FF2) carrying anti-exogenous luciferase shRNA FF2. MTS results show that shRNA knockdown of BECN1 and RIPK1 reduces the effect of Gx15-070 on cell

proliferation compared to vector control. * denotes statistically significant differences compared to control.

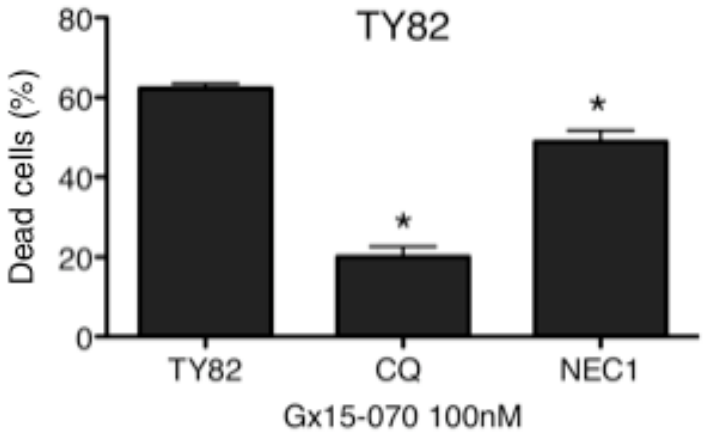

Figure 3.23: Percentage of cell death was calculated by LDH release (Cyto Tox assay) after 48-hour 100nM Gx15-070 treatment for TY82 cell line. Both necroptosis inhibitor NEC1 (30μM) and autophagy inhibitor CQ (25μM) significantly reduced the amount of cell death (One way ANOVA $p<0.0001$); Dunn post-hoc p value was <0.05 for all cells treated with inhibitors plus Gx15-070 compared to cells treated by Gx15-070 alone.

4. Discussion and conclusions

4. **Discussion and conclusions**

The evaluation of genomic aberrations of TETs revealed CDKN2A as candidate prognostic factors and BCL2 antiapoptotic proteins targets suitable for therapy. Firstly, we evaluated the expression of BRD4 –NUT fusion gene and the frequency of KIT mutations, two known genomic aberrations of TETs: but a remarkably low frequency was estimated for these molecular events. Thus, a genome wide approach was adopted starting from whole genome sequencing of a B3 thymoma. Whole exome sequencing was adopted to search for recurrent mutations in TETs and to expand knowledge learned from whole genome sequencing. An heterogeneous pattern of mutations was estimated from exome sequencing data, however, recurrent CN loss interesting CDKN2A and CDKN2B loci as well as CN gains of BCL2 were identified. Therefore the presence of these genomic aberrations was determined in a larger series of FFPE tumors collected retrospectively. Combining GISTIC analysis and patients' survival data, we established that focal CN gain of BCL2 and CN loss of CDKN2A/B loci were the only CN aberrations that significantly correlated with both DRS and TTP. Moreover, loss of $p16^{INK4}$ expression was associated with worse prognosis. Using siRNA and small molecule inhibitor approaches, we showed that TET cells underwent autophagy-dependent necroptosis after Gx15-070 treatment and that ABT263-sorafenib combination inhibited TET cell growth, providing the first preclinical evidence that deregulated BCL2 family genes may serve as suitable targets for TET therapies.

Large arm-level aberrations identified in our study are in general agreement with genetic alterations reported by conventional CGH [115,222,223]. Only few CN aberrations and LOHs have been reported for type A thymomas, which have a very indolent behavior and excellent survival [223]. B2/B3 thymomas showed frequent arm-level CN gain of 1q and loss of

chromosome 6, together with other CN aberrations that are present in less than 20% of the cases. B3 thymomas and TCs displayed a pattern of CN aberrations similar to B2/B3 tumors except for the losses of 13q, 16q and 17p, which were not observed in B2/B3 tumors. Consistent with data from frozen tumors and previous reports [95,222], hierarchical cluster analysis of arm-level CN aberrations revealed that type A thymomas were very distantly related to aggressive tumors (B3 and C), suggesting that arm-level CN aberrations associates with aggressive disease. In addition, loss of 13q, which has been previously described in B3 and TC by conventional CGH [115], correlated with worse prognosis. RB1, a well-characterized tumor suppressor gene, has been mapped to 13q. From the patients evaluated for exome sequencing, 29% presented deletion of chromosome 13q: all of them were infiltrating tumors (stage IIB-IVB) and classified as aggressive histotypes: 2 thymic carcinomas, 3 B and 2 B2 thymomas. We found only one TET with concomitant loss of 13q and CDKN2A locus. CDKN2A encodes p16INK4 and p14ARF via alterative splicing. As p16INK4, an inhibitor of CDK4-cyclin D, acts upstream of RB, inactivation of either gene will be in theory sufficient to compromise the RB pathway. The near mutual exclusive loss of 13q and CDKN2A which together represented 15% (9/59) of TETs in our series suggests that the RB pathway plays an important role in TET pathogenesis.

Using GISTIC algorithm we identified several cancer related genes involved in cell cycle control (CDKN2A/B and CDK4), or intracellular signal transduction (AKT1, PIK3CD and HRAS). Interestingly many of these genes (BCL2, BCL-XL, PDCD1, CRK) were related to apoptosis control, and BCL2 CN gain correlated with poorer TTP and DRS. CN gain of MLC1, another member of the BCL2 family gene, was found in 51% of TETs. This CN gain was more frequent in aggressive histotypes (83% B2/B3, 70% B3 and 57%TC). However,

MCL1 CN gain was mainly the result of the whole 1q gain rather than focal MCL1 CN amplification.

The oncogenic role of BCL2 is well-known in follicular lymphomas in which constitutive BCL2 activation due to IgH-BLC2 juxtaposition is thought to result in lymphomagenesis by interfering with the normal apoptosis of B lymphocytes [224]. BCL2 overexpression was observed in other types of lymphoproliferative disorders and small cell lung cancer [218]. In addition to their involvement in regulation of apoptosis, BCL2 family members are also involved in the regulation of autophagy and necroptosis pathways. We validated the functional significance of BCL2 family genes in TET cells via siRNA approaches, and demonstrated that all TET cell lines (T1889, TY82 and T1682) were addicted to BCL2, whereas T1889 and TY82 required MCL1 for growth and survival. More importantly, we showed that sorafenib (a multi-tyrosine kinase inhibitor), was capable of decreasing MCL1 expression [219] and that ABT263/sorafenib combination was highly synergic in inhibiting TET cell proliferation. We also showed that Gx15-070, a pan inhibitor of BH3 BCL2 anti-apoptotic family members, potently inhibited TET cell proliferation and induced cell death. Interestingly, cell death could be rescued by Beclin1, RIPK1 knockdown or by autophagy and necroptosis inhibition, suggesting that Gx15-070-induced a block of cell proliferation autophagy-dependent. Taken together, our data strongly indicate that BCL2 family genes are deregulated in TET cells and potential targets for TET treatment. The effect of Gx15-070 was not limited to in-vitro models of TET, indeed a mouse xenograft of TY82 was established and inhibition of cell proliferation demonstrated. Tumors in the 10 treated mice grow slower than those in the 10 untreated animals (Figure 3.19). These data support the design of a phase 2 clinical trial of Gx15-070 in TET patients since safety data are already available from phase I reports.

In conclusion, we identified CN losses of CDKN2A and 13q as poor prognostic candidate markers in TETs, implying that RB pathway deregulation may be important in TET pathogenesis. Focal BCL2 amplification suggests that this gene is deregulated in TETs and Gx15-070 may represent a novel treatment strategy for patients.

5. References

5. References

1. Bonfanti, P.*, et al.* Microenvironmental reprogramming of thymic epithelial cells to skin multipotent stem cells. *Nature* **466**, 978-982.
2. Rodewald, H.R. Thymus organogenesis. *Annu Rev Immunol* **26**, 355-388 (2008).
3. Blackburn, C.C. & Manley, N.R. Developing a new paradigm for thymus organogenesis. *Nat Rev Immunol* **4**, 278-289 (2004).
4. Rosai J. & G.D., L. Tumors of the Thymus. *Atlas of Tumors Pathology* (1976).
5. de Jong, W.K.*, et al.* Thymic epithelial tumours: a population-based study of the incidence, diagnostic procedures and therapy. *Eur J Cancer* **44**, 123-130 (2008).
6. Gadalla, S.M.*, et al.* A population-based assessment of mortality and morbidity patterns among patients with thymoma. *Int J Cancer* **128**, 2688-2694.
7. Engels, E.A. Epidemiology of thymoma and associated malignancies. *J Thorac Oncol* **5**, S260-265.
8. Welsh, J.S.*, et al.* Association between thymoma and second neoplasms. *JAMA* **283**, 1142-1143 (2000).
9. Souadjian, J.V., Silverstein, M.N. & Titus, J.L. Thymoma and cancer. *Cancer* **22**, 1221-1225 (1968).
10. Pan, C.C., Chen, P.C., Wang, L.S., Chi, K.H. & Chiang, H. Thymoma is associated with an increased risk of second malignancy. *Cancer* **92**, 2406-2411 (2001).
11. Travis, L.B., Boice, J.D., Jr. & Travis, W.D. Second primary cancers after thymoma. *Int J Cancer* **107**, 868-870 (2003).
12. Saib, A.*, et al.* Human foamy virus infection in myasthenia gravis. *Lancet* **343**, 666 (1994).
13. Liu, W.T., Kao, K.P., Liu, Y.C. & Chang, K.S. Human foamy virus genome in the thymus of myasthenia gravis patients. *Zhonghua Min Guo Wei Sheng Wu Ji Mian Yi Xue Za Zhi* **29**, 162-165 (1996).
14. Li, H.*, et al.* Absence of human T-cell lymphotropic virus type I and human foamy virus in thymoma. *Br J Cancer* **90**, 2181-2185 (2004).
15. Kuzmenok, O.I.*, et al.* Myasthenia gravis accompanied by thymomas not related to foamy virus genome in Belarusian's patients. *Int J Neurosci* **117**, 1603-1610 (2007).
16. Manca, N.*, et al.* Detection of HTLV-I tax-rex and pol gene sequences of thymus gland in a large group of patients with myasthenia gravis. *J Acquir Immune Defic Syndr* **29**, 300-306 (2002).
17. Mann, R.B.*, et al.* In situ localization of Epstein-Barr virus in thymic carcinoma. *Mod Pathol* **5**, 363-366 (1992).
18. Wu, T.C. & Kuo, T.T. Study of Epstein-Barr virus early RNA 1 (EBER1) expression by in situ hybridization in thymic epithelial tumors of Chinese patients in Taiwan. *Hum Pathol* **24**, 235-238 (1993).
19. Chen, P.C., Pan, C.C., Yang, A.H., Wang, L.S. & Chiang, H. Detection of Epstein-Barr virus genome within thymic epithelial tumours in Taiwanese patients by nested PCR, PCR in situ hybridization, and RNA in situ hybridization. *J Pathol* **197**, 684-688 (2002).
20. Engel, P.J. Absence of latent Epstein-Barr virus in thymic epithelial tumors as demonstrated by Epstein-Barr-encoded RNA(EBER) in situ hybridization. *APMIS* **108**, 393-397 (2000).

21. Rosai, J., Higa, E. & Davie, J. Mediastinal endocrine neoplasm in patients with multiple endocrine adenomatosis. A previously unrecognized association. *Cancer* **29**, 1075-1083 (1972).
22. Ferolla, P.*, et al.* Thymic neuroendocrine carcinoma (carcinoid) in multiple endocrine neoplasia type 1 syndrome: the Italian series. *J Clin Endocrinol Metab* **90**, 2603-2609 (2005).
23. Teh, B.T.*, et al.* Thymic carcinoids in multiple endocrine neoplasia type 1. *Ann Surg* **228**, 99-105 (1998).
24. Travis, W.D., Brambilla, E., Muller-Hermelink, H.K. & Harris, C.C. *Pathology and genetics: Tumors of the lung, pleura, thymus and heart.*, (IARC Press, Lyon, France, 2004).
25. Yamakawa, Y.*, et al.* A tentative tumor-node-metastasis classification of thymoma. *Cancer* **68**, 1984-1987 (1991).
26. Tsuchiya, R., Koga, K., Matsuno, Y., Mukai, K. & Shimosato, Y. Thymic carcinoma: proposal for pathological TNM and staging. *Pathol Int* **44**, 505-512 (1994).
27. Bedini, A.V.*, et al.* Proposal of a novel system for the staging of thymic epithelial tumors. *Ann Thorac Surg* **80**, 1994-2000 (2005).
28. Kondo, K. & Monden, Y. Therapy for thymic epithelial tumors: a clinical study of 1,320 patients from Japan. *Ann Thorac Surg* **76**, 878-884; discussion 884-875 (2003).
29. Kondo, K. Tumor-node metastasis staging system for thymic epithelial tumors. *J Thorac Oncol* **5**, S352-356.
30. Suster, S. & Moran, C.A. Thymoma classification: current status and future trends. *Am J Clin Pathol* **125**, 542-554 (2006).
31. Chen, G.*, et al.* New WHO histologic classification predicts prognosis of thymic epithelial tumors: a clinicopathologic study of 200 thymoma cases from China. *Cancer* **95**, 420-429 (2002).
32. Rieker, R.J.*, et al.* Histologic classification of thymic epithelial tumors: comparison of established classification schemes. *Int J Cancer* **98**, 900-906 (2002).
33. Verghese, E.T.*, et al.* Interobserver variation in the classification of thymic tumours--a multicentre study using the WHO classification system. *Histopathology* **53**, 218-223 (2008).
34. Giaccone, G., Wilmink, H., Paul, M.A. & van der Valk, P. Systemic treatment of malignant thymoma: a decade experience at a single institution. *Am J Clin Oncol* **29**, 336-344 (2006).
35. Detterbeck, F.C. & Parsons, A.M. Thymic tumors. *Ann Thorac Surg* **77**, 1860-1869 (2004).
36. Regnard, J.F.*, et al.* Prognostic factors and long-term results after thymoma resection: a series of 307 patients. *J Thorac Cardiovasc Surg* **112**, 376-384 (1996).
37. Maggi, G.*, et al.* Thymoma: results of 241 operated cases. *Ann Thorac Surg* **51**, 152-156 (1991).
38. Verley, J.M. & Hollmann, K.H. Thymoma. A comparative study of clinical stages, histologic features, and survival in 200 cases. *Cancer* **55**, 1074-1086 (1985).
39. Nakahara, K.*, et al.* Thymoma: results with complete resection and adjuvant postoperative irradiation in 141 consecutive patients. *J Thorac Cardiovasc Surg* **95**, 1041-1047 (1988).
40. Wilkins, K.B.*, et al.* Clinical and pathologic predictors of survival in patients with thymoma. *Ann Surg* **230**, 562-572; discussion 572-564 (1999).

41. Blumberg, D.*, et al.* Thymoma: a multivariate analysis of factors predicting survival. *Ann Thorac Surg* **60**, 908-913; discussion 914 (1995).
42. Quintanilla-Martinez, L.*, et al.* Thymoma. Histologic subclassification is an independent prognostic factor. *Cancer* **74**, 606-617 (1994).
43. Pan, C.C., Wu, H.P., Yang, C.F., Chen, W.Y. & Chiang, H. The clinicopathological correlation of epithelial subtyping in thymoma: a study of 112 consecutive cases. *Hum Pathol* **25**, 893-899 (1994).
44. Elert, O., Buchwald, J. & Wolf, K. Epithelial thymus tumors--therapy and prognosis. *Thorac Cardiovasc Surg* **36**, 109-113 (1988).
45. Sakamoto, M.*, et al.* Survival after extended thymectomy for thymoma. *Eur J Cardiothorac Surg* **41**, 623-627.
46. Wang, L.S., Huang, M.H., Lin, T.S., Huang, B.S. & Chien, K.Y. Malignant thymoma. *Cancer* **70**, 443-450 (1992).
47. Sugiura, H.*, et al.* Long-term results of surgical treatment for invasive thymoma. *Anticancer Res* **19**, 1433-1437 (1999).
48. Liu, H.C.*, et al.* Debulking surgery for advanced thymoma. *Eur J Surg Oncol* **32**, 1000-1005 (2006).
49. Ruffini, E.*, et al.* Recurrence of thymoma: analysis of clinicopathologic features, treatment, and outcome. *J Thorac Cardiovasc Surg* **113**, 55-63 (1997).
50. Regnard, J.F.*, et al.* Results of re-resection for recurrent thymomas. *Ann Thorac Surg* **64**, 1593-1598 (1997).
51. Haniuda, M.*, et al.* Recurrence of thymoma: clinicopathological features, re-operation, and outcome. *J Surg Oncol* **78**, 183-188 (2001).
52. Okumura, M.*, et al.* Outcome of surgical treatment for recurrent thymic epithelial tumors with reference to world health organization histologic classification system. *J Surg Oncol* **95**, 40-44 (2007).
53. Urgesi, A.*, et al.* Aggressive treatment of intrathoracic recurrences of thymoma. *Radiother Oncol* **24**, 221-225 (1992).
54. Lucchi, M.*, et al.* Management of pleural recurrence after curative resection of thymoma. *J Thorac Cardiovasc Surg* **137**, 1185-1189 (2009).
55. Girard, N. & Mornex, F. The role of radiotherapy in the management of thymic tumors. *Thorac Surg Clin* **21**, 99-105, vii.
56. Fuller, C.D., Housman, D.M. & Thomas, C.R. Radiotherapy for thymoma and thymic carcinoma. *Hematol Oncol Clin North Am* **22**, 489-507 (2008).
57. Korst, R.J., Kansler, A.L., Christos, P.J. & Mandal, S. Adjuvant radiotherapy for thymic epithelial tumors: a systematic review and meta-analysis. *Ann Thorac Surg* **87**, 1641-1647 (2009).
58. Spaggiari, L., Casiraghi, M. & Guarize, J. Multidisciplinary treatment of malignant thymoma. *Curr Opin Oncol* **24**, 117-122.
59. Curran, W.J., Jr., Kornstein, M.J., Brooks, J.J. & Turrisi, A.T., 3rd. Invasive thymoma: the role of mediastinal irradiation following complete or incomplete surgical resection. *J Clin Oncol* **6**, 1722-1727 (1988).
60. Cowen, D.*, et al.* Thymoma: results of a multicentric retrospective series of 149 non-metastatic irradiated patients and review of the literature. FNCLCC trialists. Federation Nationale des Centres de Lutte Contre le Cancer. *Radiother Oncol* **34**, 9-16 (1995).

61. Mornex, F.*, et al.* Radiotherapy and chemotherapy for invasive thymomas: a multicentric retrospective review of 90 cases. The FNCLCC trialists. Federation Nationale des Centres de Lutte Contre le Cancer. *Int J Radiat Oncol Biol Phys* **32**, 651-659 (1995).
62. Mangi, A.A.*, et al.* Adjuvant radiation therapy for stage II thymoma. *Ann Thorac Surg* **74**, 1033-1037 (2002).
63. Pollack, A.*, et al.* Thymoma: treatment and prognosis. *Int J Radiat Oncol Biol Phys* **23**, 1037-1043 (1992).
64. Jackson, M.A. & Ball, D.L. Post-operative radiotherapy in invasive thymoma. *Radiother Oncol* **21**, 77-82 (1991).
65. Kunitoh, H.*, et al.* A phase-II trial of dose-dense chemotherapy in patients with disseminated thymoma: report of a Japan Clinical Oncology Group trial (JCOG 9605). *Br J Cancer* **101**, 1549-1554 (2009).
66. Loehrer, P.J., Sr.*, et al.* Cisplatin plus doxorubicin plus cyclophosphamide in metastatic or recurrent thymoma: final results of an intergroup trial. The Eastern Cooperative Oncology Group, Southwest Oncology Group, and Southeastern Cancer Study Group. *J Clin Oncol* **12**, 1164-1168 (1994).
67. Fornasiero, A.*, et al.* Chemotherapy for invasive thymoma. A 13-year experience. *Cancer* **68**, 30-33 (1991).
68. Grassin, F.*, et al.* Combined etoposide, ifosfamide, and cisplatin in the treatment of patients with advanced thymoma and thymic carcinoma. A French experience. *J Thorac Oncol* **5**, 893-897.
69. Loehrer, P.J., Sr.*, et al.* Combined etoposide, ifosfamide, and cisplatin in the treatment of patients with advanced thymoma and thymic carcinoma: an intergroup trial. *Cancer* **91**, 2010-2015 (2001).
70. Giaccone, G.*, et al.* Cisplatin and etoposide combination chemotherapy for locally advanced or metastatic thymoma. A phase II study of the European Organization for Research and Treatment of Cancer Lung Cancer Cooperative Group. *J Clin Oncol* **14**, 814-820 (1996).
71. Bjerrum, O.W., Kiss, K. & Daugaard, G. Combination chemotherapy with a five-drug regimen for invasive thymoma. *Acta Oncol* **35**, 71-73 (1996).
72. Furugen, M.*, et al.* Combination chemotherapy with carboplatin and paclitaxel for advanced thymic cancer. *Jpn J Clin Oncol* **41**, 1013-1016.
73. Lemma, G.L.*, et al.* Phase II study of carboplatin and paclitaxel in advanced thymoma and thymic carcinoma. *J Clin Oncol* **29**, 2060-2065.
74. Loehrer, P.J.*, et al.* A phase II trial of pemetrexed in patients with recurrent thymoma or thymic carcinoma. *Journal of Clinical Oncology* **24**(2006).
75. Bonomi, P.D., Finkelstein, D., Aisner, S. & Ettinger, D. EST 2582 phase II trial of cisplatin in metastatic or recurrent thymoma. *Am J Clin Oncol* **16**, 342-345 (1993).
76. Palmieri, G.*, et al.* Preliminary results of phase II study of capecitabine and gemcitabine (CAP-GEM) in patients with metastatic pretreated thymic epithelial tumors (TETs). *Ann Oncol* **21**, 1168-1172.
77. Venuta, F.*, et al.* Multimodality treatment of thymoma: a prospective study. *Ann Thorac Surg* **64**, 1585-1591; discussion 1591-1582 (1997).
78. Kunitoh, H.*, et al.* A phase II trial of dose-dense chemotherapy, followed by surgical resection and/or thoracic radiotherapy, in locally advanced thymoma: report of a Japan Clinical Oncology Group trial (JCOG 9606). *Br J Cancer* **103**, 6-11.

79. Ishikawa, Y., *et al.* Multimodality therapy for patients with invasive thymoma disseminated into the pleural cavity: the potential role of extrapleural pneumonectomy. *Ann Thorac Surg* **88**, 952-957 (2009).
80. Wright, C.D., *et al.* Induction chemoradiotherapy followed by resection for locally advanced Masaoka stage III and IVA thymic tumors. *Ann Thorac Surg* **85**, 385-389 (2008).
81. Yokoi, K., *et al.* Multidisciplinary treatment for advanced invasive thymoma with cisplatin, doxorubicin, and methylprednisolone. *J Thorac Oncol* **2**, 73-78 (2007).
82. Lucchi, M., *et al.* Neoadjuvant chemotherapy for stage III and IVA thymomas: a single-institution experience with a long follow-up. *J Thorac Oncol* **1**, 308-313 (2006).
83. Jacot, W., Quantin, X., Valette, S., Khial, F. & Pujol, J.L. Multimodality treatment program in invasive thymic epithelial tumor. *Am J Clin Oncol* **28**, 5-7 (2005).
84. Berruti, A., *et al.* Primary chemotherapy with adriamycin, cisplatin, vincristine and cyclophosphamide in locally advanced thymomas: a single institution experience. *Br J Cancer* **81**, 841-845 (1999).
85. Shin, D.M., *et al.* A multidisciplinary approach to therapy for unresectable malignant thymoma. *Ann Intern Med* **129**, 100-104 (1998).
86. Rea, F., *et al.* Chemotherapy and operation for invasive thymoma. *J Thorac Cardiovasc Surg* **106**, 543-549 (1993).
87. Efficace, F., *et al.* Health-related quality of life in chronic myeloid leukemia patients receiving long-term therapy with imatinib compared with the general population. *Blood* **118**, 4554-4560.
88. Maemondo, M., *et al.* Gefitinib or chemotherapy for non-small-cell lung cancer with mutated EGFR. *N Engl J Med* **362**, 2380-2388.
89. Zhou, C., *et al.* Erlotinib versus chemotherapy as first-line treatment for patients with advanced EGFR mutation-positive non-small-cell lung cancer (OPTIMAL, CTONG-0802): a multicentre, open-label, randomised, phase 3 study. *Lancet Oncol* **12**, 735-742.
90. Christodoulou, C., *et al.* Response of malignant thymoma to erlotinib. *Ann Oncol* **19**, 1361-1362 (2008).
91. Farina, G., *et al.* Response of thymoma to cetuximab. *Lancet Oncol* **8**, 449-450 (2007).
92. Palmieri, G., *et al.* Cetuximab is an active treatment of metastatic and chemorefractory thymoma. *Front Biosci* **12**, 757-761 (2007).
93. Strobel, P., *et al.* Thymic carcinoma with overexpression of mutated KIT and the response to imatinib. *N Engl J Med* **350**, 2625-2626 (2004).
94. Buti, S., *et al.* Impressive response with imatinib in a heavily pretreated patient with metastatic c-KIT mutated thymic carcinoma. *J Clin Oncol* **29**, e803-805.
95. Girard, N., *et al.* Comprehensive genomic analysis reveals clinically relevant molecular distinctions between thymic carcinomas and thymomas. *Clin Cancer Res* **15**, 6790-6799 (2009).
96. Bisagni, G., *et al.* Long lasting response to the multikinase inhibitor bay 43-9006 (Sorafenib) in a heavily pretreated metastatic thymic carcinoma. *J Thorac Oncol* **4**, 773-775 (2009).
97. Disel, U., *et al.* Promising efficacy of sorafenib in a relapsed thymic carcinoma with C-KIT exon 11 deletion mutation. *Lung Cancer* **71**, 109-112.

98. Li, X.F., Chen, Q., Huang, W.X. & Ye, Y.B. Response to sorafenib in cisplatin-resistant thymic carcinoma: a case report. *Med Oncol* **26**, 157-160 (2009).
99. Strobel, P.*, et al.* Sunitinib in metastatic thymic carcinomas: laboratory findings and initial clinical experience. *Br J Cancer* **103**, 196-200.
100. Dham, A., Truskinovsky, A.M. & Dudek, A.Z. Thymic carcinoid responds to neoadjuvant therapy with sunitinib and octreotide: a case report. *J Thorac Oncol* **3**, 94-97 (2008).
101. Zucali, P.A.*, et al.* Insulin-like growth factor-1 receptor and phosphorylated AKT-serine 473 expression in 132 resected thymomas and thymic carcinomas. *Cancer* **116**, 4686-4695.
102. Giaccone, G.*, et al.* Phase II study of belinostat in patients with recurrent or refractory advanced thymic epithelial tumors. *J Clin Oncol* **29**, 2052-2059.
103. Palmieri, G.*, et al.* Somatostatin analogs and prednisone in advanced refractory thymic tumors. *Cancer* **94**, 1414-1420 (2002).
104. Gordon, M.S., Battiato, L.A., Gonin, R., Harrison-Mann, B.C. & Loehrer, P.J., Sr. A phase II trial of subcutaneously administered recombinant human interleukin-2 in patients with relapsed/refractory thymoma. *J Immunother Emphasis Tumor Immunol* **18**, 179-184 (1995).
105. Kelly, R.J., Petrini, I., Rajan, A., Wang, Y. & Giaccone, G. Thymic malignancies: from clinical management to targeted therapies. *J Clin Oncol* **29**, 4820-4827.
106. Kurup, A., Burns, M., Dropcho, S., Pao, W. & Loehrer, P.J. Phase II study of gefitinib treatment in advanced thymic malignancies. *Journal of Clinical Oncology* **23**(2005).
107. Bedano, P.M.*, et al.* A phase II trial of erlotinib plus bevacizumab in patients with recurrent thymoma or thymic carcinoma. *Journal of Clinical Oncology* **26**(2008).
108. Giaccone, G.*, et al.* Imatinib mesylate in patients with WHO B3 thymomas and thymic carcinomas. *J Thorac Oncol* **4**, 1270-1273 (2009).
109. Salter, J.T.*, et al.* Imatinib for the treatment of thymic carcinoma. *Journal of Clinical Oncology* **26**(2008).
110. Palmieri, G.*, et al.* Imatinib mesylate in thymic epithelial malignancies. *Cancer Chemother Pharmacol* **69**, 309-315.
111. Rajan, A.*, et al.* Phase II study of the insulin-like growth factor-1 receptor (IGF-1R) antibody cixutumumab (C) in patients (pts) with thymoma (T) and thymic carcinoma (TC). *Journal of Clinical Oncology* **28**(2010).
112. Loehrer, P.J., Sr., Wang, W., Johnson, D.H., Aisner, S.C. & Ettinger, D.S. Octreotide alone or with prednisone in patients with advanced thymoma and thymic carcinoma: an Eastern Cooperative Oncology Group Phase II Trial. *J Clin Oncol* **22**, 293-299 (2004).
113. Nelson, R.P., Jr. & Pascuzzi, R.M. Paraneoplastic syndromes in thymoma: an immunological perspective. *Curr Treat Options Oncol* **9**, 269-276 (2008).
114. Herens, C.*, et al.* Deletion (6)(p22p25) is a recurrent anomaly of thymoma: report of a second case and review of the literature. *Cancer Genet Cytogenet* **146**, 66-69 (2003).
115. Zettl, A.*, et al.* Recurrent genetic aberrations in thymoma and thymic carcinoma. *Am J Pathol* **157**, 257-266 (2000).
116. Girard, N. Thymic tumors: relevant molecular data in the clinic. *J Thorac Oncol* **5**, S291-295.

117. Suzuki, E.*, et al.* Expression and mutation statuses of epidermal growth factor receptor in thymic epithelial tumors. *Jpn J Clin Oncol* **36**, 351-356 (2006).
118. Ionescu, D.N., Sasatomi, E., Cieply, K., Nola, M. & Dacic, S. Protein expression and gene amplification of epidermal growth factor receptor in thymomas. *Cancer* **103**, 630-636 (2005).
119. A. Kurup, M.B., S. Dropcho, W. Pao, P. J. Loehrer. Phase II study of gefitinib treatment in advanced thymic malignancies. *Journal of Clinical Oncology* **23**, Part I of II (June 1 Supplement):7068 (2005).
120. Aisner, S.C.*, et al.* Epidermal growth factor receptor, C-kit, and Her2/neu immunostaining in advanced or recurrent thymic epithelial neoplasms staged according to the 2004 World Health Organization in patients treated with octreotide and prednisone: an Eastern Cooperative Oncology Group study. *J Thorac Oncol* **5**, 885-892.
121. Henley, J.D., Cummings, O.W. & Loehrer, P.J., Sr. Tyrosine kinase receptor expression in thymomas. *J Cancer Res Clin Oncol* **130**, 222-224 (2004).
122. Pan, C.C., Chen, P.C. & Chiang, H. KIT (CD117) is frequently overexpressed in thymic carcinomas but is absent in thymomas. *J Pathol* **202**, 375-381 (2004).
123. Nakagawa, K.*, et al.* Immunohistochemical KIT (CD117) expression in thymic epithelial tumors. *Chest* **128**, 140-144 (2005).
124. Tsuchida, M.*, et al.* Absence of gene mutations in KIT-positive thymic epithelial tumors. *Lung Cancer* **62**, 321-325 (2008).
125. Vasamiliette, J.*, et al.* Treatment monitoring with 18F-FDG PET in metastatic thymoma after 90Y-Dotatoc and selective internal radiation treatment (SIRT). *Hell J Nucl Med* **12**, 271-273 (2009).
126. Salter JT LD, Y.C., Loehrer PJ, Risley L, Chiorean EG. Imatinib for the treatment of thymic carcinoma. *Journal of Clinical Oncology* **26**, 8116 (2008).
127. Yoh, K.*, et al.* Mutational status of EGFR and KIT in thymoma and thymic carcinoma. *Lung Cancer* **62**, 316-320 (2008).
128. Girard, N.*, et al.* Insulin-like growth factor-1 receptor expression in thymic malignancies. *J Thorac Oncol* **5**, 1439-1446.
129. Heinrich, M.C.*, et al.* Primary and secondary kinase genotypes correlate with the biological and clinical activity of sunitinib in imatinib-resistant gastrointestinal stromal tumor. *J Clin Oncol* **26**, 5352-5359 (2008).
130. Brocheriou, I., Carnot, F. & Briere, J. Immunohistochemical detection of bcl-2 protein in thymoma. *Histopathology* **27**, 251-255 (1995).
131. Chen, F.F.*, et al.* Immunohistochemical localization of Mcl-1 and bcl-2 proteins in thymic epithelial tumours. *Histopathology* **29**, 541-547 (1996).
132. Dorfman, D.M., Shahsafaei, A. & Miyauchi, A. Immunohistochemical staining for bcl-2 and mcl-1 in intrathyroidal epithelial thymoma (ITET)/carcinoma showing thymus-like differentiation (CASTLE) and cervical thymic carcinoma. *Mod Pathol* **11**, 989-994 (1998).
133. Hiroshima, K.*, et al.* Proliferative activity and apoptosis in thymic epithelial neoplasms. *Mod Pathol* **15**, 1326-1332 (2002).
134. Khoury, T.*, et al.* Apoptosis-related (survivin, Bcl-2), tumor suppressor gene (p53), proliferation (Ki-67), and non-receptor tyrosine kinase (Src) markers expression and correlation with clinicopathologic variables in 60 thymic neoplasms. *Chest* **136**, 220-228 (2009).

135. Pan, C.C., Chen, P.C., Wang, L.S., Lee, J.Y. & Chiang, H. Expression of apoptosis-related markers and HER-2/neu in thymic epithelial tumours. *Histopathology* **43**, 165-172 (2003).
136. Stefanaki, K.*, et al.* Expression of p53, mdm2, p21/waf1 and bcl-2 proteins in thymomas. *Histopathology* **30**, 549-555 (1997).
137. Tateyama, H.*, et al.* Apoptosis, bcl-2 protein, and Fas antigen in thymic epithelial tumors. *Mod Pathol* **10**, 983-991 (1997).
138. Park, S.H., Kim, H.K., Kim, H. & Ro, J.Y. Apoptosis in thymic epithelial tumors. *Pathol Res Pract* **198**, 461-467 (2002).
139. Engel, P., Francis, D. & Graem, N. Expression of bcl-2 in fetal thymus, thymomas and thymic carcinomas. Association with p53 expression and review of the literature. *APMIS* **106**, 449-455 (1998).
140. Kaira, K.*, et al.* Biologic correlation of 2-[18F]-fluoro-2-deoxy-D-glucose uptake on positron emission tomography in thymic epithelial tumors. *J Clin Oncol* **28**, 3746-3753.
141. Nabarra, B., Pontoux, C., Godard, C., Osborne-Pellegrin, M. & Ezine, S. Neoplastic transformation and angiogenesis in the thymus of transgenic mice expressing SV40 T and t antigen under an L-pyruvate kinase promoter (SV12 mice). *Int J Exp Pathol* **86**, 397-413 (2005).
142. Weirich, G.*, et al.* p53 alterations in thymic epithelial tumours. *Virchows Arch* **431**, 17-23 (1997).
143. Tateyama, H.*, et al.* p53 protein expression and p53 gene mutation in thymic epithelial tumors. An immunohistochemical and DNA sequencing study. *Am J Clin Pathol* **104**, 375-381 (1995).
144. Pich, A.*, et al.* p53 expression and proliferative activity predict survival in non-invasive thymomas. *Int J Cancer* **69**, 180-183 (1996).
145. Oyama, T.*, et al.* p53 alteration, proliferating cell nuclear antigen, and nucleolar organizer regions in thymic epithelial tumors. *Int J Mol Med* **1**, 823-826 (1998).
146. Mineo, T.C., Ambrogi, V., Mineo, D. & Baldi, A. Long-term disease-free survival of patients with radically resected thymomas: relevance of cell-cycle protein expression. *Cancer* **104**, 2063-2071 (2005).
147. Hirabayashi, H.*, et al.* p16INK4, pRB, p53 and cyclin D1 expression and hypermethylation of CDKN2 gene in thymoma and thymic carcinoma. *Int J Cancer* **73**, 639-644 (1997).
148. Hino, N., Kondo, K., Miyoshi, T., Uyama, T. & Monden, Y. High frequency of p53 protein expression in thymic carcinoma but not in thymoma. *Br J Cancer* **76**, 1361-1366 (1997).
149. Hayashi, Y.*, et al.* Thymoma: tumour type related to expression of epidermal growth factor (EGF), EGF-receptor, p53, v-erb B and ras p21. *Virchows Arch* **426**, 43-50 (1995).
150. Gilhus, N.E.*, et al.* Oncogene proteins and proliferation antigens in thymomas: increased expression of epidermal growth factor receptor and Ki67 antigen. *J Clin Pathol* **48**, 447-455 (1995).
151. Comin, C.E., Messerini, L., Novelli, L., Boddi, V. & Dini, S. KI-67 antigen expression predicts survival and correlates with histologic subtype in the WHO classification of thymic epithelial tumors. *Int J Surg Pathol* **12**, 395-400 (2004).

152. Chen, F.F., Yan, J.J., Jin, Y.T. & Su, I.J. Detection of bcl-2 and p53 in thymoma: expression of bcl-2 as a reliable marker of tumor aggressiveness. *Hum Pathol* **27**, 1089-1092 (1996).
153. Hirose, Y.*, et al.* Aberrant methylation of tumour-related genes in thymic epithelial tumours. *Lung Cancer* **64**, 155-159 (2009).
154. Tsuji, T.*, et al.* Malignant transformation of thymoma in recipient rats by heterotopic thymus transplantation from HTLV-I transgenic rats. *Lab Invest* **85**, 851-861 (2005).
155. Masaoka, A.*, et al.* Thymectomy and malignancy. *Eur J Cardiothorac Surg* **8**, 251-253 (1994).
156. Haack, H.*, et al.* Diagnosis of NUT midline carcinoma using a NUT-specific monoclonal antibody. *Am J Surg Pathol* **33**, 984-991 (2009).
157. French, C.A.*, et al.* BRD4 bromodomain gene rearrangement in aggressive carcinoma with translocation t(15;19). *Am J Pathol* **159**, 1987-1992 (2001).
158. Allander, S.V.*, et al.* Gastrointestinal stromal tumors with KIT mutations exhibit a remarkably homogeneous gene expression profile. *Cancer Res* **61**, 8624-8628 (2001).
159. Drmanac, R.*, et al.* Human genome sequencing using unchained base reads on self-assembling DNA nanoarrays. *Science* **327**, 78-81.
160. Reich, M.*, et al.* GenePattern 2.0. *Nat Genet* **38**, 500-501 (2006).
161. Ehemann, V.*, et al.* Establishment, characterization and drug sensitivity testing in primary cultures of human thymoma and thymic carcinoma. *Int J Cancer* **122**, 2719-2725 (2008).
162. Chiarenza, A.*, et al.* Tamoxifen inhibits nerve growth factor-induced proliferation of the human breast cancerous cell line MCF-7. *Cancer Res* **61**, 3002-3008 (2001).
163. Harada, T.*, et al.* Characterization of epidermal growth factor receptor mutations in non-small-cell lung cancer patients of African-American ancestry. *Oncogene*.
164. Petrini, I.*, et al.* Expression and mutational status of c-kit in thymic epithelial tumors. *J Thorac Oncol* **5**, 1447-1453.
165. French, C.A.*, et al.* Midline carcinoma of children and young adults with NUT rearrangement. *J Clin Oncol* **22**, 4135-4139 (2004).
166. French, C.A.*, et al.* BRD4-NUT fusion oncogene: a novel mechanism in aggressive carcinoma. *Cancer Res* **63**, 304-307 (2003).
167. Wu, S.Y. & Chiang, C.M. The double bromodomain-containing chromatin adaptor Brd4 and transcriptional regulation. *J Biol Chem* **282**, 13141-13145 (2007).
168. French, C.A.*, et al.* BRD-NUT oncoproteins: a family of closely related nuclear proteins that block epithelial differentiation and maintain the growth of carcinoma cells. *Oncogene* **27**, 2237-2242 (2008).
169. Florence, B. & Faller, D.V. You bet-cha: a novel family of transcriptional regulators. *Front Biosci* **6**, D1008-1018 (2001).
170. LeRoy, G., Rickards, B. & Flint, S.J. The double bromodomain proteins Brd2 and Brd3 couple histone acetylation to transcription. *Mol Cell* **30**, 51-60 (2008).
171. Dey, A.*, et al.* A bromodomain protein, MCAP, associates with mitotic chromosomes and affects G(2)-to-M transition. *Mol Cell Biol* **20**, 6537-6549 (2000).
172. Jang, M.K.*, et al.* The bromodomain protein Brd4 is a positive regulatory component of P-TEFb and stimulates RNA polymerase II-dependent transcription. *Mol Cell* **19**, 523-534 (2005).
173. Yang, Z.*, et al.* Recruitment of P-TEFb for stimulation of transcriptional elongation by the bromodomain protein Brd4. *Mol Cell* **19**, 535-545 (2005).

174. Kuzume, T.*, et al.* Establishment and characterization of a thymic carcinoma cell line (Ty-82) carrying t(15;19)(q15;p13) chromosome abnormality. *Int J Cancer* **50**, 259-264 (1992).
175. Kubonishi, I.*, et al.* Novel t(15;19)(q15;p13) chromosome abnormality in a thymic carcinoma. *Cancer Res* **51**, 3327-3328 (1991).
176. Toretsky, J.A.*, et al.* Translocation (11;15;19): a highly specific chromosome rearrangement associated with poorly differentiated thymic carcinoma in young patients. *Am J Clin Oncol* **26**, 300-306 (2003).
177. Lee, A.C.*, et al.* Disseminated mediastinal carcinoma with chromosomal translocation (15;19). A distinctive clinicopathologic syndrome. *Cancer* **72**, 2273-2276 (1993).
178. Dotto, J., Pelosi, G. & Rosai, J. Expression of p63 in thymomas and normal thymus. *Am J Clin Pathol* **127**, 415-420 (2007).
179. Pan, C.C., Chen, P.C., Chou, T.Y. & Chiang, H. Expression of calretinin and other mesothelioma-related markers in thymic carcinoma and thymoma. *Hum Pathol* **34**, 1155-1162 (2003).
180. Kees, U.R., Mulcahy, M.T. & Willoughby, M.L. Intrathoracic carcinoma in an 11-year-old girl showing a translocation t(15;19). *Am J Pediatr Hematol Oncol* **13**, 459-464 (1991).
181. Edling, C.E. & Hallberg, B. c-Kit--a hematopoietic cell essential receptor tyrosine kinase. *Int J Biochem Cell Biol* **39**, 1995-1998 (2007).
182. Corless, C.L., Fletcher, J.A. & Heinrich, M.C. Biology of gastrointestinal stromal tumors. *J Clin Oncol* **22**, 3813-3825 (2004).
183. Pan, C.C., Chen, P.C. & Chiang, H. Overexpression of KIT (CD117) in chromophobe renal cell carcinoma and renal oncocytoma. *Am J Clin Pathol* **121**, 878-883 (2004).
184. Inokuchi, K.*, et al.* Abnormality of c-kit oncoprotein in certain patients with chronic myelogenous leukemia--potential clinical significance. *Leukemia* **16**, 170-177 (2002).
185. Heinrich, M.C.*, et al.* Kinase mutations and imatinib response in patients with metastatic gastrointestinal stromal tumor. *J Clin Oncol* **21**, 4342-4349 (2003).
186. Medeiros, F.*, et al.* KIT-negative gastrointestinal stromal tumors: proof of concept and therapeutic implications. *Am J Surg Pathol* **28**, 889-894 (2004).
187. Bauer, S.*, et al.* Response to imatinib mesylate of a gastrointestinal stromal tumor with very low expression of KIT. *Cancer Chemother Pharmacol* **51**, 261-265 (2003).
188. Wilhelm, S.M.*, et al.* BAY 43-9006 exhibits broad spectrum oral antitumor activity and targets the RAF/MEK/ERK pathway and receptor tyrosine kinases involved in tumor progression and angiogenesis. *Cancer Res* **64**, 7099-7109 (2004).
189. Kruger, S.*, et al.* The c-kit (CD117) sequence variation M541L, but not N564K, is frequent in the general population, and is not associated with CML in Caucasians. *Leukemia* **20**, 354-355; discussion 356-357 (2006).
190. Salter JT, L.D., Yiannoutsos C, Loehrer PJ, Risley L, Chiorean EG. Imatinib for the treatment of thymic carcinoma. *Journal of Clinical Oncoogy* **26**, 8116 (2008).
191. Giaccone, G.M., PhD; Rajan, Arun MD; Ruijter, Rita RN; Smit, Egbert MD, PhD; van Groeningen, Cees MD, PhD; Hogendoorn, Pancras C. W. MD, PhD. Imatinib Mesylate in Patients with WHO B3 Thymomas and Thymic Carcinomas. *Journal of Thoracic Oncology* **4**, 1270-1273 (2009).
192. Vasamiliette, J.*, et al.* Treatment monitoring with (18)F-FDG PET in metastatic thymoma after (90)Y-Dotatoc and selective internal radiation treatment (SIRT). *Hell J Nucl Med* **12**, 271-273 (2009).

193. Mardis, E.R., *et al.* Recurring mutations found by sequencing an acute myeloid leukemia genome. *N Engl J Med* **361**, 1058-1066 (2009).
194. Roberts, A., Pimentel, H., Trapnell, C. & Pachter, L. Identification of novel transcripts in annotated genomes using RNA-Seq. *Bioinformatics* **27**, 2325-2329.
195. Zhou, M.I., *et al.* Jade-1, a candidate renal tumor suppressor that promotes apoptosis. *Proc Natl Acad Sci U S A* **102**, 11035-11040 (2005).
196. Doyon, Y., *et al.* ING tumor suppressor proteins are critical regulators of chromatin acetylation required for genome expression and perpetuation. *Mol Cell* **21**, 51-64 (2006).
197. Hayashida, Y., *et al.* PPP1R3 gene (protein phosphatase 1) alterations in colorectal cancer and its relationship to metastasis. *Oncol Rep* **13**, 1223-1227 (2005).
198. Winter, S.L., Bosnoyan-Collins, L., Pinnaduwage, D. & Andrulis, I.L. The interaction of PP1 with BRCA1 and analysis of their expression in breast tumors. *BMC Cancer* **7**, 85 (2007).
199. Ghetu, A.F., *et al.* Structure of a BCOR corepressor peptide in complex with the BCL6 BTB domain dimer. *Mol Cell* **29**, 384-391 (2008).
200. Wamstad, J.A., Corcoran, C.M., Keating, A.M. & Bardwell, V.J. Role of the transcriptional corepressor Bcor in embryonic stem cell differentiation and early embryonic development. *PLoS One* **3**, e2814 (2008).
201. Fan, Z., *et al.* BCOR regulates mesenchymal stem cell function by epigenetic mechanisms. *Nat Cell Biol* **11**, 1002-1009 (2009).
202. Ng, D., *et al.* Oculofaciocardiodental and Lenz microphthalmia syndromes result from distinct classes of mutations in BCOR. *Nat Genet* **36**, 411-416 (2004).
203. Grossmann, V., *et al.* Whole-exome sequencing identifies somatic mutations of BCOR in acute myeloid leukemia with normal karyotype. *Blood* **118**, 6153-6163.
204. Fernandez-Valdivia, R., Zhang, Y., Pai, S., Metzker, M.L. & Schumacher, A. l7Rn6 encodes a novel protein required for clara cell function in mouse lung development. *Genetics* **172**, 389-399 (2006).
205. Beckmann, J., *et al.* Human teneurin-1 is a direct target of the homeobox transcription factor EMX2 at a novel alternate promoter. *BMC Dev Biol* **11**, 35.
206. Ostrovnaya, I., Nanjangud, G. & Olshen, A.B. A classification model for distinguishing copy number variants from cancer-related alterations. *BMC Bioinformatics* **11**, 297.
207. Shlien, A. & Malkin, D. Copy number variations and cancer. *Genome Med* **1**, 62 (2009).
208. Beroukhim, R., *et al.* Assessing the significance of chromosomal aberrations in cancer: methodology and application to glioma. *Proc Natl Acad Sci U S A* **104**, 20007-20012 (2007).
209. Beroukhim, R., *et al.* The landscape of somatic copy-number alteration across human cancers. *Nature* **463**, 899-905.
210. Luh, F.Y., *et al.* Structure of the cyclin-dependent kinase inhibitor p19Ink4d. *Nature* **389**, 999-1003 (1997).
211. Clark, P.A., Llanos, S. & Peters, G. Multiple interacting domains contribute to p14ARF mediated inhibition of MDM2. *Oncogene* **21**, 4498-4507 (2002).
212. Kumar, P., Henikoff, S. & Ng, P.C. Predicting the effects of coding non-synonymous variants on protein function using the SIFT algorithm. *Nat Protoc* **4**, 1073-1081 (2009).

213. Chiecchio, L.*, et al.* Deletion of chromosome 13 detected by conventional cytogenetics is a critical prognostic factor in myeloma. *Leukemia* **20**, 1610-1617 (2006).
214. van den Berg, J., Johannsson, O., Hakansson, S., Olsson, H. & Borg, A. Allelic loss at chromosome 13q12-q13 is associated with poor prognosis in familial and sporadic breast cancer. *Br J Cancer* **74**, 1615-1619 (1996).
215. D'Andrea, A.D. & Grompe, M. The Fanconi anaemia/BRCA pathway. *Nat Rev Cancer* **3**, 23-34 (2003).
216. Kim, M.*, et al.* Homozygous deletion of CDKN2A (p16, p14) and CDKN2B (p15) genes is a poor prognostic factor in adult but not in childhood B-lineage acute lymphoblastic leukemia: a comparative deletion and hypermethylation study. *Cancer Genet Cytogenet* **195**, 59-65 (2009).
217. Lal, A.*, et al.* p16(INK4a) translation suppressed by miR-24. *PLoS One* **3**, e1864 (2008).
218. Shoemaker, A.R.*, et al.* Activity of the Bcl-2 family inhibitor ABT-263 in a panel of small cell lung cancer xenograft models. *Clin Cancer Res* **14**, 3268-3277 (2008).
219. Inuzuka, H.*, et al.* SCF(FBW7) regulates cellular apoptosis by targeting MCL1 for ubiquitylation and destruction. *Nature* **471**, 104-109.
220. Nguyen, M.*, et al.* Small molecule obatoclax (GX15-070) antagonizes MCL-1 and overcomes MCL-1-mediated resistance to apoptosis. *Proc Natl Acad Sci U S A* **104**, 19512-19517 (2007).
221. Bonapace, L.*, et al.* Induction of autophagy-dependent necroptosis is required for childhood acute lymphoblastic leukemia cells to overcome glucocorticoid resistance. *J Clin Invest* **120**, 1310-1323.
222. Penzel, R.*, et al.* Clusters of chromosomal imbalances in thymic epithelial tumours are associated with the WHO classification and the staging system according to Masaoka. *Int J Cancer* **105**, 494-498 (2003).
223. Inoue, M.*, et al.* Correlating genetic aberrations with World Health Organization-defined histology and stage across the spectrum of thymomas. *Cancer Res* **63**, 3708-3715 (2003).
224. Hockenbery, D., Nunez, G., Milliman, C., Schreiber, R.D. & Korsmeyer, S.J. Bcl-2 is an inner mitochondrial membrane protein that blocks programmed cell death. *Nature* **348**, 334-336 (1990).

6. Acknowledgment

Giuseppe Giaccone and Yisong Wang supervised the experimental procedures. Sean Davis provided part of the next generation sequencing data analysis. Paolo A. Zucali provided FFPE tumor samples and clinical data from patients treated at Humanitas Cancer Center (Milan). Marco Lucchi provided the frozen tumor from Pisa University Hospital. Sara Galimberti, Mario Petrini and Morrow Betsy reviewed and corrected this dissertation.

7. Abbreviations

TET Thymic epithelial tumors

WHO World Health Organization

CN Copy number

CGH Comparative genomic hybridization

FISH Fluorescence in situ hybridization

DN double negative

DP double positive

SP single positive

MEC medulla epithelial cell

CEC Cortex epithelial cell

DC dendritic cell

TCR T cell receptor

SEER Surveillance, Epidemiology and End Results

TC thymic carcinoma

SIR Standardized incidence ratio

AIDS Acquired immune deficiency syndrome

EBV Epstein Barr virus

MEN1 Multiple endocrine neoplasm

MG Myasthenia gravis

OS overall survival

DRS Disease related survival

TTP Time to progression

RR Response rate

CR complete response

PR partial response

SD stable disease

ACTH Adrenocorticotropic hormone

IMRT Intensity modulated radiotherapy

R0 Complete resection

R1 Microscopically incomplete resection

R2 Macroscopically incomplete resection

CI Confidence interval

GH Growth hormone

SV40 simian virus 40

FFPE Formalin fixed paraffin embedded

BAC Bacterial artificial chromosome

DAB 3',3'-diaminobenzidine

HRP Horseradish peroxidase

TBS Tris buffered saline

TBST Tris buffered saline and tween 20

H&E Haematoxylin & Eosin

DNBs DNA nano-balls

SNV single nucleotide variation

SNP single nucleotide polymorphism

INDEL insertion/deletion

OCT optimal cutting temperature

EDTA Ethylenediaminetetraacetic acid

GISTIC Genomic Identification of Significant Targets in Cancer

GATK Genome Analysis Tool Kit

RIN RNA integrity number

GA-II Genome analyzer-II

7AAD 7-amino-actinomycin D

MTS 3-(4,5-dimethylthiazol-2-yl)-5-(3-carboxymethoxyphenyl)-2-(4-sulfophenyl)-2H-tetrazolium assay

IHC Immunohistochemistry

Uk Unknown

Nr Not reached

miRNA Micro RNA

siRNA Small interference RNA

shRNA Small hairpin RNA

scRNA Scramble siRNA

CIx Combination Index

NEC1 Necrostatin 1

QC Chloroquine

FF2 Fire fly luciferase